1964

An investigation of crack occurrence in the end regions of pretensioned prestressed concrete beams

D. M. Miller
Lehigh University

AN INVESTIGATION OF CRACK OCCURRENCE IN THE END REGIONS OF PRETENSIONED PRESTRESSED CONCRETE BEAMS

by

D. M. Miller

This thesis presents the results of an experimental investigation of the probable causes of crack occurrence in the end regions of pretensioned prestressed concrete beams used for highway bridges. Even though the occurrence of surface cracks in pretensioned highway bridge beams probably causes no immediate effect on beam service performance, it is generally felt that such members should be free of cracks when delivered for erection at a bridge site. This is required in order to provide greater durability of bridge structures, and to eliminate the adverse effects on appearance caused by cracks. However, cracks have been observed in many of the pretensioned highway beams prior to their being erected. These cracks appeared principally in the top fibers near the ends of beams, and to a lesser extent in the end faces and in top fibers away from the beam ends. Neither the cause of this cracking nor the exact time during fabrication or storage at which cracks formed was known.

From consideration of the beam fabrication process and the characteristics of the cracks that were observed, it seemed certain that the cause of cracking was due to one or a combination of the following:

1. Temperature effects created by cement hydration and steam curing.
2. The effects of concrete shrinkage.
3. The effects caused by transfer of the prestress force.

In order to determine accurately the conditions leading to the occurrence of beam cracking it would be necessary to define completely the concrete stress distributions present in the end regions of pretensioned beams from the time of casting to and including the time of prestress transfer. However, since a mathematical stress determination was not feasible for this investigation, an experimental approach was used.

The experimental study consisted of the determination during the fabrication process of the temperature and strain distribution in the end zones of two full sized prestressed concrete beams. The beams were fabricated in a commercial prestressing plant under standard conditions as specified for beams used for highway bridges. A strain measuring device was developed which consisted of a temperature compensating metallic foil gage bonded to a slender piece of mild steel. The first beam test included 24 thermocouples and 59 strain measuring devices embedded in the end zones of the member. The second beam test included 24 thermocouples and 60 strain measuring devices embedded in one end zone of the member. The temperature and strain distribution was obtained at intervals during the curing process. These data are presented and discussed in detail.

The exact cause of the beam cracking was not determined in this investigation. However, knowledge was gained which pointed to probable causes, and it is hoped, that this, along with other information obtained in the research, may be helpful in reducing beam cracking.

AN INVESTIGATION OF CRACK OCCURRENCE
IN THE END REGIONS OF
PRETENSIONED PRESTRESSED CONCRETE BEAMS

by

D. M. Miller

A THESIS

Presented to the Graduate Faculty
of Lehigh University
in Candidacy for the Degree of
Master of Science

Lehigh University

1964

This thesis is accepted and approved in partial fulfillment of the requirements for the degree of Master of Science.

March 10, 1964
(Date)

C. F. Hulsbos
Professor in Charge

W. J. Eney
Professor W. J. Eney, Head
Department of Civil Engineering

ACKNOWLEDGEMENTS

This work has been carried out under the auspices of the Institute of Research of Lehigh University, and was sponsored by the Pennsylvania Department of Highways. The major tests involved in the investigation were conducted at the Schuylkill Products Company plant in Cressona, Pennsylvania, and the remainder of the work was done in the Department of Civil Engineering at the Fritz Engineering Laboratory.

The author wishes to express his appreciation for the assistance and patience of the management and staff of the Schuylkill Products Company, and for the advice and assistance given during the investigation by Pennsylvania Department of Highways personnel.

In addition, the continued advice and helpful criticism given by his thesis supervisor, Professor C. L. Hulsbos,and the assistance during various stages of the project of Messrs. W. F. Chen, Erol Yarimci, and F. S. Ople, Jr. are greatly appreciated.

TABLE OF CONTENTS

LIST OF TABLES

LIST OF FIGURES

1. INTRODUCTION

1.1 THE CRACKING PROBLEM

Even though the occurrence of surface cracks in pretensioned highway bridge beams probably causes no immediate effect on beam service performance, it is generally felt that such members should be free of cracks when delivered for erection at a bridge site. This is required in order to provide greater durability of bridge structures, and to eliminate the adverse effects on appearance caused by cracks. However, cracks have been observed in many of the pretensioned highway beams fabricated for the Pennsylvania Department of Highways (PDH) prior to their being erected. These cracks appeared principally in the top fibers near the ends of beams, and to a lesser extent in the end faces and in top fibers away from the beam ends. Neither the cause of this cracking nor the exact time during fabrication or storage at which the cracks formed was known. The cracks were relatively fine, with measured widths averaging about 0.002 in.

Figure 1 shows the location of typical cracks occurring in the end of a rectangular pretensioned beam. In most cases only a few cracks were observed in any one beam, and those which most commonly occurred are marked A in the figure. When cracks appeared in the end face of a beam, they generally occurred below the mid depth, and ran horizontally from the edges or diagonally near the lower corners. The most common types of end face cracks are marked B in Fig. 1.

From consideration of the beam fabrication process and the characteristics of the cracks that were observed, it seemed certain that the cause of the cracking was one or a combination of the following:

1. Temperature effects created by cement hydration and and steam curing.
2. The effects of concrete shrinkage.
3. The effects caused by transfer of the prestress force.

In all probability shrinkage is very slight during most of the beam fabrication process since, from the time of casting to the time of prestress transfer the enclosure of beam surfaces by forms and tarpaulins, and the application of steam curing prevent the escape of concrete void water. With negligible shrinkage during this time, it was felt that any concrete stresses of important magnitude occurring during the curing phase of fabrication could be attributed to temperature effects.

In Pennsylvania fabricating plants, the temperature in some parts of steam cured beams may rise to 180F or higher within a few hours after casting. It was considered possible that such large temperature changes along with the temperature gradients occurring early in the curing cycle could produce significant stresses in the hardening concrete.

Concrete shrinkage begins at the termination of steam curing, but probably does not become significant until beam surfaces are uncovered. If tarpaulins and forms are removed immediately upon cessation of steam application, the shrinkage rate will be quite high due to the accelerated evaporation caused by the temperature difference between the not yet cooled beam and the surrounding air. The resulting deformations would not induce stress unless they are restrained in some way. However,

longitudinal shrinkage would be impeded at strand level by the bond between concrete and strands, and if beam surfaces were thus exposed prior to prestress transfer, this restrain could cause cracking.

In addition, if the temperature difference mentioned above is large, significant surface tensile stresses could be caused by uncovering the beams. According to Goodier[1], if a part or the whole of the surface of an elastic body experiences a sudden decrease in temperature, ΔT, tensile stress is developed in the surface layer of the body wherever the cooling occurs equal to

$$\frac{E \alpha \Delta T}{1 - \nu}$$

in which E is the elastic modulus

α is the coefficient of thermal expression, and

ν is poisson's ratio.

Since this formula gives the stress caused by "sudden" cooling, it does not accurately represent effects of the relatively gradual temperature changes occurring upon the removal of forms from steam cured beams. However, stress values determined with the formula are larger than the surface stresses actually induced, and, therefore, represent an upper bound. If typical values for concrete are substituted for E, α, and ν, and ΔT is set equal to unity, the above formula gives a value of induced tensile stress of approximately 30 psi for each Fahrenheit degree difference in temperature. If ΔT were large, and the induced tensile stress approached this magnitude, cracking would occur. It is important to note, however, that even if this temperature induced stress is not large enough in itself to cause cracking, it adds to the effects of concrete shrinkage, and, therefore, increases the probability of crack occurrence.

If however, the possibility of harmful temperature or shrinkage effects is disregarded, the cracking in Fig. 1 could be imagined to arise solely from the effects of prestress transfer. The fact that most cracks observed were in the top surfaces near beam ends might indicate excessive initial prestress due to overtensioning of prestressing strands, or insufficient concrete strength for the tensile stresses allowed in design. Similarly, the end face cracks could have been caused by the "bursting" and "spalling" effects[2] of the complex end-zone stress distribution produced by prestress transfer.

1.2 BACKGROUND TO THE RESEARCH PROJECT

In attempting to solve the problem, a method for alleviating cracking by diminishing the prestress transfer effects was given particular consideration by highway officials and beam fabricators. The method consisted of unbonding a number of strands for a sufficient distance from the ends of beams to partly dissipate end stress concentrations, and, by thus increasing the average transfer distance, to reduce possibly excessive stresses near the beam ends. Although there are a number of ways to prevent bond between prestressing strand and the surrounding concrete, one method which had been previously investigated[3,4] was shown particular interest. This method involved painting the prestressing strands with a bond retarding chemical prior to beam casting. Unlike other unbonding procedures, this chemical method was believed to only temporarily eliminate bond, and supposedly could permit sufficient bond increase with time to exclude the possibility of a reduction in member strength due to a flexural bond failure.

On September 22, 1961 a research proposal to investigate the bond retardant method was sent to the PDH by Lehigh University. The proposed research included pull-out tests to study the effectiveness of the chemical agent in eliminating and re-establishing bond between steel strands and concrete. In addition, static and repeated load tests were to be conducted on beams in which some unbonded strands were included. These beams were to be fabricated in the Fritz Laboratory.

The proposal was not approved, but instead a more comprehensive study was drawn up by the PDH and sent to Lehigh University on November 9, 1961. This suggested investigation included extensive pull-out tests, strain measurement in the end regions of full-scale highway beams with bonded and unbonded strands, and a study to evaluate the side effects of bond retardant coatings. A revised proposal was submitted to the PDH on January 8, 1962 which included most of the suggested testing program, but omitted the side effects study.

In discussions which followed, however, it was decided to change the emphasis of the investigation from a study of one possible solution to the cracking problem, to an evaluation of the cause of cracking. Consideration of the unbonding investigation was then discontinued, at least temporarily, and attention was turned to the problem of determining the conditions in the end regions of pretensioned beams which are brought about by the three crack causing effects previously listed. A new proposal was offered to the PDH on June 9, 1962 which, in general, outlined the research discussed in the remainder of this report.

2. DESCRIPTION OF THE RESEARCH PROJECT

2.1 REQUIREMENTS

In order to accurately determine the conditions leading to the occurrence of beam cracking, it would be necessary to define completely the concrete stress distributions present in the end regions of pre-tensioned beams from the time of concrete casting to and including the time of prestress transfer. If such a stress analysis were practicable, it would be accomplished by using the mathematical theories of elasticity and plasticity, or by employing a combination of mathematical and experimental methods. However, as will be discussed in Section 2.2, a mathematical stress determination is not feasible for this investigation, and, for the most part, an entirely experimental approach must be used.

Since stresses are not directly determined in an experimental analysis, but are arrived at indirectly using indicated strain values, this research involves an investigation of strains which are associated with the concrete stresses present during beam fabrication. In addition, it is desired to determine, if possible, the relative influence of temperature changes, shrinkage, and prestress transfer in causing these stresses.

It was originally planned that three beam tests would be included in the investigation, and that two rectangular box beams and one I-beam would be used. However, difficulties arising primarily in instrumentation development and test scheduling prescribed that only two box beam tests be conducted. The first of these tests was conducted in

October, 1962 using a sixteen foot beam. The second, and more conclusive test was conducted using a full size bridge beam in August, 1963.

In order to duplicate as closely as possible typical bridge beam fabrication conditions, it was required that only PDH standard cross sections be used in this study, and that reinforcement, concrete curing, and handling be provided according to current fabrication specifications. Because the Fritz Laboratory facilities were not adequate to meet these requirements, it was decided that the beam tests would be conducted at the Schuylkill Products Company plant in Cressona, Pennsylvania. This firm has for some time been employed in the fabrication of Pennsylvania highway bridge beams.

2.2 LIMITATIONS

The most severe limitations in this investigation are the necessity to rely almost entirely on experimental strain determination, and the difficulty of minimizing experimental error.

In order for a mathematical stress analysis to be attainable for this investigation, the elastic and inelastic behavior of beam materials, the applied loads, and the deformational restraints would have to be accurately known for all points in the ends of a test beam throughout the time required for its fabrication[5]. However, because of the inability to account for inelastic deformations, and the lack of knowledge concerning boundary conditions and applicable stress functions, an analytical solution is not feasible. The fact that temperature and material properties vary with time and also from point to point throughout the

ends of beams, only emphasizes the impracticability of a mathematical solution. Consequently the investigation is limited to an experimental study without the advantage of an analytical check on the resulting data.

In addition, it is unusually difficult to limit experimental errors in this investigation because: (1) variations in concrete temperature alter strain readings; (2) variations of concrete elastic properties during curing change the significance of strain readings, and; (3) dampness, ambient temperature fluctuations, and other factors at the test site cause changes in instrumentation which in turn induce unaccountable errors in strain readings.

3. DEVELOPMENT OF AN INTERNAL STRAIN MEASURING DEVICE

3.1 REQUIREMENTS

It was decided that the most plausible internal strain measuring procedure would be to embed electrical devices of some kind in the concrete near the ends of the beams to be tested. This presented the problem of developing a suitable strain measuring device for that purpose.

Ideally, such a device would: (1) be sufficient dimensionally to bond with, and account for the heterogeneity of the surrounding concrete; (2) accurately indicate small and large strains in at least two known directions; (3) exhibit material properties which are identical with those of the concrete matrix, and; (4) indicate only strains which are associated with stress.

The first three of these criteria are self-explanatory; however, the last one requires some explanation. It was stated earlier that a concrete stress determination was necessary in order to accurately describe the conditions associated with beam cracking. However, stresses cannot be determined from an experimental strain analysis unless the internal and external restraints to beam deformation are known, or unless the effects of restraint (and the absence of it) can be compensated for in the measurement of strains. In explanation, we know that strains may exist in beams as the result of free expansion which involves no stress; and, conversely, restraint stresses may be induced because the material is not allowed to strain. Therefore, without knowing the deformational

restraints which would occur in test beams, it is necessary that the internal strain measuring device used in the investigation compensates for these effects, and gives only strain indications which reflect the concrete stresses actually occurring.

Since a primary cause of restraint stresses and unrestrained deformations in steam cured beams is change in temperature, these effects are discussed more thoroughly in Section 3.2.3. There it will be shown that temperature induced stresses and deformations may be at least partially accounted for experimentally.

3.2 THE STRAINOMETER

3.2.1 Description

In an attempt to contrive a strain measuring device to fulfill the requirements outlined in Section 3.1, a "strainometer" was developed, which consists of a temperature compensating metallic foil gage bonded to a slender piece of mild steel. Figure 2 gives a description of this device, and shows the wiring used in connecting strainometers to switching units. The wiring employed to connect switching units to strain indicators is also shown in the figure.

The ends of the steel piece used in making the strainometer are seen in Fig. 2 to be larger than the mid-section, and holes are drilled to afford better mechanical bond with surrounding concrete. With negligible concrete bond over the waterproofed mid-section, the strainometer has a gage length somewhat less than its total length.

In the early stages of its development, the proposed application of the strainometer was discussed with a representative of the manufacturer whose strain gage was to be used on the device. In this discussion the methods were prescribed for attaching the gage to the steel piece, wiring the gage, and waterproofing the gaged area.

The strain gage used is a Tatnall Metalfilm gage, type C6-141-B, manufactured by the Budd Company. This temperature compensating gage is bonded to one side of the steel piece by using Eastman 910 contact cement manufactured by the Eastman Kodak Company. The wire used to connect strainometers with switching units is a stranded three conductor, plastic insulated, No. 30 wire manufactured by the Alpha Wire Corporation.

Following the fabrication stage shown in Fig. 2, the wires are secured to the steel piece with heavy thread, and the device is waterproofed before it is ready for use. The waterproofing method employed is a two-step process. The gaged area is first painted with a heavy coat of Gagekote No. 1, which is a fast drying light duty waterproofing agent. Following this a thick coat of Gagekote No. 5 is applied. This material is a highly resilient two-component epoxy compound which hardens at room temperature to a pliable protective covering after twenty-four hours. Both Gagekote No. 1 and Gagekote No. 5 are distributed by Wm. T. Beam, Detroit, Michigan.

This procedure for waterproofing the strainometers used in the second beam test differed slightly from the process used for the first test, in that the Gagekote No. 5 was applied to all surfaces of the mid-section of the steel piece. On the earlier strainometers the material

was applied only on the side to which the gage and connecting strip were attached. Even though preliminary tests were made which seemingly proved the waterproofing method used on the strainometers for the first beam test to be satisfactory, the change in procedure was prompted by what appeared to be failure of the waterproofing in that test (see Section 4.4). To insure against repetition of this failure in the second beam test, the strainometers waterproofed by the new procedure were subjected to a more rigid test than those used earlier. Twenty of the devices were immersed in water for eight days while gage readings were periodically taken. It is significant that no changes in gage readings greater than give microstrain were recorded for any of the strainometers over the entire period of immersion.

Steel was chosen to form the body of the strainometer because it is chemically non-reactive with concrete, and because it exhibits thermal properties which are similar to those of hardened concrete. In turn, the foil strain gage employed was selected because of its alleged ability to compensate for errors caused by minor temperature variations in steel. Other reasons for choosing the foil-type gage were its compactness, and its relatively high sensitivity to small strains.

The use of temperature compensating strain gages permits elimination of a "dummy" gage, but presents the problem of eliminating errors due to the effect of temperature upon the lead wires connecting the gage to the measuring circuit. This problem is simply solved, however, by using the "three wire" connection shown in Fig. 2. With this connecting method, all of the lead wires can be subjected to wide resistance variation

due to temperature and still produce negligible error in the strain gage readings[6].

3.2.2 Effect of Material Differences on Strain Indications

An obvious variance between the ideal strain measuring device outlined in Section 3.1 and the device described above is that the steel strainometer and concrete exhibit different load-deformation characteristics, and that these material property differences change as the beam concrete gains strength. Because of these differences, indicated strain will not accurately represent strains occurring in beams in which strainometers are embedded.

These effects from material property differences can be alleviated to some extent if, instead of steel, an epoxy resin is used for the strainometer body which has elastic and thermal properties similar to those of concrete. The strain gage can then be encapsulated in this material instead of being attached to an outer surface, which helps to eliminate the problems of gage bonding and waterproofing. Such devices have been shown to be successful in measuring concrete strains[7] and large strains in plastics[8], and their application in this investigation was considered. It was decided, however, that the cost and time required in the development of such a device were prohibitive.

In order to determine the indicated strain errors caused by the difference in a steel strainometer, and its surrounding concrete, two compressive tests and a beam test were conducted on concrete specimens in which strainometers were embedded.

The compressive tests were run using standard 6 by 12 in. concrete cylinders with one strainometer centered along the axis of each cylinder. While loading the cylinders, strain readings were taken simultaneously from the internal strainometer and from four external, equally spaced electrical strain gages. Figure 3 gives the results of compressive tests on two cylinders, A and B. The curves show internal and average external strain variation with applied stress. The internal and external curves for each cylinder are comparable, although the greater stiffness of the steel is indicated by an increasing difference between the curves with increasing stress. It is also seen that this difference is slightly larger in the weaker cylinder for any applied stress.

In order to measure the reinforcing effect of the strainometer, three additional cylinders were cast at the same time as, and tested with cylinder B. These additional cylinders were without embedded strainometers, and the average stress-strain relationship determined from their loading is shown as a dashed line in Fig. 3. The proximity of the dashed line and the externally determined curve for cylinder B indicates that steel restraint to cylinder deformation was negligible, and that, therefore, the strain difference between the internal and external curves for each cylinder closely approximates the error in compressive strains caused by the material property differences. The initial tangent elastic moduli of cylinders A and B are also given in Fig. 3.

A test was also made wherein two strainometers were embedded in the lower flange of a pretensioned I-beam which was subsequently loaded to failure as part of another investigation being conducted in the Fritz Laboratory (see Ref. 9, Beam F-19). In this test, strainometer readings

were taken prior to beam loading and after each successive load increase until flexural cracking became excessive.

Figure 4 shows the location of the strainometers in the test beam. It also describes the loading arrangement used, and gives a theoretical stress-strain curve along with the corresponding experimental curve resulting from the test. These curves are averages of the calculated and experimental variations in stress and strain at the two strainometer locations. It should be noted that, because of inelastic deformation, the actual strain history of the beam concrete is not known, and that, therefore, the strain values in Fig. 4 represent only the strains required to afford intersection of the two curves at zero calculated average stress in the concrete.

By comparing the curves of Figs. 3 and 4, it is seen that the differences in theoretical and experimental strains at any level of compressive stress in Fig. 4 are quite similar to the differences in strain at corresponding stresses for the curves of Fig. 3. Furthermore, Fig. 4 shows that differences in strain occurring under compressive stress are comparable to those present when strainometers are subjected to similar tensile stresses. Therefore, strainometer readings involve the same magnitude of error due to elastic property differences under either tension or compression, and indicated strains are smaller than those actually occurring in either case. With this information, it is believed that approximate corrections can be applied to indicated strains occurring in hardened concrete by use of curves such as those of Fig. 3.

It should be pointed out that errors in indicated strain arising from inelastic deformations cannot be determined, and since the inelastic

deformations occurring before hardening of beam concrete and just after release of the prestress force are of similar or greater magnitude than the elastic strains, changes in strainometer readings during these times are, at best, qualitatively representative of concrete stress changes. Because of this, it is felt that the application of corrections for errors due to elastic property differences is not warranted for strains indicated before hardening of beam concrete or soon after prestress transfer. Furthermore, since concrete shrinkage is an inelastic phenomenon, strainometers cannot be expected to indicate strains which reflect stresses caused by shrinkage. Therefore changes in internal strain readings during the time in beam fabrication when shrinkage is active will not accurately represent corresponding stress changes.

3.2.3 Temperature Strains and the Effect of Temperature Change on Strain Indications

Temperature changes induce stress in a body whenever temperature deformations which would otherwise occur freely are restrained by external forces, or when the temperature distribution is such that internal restraints to deformation exist. On the other hand, if temperature distributions are constant or otherwise compatible with the free expansion tendencies of a body, and this expansion is not externally restrained, temperature changes will cause deformation without inducing stress in the body[5,10]. These two phenomena of restraint stress and unrestrained deformation were discussed earlier, and it was stated that when these effects are caused by temperature, they may be accounted for experimentally. This is accomplished by employing compensating strain measuring devices in the investigation.

By definition, an ideally temperature compensating strain measuring device having the same thermal expansion properties as the body being investigated, will indicate "apparent" strains which, when altered by the elastic properties of the body, yield actual stresses occurring in the body, whether or not the indicated strains are real. In explanation, assume that such an ideal device were embedded longitudinally at some point near midspan of a cantilever beam, and that the temperature of the beam had just been raised an equal amount throughout. Every part of the beam has elongated without inducing stress. The embedded device was deformed also, but no strain is indicated since there is no associated stress.

Suppose now that the free end of the cantilever is rigidly fixed in the same way as the other end, and that a uniform temperature increase is applied throughout the beam. No longitudinal strain will occur, however, every part of the beam including the embedded device will suffer a longitudinal stress induced by the temperature increase and added restraint. Although the device will not deform, it will indicate an apparent strain which then multiplied by the modulus of elasticity of the beam material will give the stress in the beam. Such an ideally temperature compensating device, then, would include in an experimental study the temperature stresses caused by restraint, and eliminate the harmless temperature induced strains not associated with stress.

However, as mentioned earlier, this would only be true if the thermal deformation properties of the device were identical to those of the concrete matrix. The value of the thermal coefficient of expansion for concrete increases during curing, and reaches a maximum which depends

primarily on the cement factor of the concrete mix and on the type of aggregates used. The rich concrete mixes used in prestressed bridge members in Pennsylvania would tend to produce higher values for the thermal coefficient of expansion[11]; however, if crushed limestone is used for the coarse aggregate in the concrete, the thermal coefficient may range from four to seven microstrain per F, depending on the thermal properties of the stone[12]. Since limestone was to be used in the concrete for both beam tests, even if the strain gages attached to the strainometers were ideally compensated for the steel, the difference in thermal properties would cause indicated strain errors before concrete hardening and possibly in the cured concrete.

Unfortunately no electrical strain gage is ideally temperature compensating. The nearest approach to this is exhibited by the "universally compensating" gage[6,13], which includes in its design a platinum temperature sensing element. With the use of an external calibration circuit, the characteristics of this gage can be adjusted so that temperature compensation is attained for a variety of materials over a wide temperature range. The extensive additional instrumentation needed, however, along with the higher cost (approx. $17/gage) make the application of this gage unfeasible in research in which a large number of devices would be required.

The strain gage chosen for this investigation is of a type in which the temperature coefficient of resistance of the gage alloy has been adjusted to minimize temperature strain errors for a particular material. When this "selected melt"[6] gage is bonded to an unrestrained specimen of

the material for which it is compensated, and the specimen is heated or cooled a few degrees above or below room temperature, only small strains are indicated by the gage.

A plot of these indicated strains as a function of change in temperature of the unrestrained specimen is called a temperature compensation curve. A curve of this type is supplied by strain gage manufacturers in each package of gages to indicate to the user the temperature strain error to be expected in gage application. It was originally anticipated that strainometer readings could be corrected for these errors by determining the temperature of the surrounding concrete and utilizing the temperature compensation curves supplied with the strain gages used to fabricate the strainometers.

Just prior to the first beam test the temperature compensation of the strainometers to be used was checked by placing a number of the devices in a laboratory oven and noting indicated strain at temperatures up to the maximum expected test beam temperature. It was found that none of the resulting temperature compensation curves was comparable to the one supplied by the gage manufacturer. Also, except for general shape, most of the curves were not comparable with one another. Figure 5 shows a representative group of strainometer temperature compensation curves accompanied by a plot of the corresponding curve supplied by the gage manufacturer.

It was found, however, that upon subjecting the strainometers to a second temperature cycle the curves of the first cycle were reproduced with reasonable accuracy; and that the results of additional cycles showed even closer agreement with the curves obtained from the second temperature cycle.

With this information, it was decided to determine, in the same manner, temperature compensation curves for each of the strainometers to be used in beam tests. These curves would then be applied in correcting indicated strain errors caused by changes in temperature. The curves resulting from the second temperature cycle would be used for this purpose. The assumption was made that deviation of strainometer temperature compensation curves from the gage manufacturer's curve caused no additional error in indicated strain.

The reason for the dissimilarity of the curves of Fig. 5 has never been determined, although considerable time has been spent on the problem. At first the fault was thought to be in strainometer fabrication technique, and the gage manufacturer was consulted with this in mind. Although suggestions were made which subsequently changed slightly the fabrication of strainometers used in the second beam test, the temperature compensation curves for strainometers used in both beam tests were quite similar. Furthermore, temperature compensation curves resulting from tests on a few strainometers fabricated by the gage manufacturer deviated from the curve supplied with the gages in the same way as did the curves for the strainometers used in the beam tests.

It was also suggested that the steel used in the strainometers may not have the thermal properties for which the strain gage was designed. However, results of tests run on three samples of the strainometer steel by the Department of Metallurgy of Lehigh University showed the average thermal coefficient of expansion, α_s, of the material to be 6.1 microstrain per Fahrenheit degree. The strain gage used is compensated for a material

thermal coefficient of 6.0 microstrain per Fahrenheit degree. This difference is not sufficient to explain the deviation of the curves.

3.2.4 Summary of Strainometer Qualifications

From consideration of the information given in Sections 2.3.1 through 3.2.3, an outline can be given of what can and cannot be expected from the use of the strainometers in this investigation.

First because of the differences in material properties occurring particularly in the early part of the concrete curing period, internal strain indications will not accurately reflect concrete stresses present during that time. Also, stresses caused by concrete shrinkage, and by the inelastic deformations occurring after prestress transfer will not be accurately represented by strainometer readings.

On the other hand, since the stresses occurring early in beam fabrication are probably small and are caused primarily by temperature changes, and since corrections can be applied which reduce the errors in indicated strains induced by temperature effects, it can be expected that strainometer data taken during the curing of beams will bt at least qualitatively correct. Also, by applying corrections to reduce the indicated strain errors caused by the material property differences between steel strainometers and hardened concrete, the stresses resulting from prestress release may be closely approximated from strainometer data.

4. THE FIRST BEAM TEST

4.1 GENERAL INFORMATION

The first beam test was conducted during the twenty-five day period from October 23 through November 16, 1962. A special box-shaped beam was used in the test which was four feet wide, three feet deep and sixteen feet long. This beam was located nearest the tensioning end of a bed containing a total of five beams. The other four were skewed highway bridge beams (PDH project P-5047) having the same cross section and strand pattern as the test beam. The test beam, however, was not skewed. The beams were pretensioned with 46, 7/16 in. diameter Roebling strands for which the allowable working load was 18.9 kips per strand. The test beam was positioned near the tensioning end of the prestressing bed so that the beam would be immediately affected by prestress release. The entire bed of beams was cast on October 24 with the test beam concrete placed last.

Figure 6 gives a description of the first test beam including a table of properties for the sections at which most of the internal instrumentation was located. The left end of the test beam as it is shown in Fig. 6 was nearest the tensioning end of the bed. As is seen in the figure, the left end of the beam was plain while the right end was provided with a paving notch. This use of two different beam end configurations was specified to determine what effects a paving notch might have in altering end strain distributions. Although not shown in Fig. 6, the deformed bar reinforcement used in the test beam was chosen to fulfill PDH specifications (see reference 14, S-3904), and except for the difference

required by the skewed ends, was similar to the reinforcement provided for the bridge beams that were cast in the same bed.

The decision to use a separate test beam instead of a full length highway bridge beam was made because of the infrequency of highway beams having a ninety-degree skew, and possessing both plain and notched ends. A non-skewed beam was considered desirable so that a more uniform strain distribution would be provided which in turn would afford a check on experimental strain data by taking readings at corresponding points on opposite sides of the beam.

Since the investigation pertains primarily to beam end regions, the decision was made to use a short test beam which was to be, in effect, two ends separated by a sufficient length of mid-section to dissipate the end effects caused by prestress transfer. It was felt, considering the cross section that was to be used for the test beam, that a minimum total length for this purpose should be twelve to fourteen feet. However, the shortest available length of prefabricated void material was twelve feet, hence, a sixteen foot beam was used.

The cross section and strand pattern used for the first test beam were determined by the choice of the highway bridge beams with which the test beam was to be cast. Using two criteria, the choice was made from the beams listed on a casting schedule provided by the fabricator. The criteria for selection were the magnitude of the stresses which would be induced by the prestress force, and the total length of beams to be cast in the bed containing the test beam.

It was considered desirable to use a test beam in which the stresses caused by prestress release would be relatively large. This

would afford the more critical conditions needed for studying the adverse effects of prestress transfer, and would provide a chance for better correlation between internal and external strain readings taken before and after prestress release. By PDH specification (reference 14, S-3904), the maximum temporary concrete stresses which are allowed just after prestress release are 0.60 f'_{ci} compression in the bottom, and 0.12 f'_{ci} tension in the top fibers of beams when unprestressed reinforcement is included to resist the total tensile force. Theoretically, the maximum corresponding fiber stresses caused by prestress transfer in the test beam used would be, without considering elastic losses and beam weight, 600 psi tension and 2850 psi compression. Since a minimum concrete strength of 5000 psi was required before allowing prestress transfer to the beams cast with the first test beam (S-3904), these stresses represent, respectively, 12 and 57 percent of the required concrete strength, which closely approximate the maximum allowable stress values.

It had been observed that longitudinal shrinkage occurring in pretensioned beams fabricated in the Fritz Laboratory caused an increase in the tensioning force during the curing period[15]. It was hoped that shrinkage or the combined effects of temperature and shrinkage, could be similarly detected in this investigation by an increase in the tensioning force upon cessation of steam curing. It was felt that in order to maximize this effect, a large total length of beams should be used which, in turn, would provide a greater total longitudinal shrinkage. The span of each of the bridge beams cast with the first test beam was 65'-9" making the total length of concrete cast approximately 280 feet.

4.2 INSTRUMENTATION

Instrumentation for the first beam test included six electrical dynamometers (load cells) for measurement of prestressing strand forces, 59 strainometers, 24 thermocouples, and 157 Whittemore gage points cast into the sides of the beam.

The dynamometers used in the test were constructed of approximately six inch lengths of steel pipe on each of which four electrical strain gages were attached in such a way that temperature strain errors were eliminated, and only axial deformations of the devices were measured. The dynamometers were placed on six of the strands just prior to attaching the strand anchors at the tensioning end of the prestressing bed. The strands thus instrumented in the first beam test are shown circled in Fig. 6; and, although pertinent particularly to the second beam test, Fig. 14 shows the manner in which dynamometers were used in both beam tests.

The force indicated for the six instrumented strands was used as representative of the total prestress force of all 46 strands and its variation throughout beam fabrication. Since the dynamometers were not used to establish the initial tensioning force, a means was thus provided for checking the method used by the beam fabricator for measuring this force.

Figure 7 shows the location of the strainometers and thermocouples in the first test beam. As shown in this figure, the greatest number of the strainometers were placed longitudinally near the beam surfaces in Sections I through VI, while six of the devices were placed either vertically or transversely near the left end face of the beam. The location of beam Sections I through VI is given in Fig. 6.

As shown in Fig. 7 the greatest number of strainometers were placed in the near side of the test beam and only a few were located on the far side of the beam to provide a check on corresponding strain readings taken from the near side.

As seen in Fig. 6, Sections I and VI lay entirely in the end blocks of the test beam, while sections III and IV were located sufficiently distant from the beam ends such that an analytical check on the measured strain in these sections caused by prestress release could be made. This, it was hoped, would give some indication of the accuracy of all the strainometer readings. Section II and V were located at the transitions between the end blocks and the midsection of the beam.

Concrete temperature measurement was required throughout beam fabrication in order to provide a means for correcting temperature induced errors in indicated strains, and to determine the change of temperature with time near the beam ends during the curing period. The temperature measuring instrumentation, consisting of thermocouples and an automatically recording twenty-four channel thermo-electric pyrometer, was installed and operated throughout the test by PDH Laboratory personnel. Because of the limited number of thermocouples which could be used with the pyrometer, it was not possible to measure temperature near all of the strainometers. With the assumption, however, that the temperature changes with time would be more or less symmetrical about the vertical centerline of any beam cross section, it was felt that the temperature at most of the strainometer locations could be sufficiently approximated.

As shown in Fig. 7, 22 thermocouples were embedded in the beam concrete. The other two, not shown in the figure, were used outside of

the beam; one to measure ambient temperature, and the other to measure the temperature of the steam near the top surface of the beam. Note that even with the above mentioned assumption of temperature symmetry, the temperature of strainometers in Sections IV and VI, and in the left end face of the beam, cannot be approximated. Without the ability to correct temperature induced errors, the strain data taken from these strainometers were expected to be valuable only in determining stresses caused by pre-stress transfer.

In order to provide a check on strainometer readings at release, and to permit continued external strain readings to be taken over a period of time, extensive Whittemore instrumentation was included in the first beam test. The location of the Whittemore targets on the test beam is shown in Fig. 8. In general, the targets were spaced at 5 in. intervals horizontally and vertically, making it possible to use a five inch and a ten inch Whittemore gage in either direction.

Because of the short length of time allowed between form removal and prestress release, and because of the dampness of the concrete surfaces during this time, it was not considered feasible to attach Whittemore targets to the test beam surfaces. Instead, a special type of Whittemore target was developed for the investigation which required embedment of 3/4 in. long cadmium plated steel inserts in the beam concrete. Figure 9 shows two stages in the installation of the target. The internally threaded inserts were first secured to the concrete forms by means of small screws, as seen in Fig. 9a. After beam casting but before form removal, these screws were taken out; and immediately after form removal, flat-headed brass screws in which Whittemore points had been drilled were inserted in

the embedded inserts. A completed target installation is shown in Fig. 9b. The steel inserts for the Whittemore instrumentation of the first test beam were attached to the beam forms on October 22.

4.3 DESCRIPTION OF THE TEST

Table 1 gives a chronological record of the more important phases of the first beam test from the time of strand tensioning to the final Whittemore readings.

The prestressing strands for the first beam test were tensioned on the night of October 23. The process of strand tensioning involves moving the tensioning head at the live end of the prestressing bed by means of four hydraulic jacks. The force applied to the strands is determined indirectly by noting the distance through which the tensioning head travels. When the prescribed strand elongation is reached the head is stopped, and the hydraulic tensioning jacks are replaced with four mechanical holding jacks. This substitution is made so that the hydraulic jacks are available for use elsewhere in the plant. Release of the prestress force after the curing period is accomplished by reversing the tensioning process.

With strand tensioning completed, the strainometers and thermocouples were installed within the beam forms on the morning of the day of casting. Strainometers to be placed in the top, bottom, and left end face of the test beam were installed individually by wiring them to 1/8" diameter steel rods, after these had been attached to deformed bar re-

inforcement or strands. The strainometers to be placed along the sides of the beam, however, were first wired to frames made from the 1/8" diameter rod, which in turn were positioned within the forms, and attached to the adjacent deformed bars.

Prior to placing concrete in the test beam forms, dynamometer and initial strainometer readings were taken, and the temperature recording equipment was checked and put into operation. The test beam was then cast. The concrete mix used for both beam tests is presented in Appendix I along with data on the gradation of the concrete aggregates. Unfortunately, during concrete placement seven of the 39 strainometers in the left end of the test beam were contacted by vibrators and rendered inoperative.

After the first test beam was cast, strainometer and dynamometer readings were taken at two to three hour intervals for the first 12 hours, and then at slightly longer intervals until after prestress transfer. The concrete temperature at each thermocouple point was recorded every 12 minutes until 8:30 PM on October 26 when the pryometer was turned off for the weekend. Temperature measurement was started again at 11:45 AM on October 29 and was finally discontinued at 9:30 AM on October 31.

Throughout the test the ambient temperature ranged from approximately 40 to 60F. Because of these relatively low temperatures the water vapor resulting from steam curing filled the area in the vicinity of the beams with fog.

Transfer of the prestress force was achieved by gradually decreasing the hydraulic pressure in the tensioning jacks, and release was terminated by cutting the strands with an acetylene torch, first at the tensioning end of the bed and then between each of the beams.

Whittemore readings were taken prior to and immediately after prestress release using both a five inch and a ten inch gage horizontally and vertically. Vertical strains caused by release however, were too small to be indicated by either device, and further vertical readings were not taken. Although successful tests were made in the Fritz Laboratory on Whittemore targets such as those used in the first beam test, many of the steel inserts embedded in the test beam were found to be loose upon removal of the forms. As a result, much of the Whittemore data are unreliable.

The concrete strength in the first test beam was checked periodically by testing concrete cylinders which had been cast and cured with the test beam. The test cylinders were made using metal molds provided by the beam fabricator. Listed in Table 2 are average values of initial tangent elastic moduli and ultimate strength for four groups of three cylinders. The stress-strain curves resulting from these cylinder tests and others made in the second beam test are given in Appendix II. These tests were made using the cylinder testing machine at the Schuylkill Products Company plant.

The last strainometer readings were taken on October 29, after which the strainometer instrumentation was disconnected. The test beam was then removed from the prestressing bed and placed on blocks. The final Whittemore readings were taken on November 16, 1962.

4.4 RESULTS AND CONCLUSIONS - FIRST BEAM TEST

Results from the dynamometer instrumentation are presented in Table 3 and in Fig. 10. The table gives the strand force values deter-

mined for the six instrumented strands, and also the average of these values at various times during the test. The maximum, minimum, and average strand forces are presented graphically in Fig. 10 along with another curve describing the variation of concrete temperature at the level of the prestressing strands during the test. The circled numbers appearing in Fig. 10 refer to phases of the first beam test which are similarly denoted in Table 1.

The slight change in prestress force occurring up to the time of casting the first test beam, as seen in Fig. 10, was apparently caused by jack substitution, strand relaxation, and the gradual increase in temperature along the prestressing bed due to hydration in the concrete placed for the highway bridge beams. The considerable prestress changes occurring after completion of beam casting, however, were no doubt caused by temperature changes brought about by increasing cement hydration, steam curing, and subsequent cooling. The dependence of the prestress force upon strand temperature during the curing period is definitely seen by comparing the curves of Fig. 10.

However, just prior to prestress release the strand force increased at a much higher rate than the corresponding rate of decrease in strand temperature, as seen in Fig. 10. Also, at the same time vertical cracks were observed at intervals of eight to ten feet in the sides of the bridge beams occupying the remainder of the prestressing bed. Since the increase in strand force and the beam cracking occurred after cessation of steam curing and during the time when forms were being removed, it is probable that these effects were caused by a combination of concrete shrinkage and cooling of the uncovered beam surfaces. The presence of

significant concrete shrinkage in the beams was almost assured by the length of the time interval between form removal and prestress release, as seen in Table 1, and by the fact that no attempt was made to keep the beam surfaces moist during this time. In addition, the approximately 20F difference between beam surface temperatures and the temperature of the surrounding air may have caused significant surface tensile stresses when forms were removed.

It should be noted that although the prestress information given in Table 3 and in Fig. 10 reflects, more or less, the average of variations occurring over the entire length of the prestressing bed, the temperature information with which it is compared was taken from a relatively short length of the bed and is probably not as representative as the prestress data.

The bridge beam cracks were no longer visible after release of the prestress force, and no cracking was observed in the test beam. The average prestress force per strand transferred to the beams, as seen in Table 3, was 19.5 kips, which exceeds the prescribed 18.9 kip force by 3.2 percent based on the latter value.

Some of the results from internal strain readings taken prior to and just after release of prestress are given in Figs. 11a and 11b. In these figures, the variation with time of temperature and apparent strain is shown for vertical Sections I and II. The numbers used to denote the various temperature distributions in Fig. 11 also indicate the time elapsed in hours since completion of test beam casting. The strain values in Fig. 11 were determined from strainometer readings

which have been corrected for temperature induced errors, and for errors at prestress release caused by material differences.

Results from other sections of the beam are not included in Fig. 11 partly because insufficient temperature data and inoperative strainometers did now allow their determination. In addition, even though strain readings were taken from most of the devices during the test, it became apparent upon reduction of these data that many of the strainometers were not operating well enough to yield strain information of any value.

The defective strainometer operation may have been brought about by a number of possible causes, among which are the adverse atmospheric conditions at the plant during beam fabrication, and the possibility of faulty strainometer fabrication technique. However, during subsequent conferences with representatives of the Budd Co. concerning this problem, it was discovered that a primary cause of the trouble lay in the waterproofing method which had been used. Consequently, a more satisfactory waterproofing process was devised which, along with some minor changes in fabrication technique, was employed in making the strainometers used in the second beam test. The waterproofing methods used for the strainometers for both beam tests were outlined in Section 3.2.1.

As seen in Fig. 11, the points denoting strain values are connected by straight lines, whereas the temperature distributions are presented as curves. As will be shown more conclusively in the results of the second beam test (Section 5.4), temperature data given by the equipment used in this investigation are of sufficient accuracy to warrant representation as smooth curves. On the other hand, the strain distributions, parti-

cularly those from the first beam test, caused by effects other than pre-stress release are not regular enough to suggest fitting them with smooth curves. The temperature curves in Fig. 11 are second degree parabolas determined by the Sterling interpolation method[16]. The open circles denote points determined directly from the temperature readings, and the points enclosed with squares are interpolated values.

Little can be derived from the strain distributions of Fig. 11 which could be considered conclusive. Although, as stated earlier, the concrete stresses occurring during the curing period of beam fabrication are most likely caused by temperature effects, the changes with time of the apparent strain distributions of Fig. 11 do not, in general, follow the corresponding temperature changes in either section. Also, the only comparisons which can be readily made between the strain distributions in Section I and those in Section II are that they shift longitudinally in generally the same manner with time, and that they are similar in shape near the upper surface of the beam. Additionally, it can be seen that many of the strain distributions of Fig. 11 exhibit only compressive values, which, assuming these results are qualitatively correct, is possible only if predominantly tensile stresses existed farther inward from the surfaces of the beam. Since however, strainometers were not placed in the interior of the end regions, it is not known if tension occurred there.

These results suggested not only that strainometer operation had to be improved before a second beam test could be made, but that in order to check the occurrence of predominantly compressive strains near the sur-

faces of the first test beam, at least one beam section in the second test should be thoroughly instrumented over the entire cross section instead of near the beam surfaces only. Also, for strainometers to be used more effectively, it would be necessary to locate thermocouples so that the temperatures near all of the devices could be accurately determined.

It is seen from the temperature distribution curve of Fig. 11 that upon application of steam curing the upper part of the first test beam received most of the applied heat, and that the subsequent temperature rise was much more rapid there than nearer the bottom of the beam. This difference in temperature dissipated with time; however, more or less constant temperatures were not attained in either beam section until a few hours before prestress release (the elapsed time at release was approx. 45 hours). This means that concrete near the bottom of the beam received less of the effect of steam curing, and received it later than concrete nearer the beam's upper surface. It has been shown[17,18] that both the maximum temperature to which the concrete is subjected during steam curing, and the time lapse between concrete placement and the application of steam curing significantly influence the resulting strength of the concrete. It is doubtful, because of this, that concrete strength properties throughout the test beam were uniform at transfer of prestress.

The results of the internal and external strain readings taken just before and shortly after release of prestress are indicated in Figs. 12a through 12d. These figures show stresses determined from the strains given by strainometers and Whittemore gage readings at various levels in Section I through VI of the first test beam. Theoretical stress distributions are also included in those figures which pertain to the beam sections

for which such analyses are possible.

In addition to the information given in Fig. 12, all of the strains (except vertical strains) determined from readings of the five and ten inch Whittemore gages in the first beam test are presented in Tables 4 and 5 respectively. The stresses shown in Fig. 12 were determined from the Whittemore strain values in Tables 4 and 5 by use of the concrete elastic modulus at release (see Table 2). The strainometer values were obtained similarly, except that corrections had to be made at higher strain levels for the elastic dissimilarity of the materials. However, no temperature corrections were required for the strainometer readings involved since the temperature change occurring over the time of prestress release was negligible.

Figure 12a shows the experimentally determined stresses and the theoretical stress distribution for the equivalent Sections III and IV. As noted before these are the only internally instrumented sections to which an analytical stress determination at release could be applied directly. The theoretical distributions in Fig. 12 include the effects of elastic prestress loss. As seen in this figure, the agreement between experimental and theoretical values is good except at the level near the bottom fiber. The small discrepancies noted in the Whittemore values above the neutral axis should be disregarded since the precisions of the instruments used are of comparable magnitude to the prestress transfer strains present in that part of the beam surface. The capital letters denoting the various levels of each section in Fig. 12 are identified in Fig. 8.

Figure 12b gives similar information for the equivalent Sections II and V; although, in this case, a flexural analysis cannot be applied directly

as a check because of the sudden change in cross section and the unknown prestress transfer length. Assuming, however, that the entire prestress force is applied at this section, the actual stress distribution would have to lie somewhere between the bounding theoretical distributions determined from the properties of the sections immediately adjoining Sections II and V. These stress bounds are shown in the figure, and the majority of the experimental points can be seen to fall within them. Figures 12c and 12d show the experimental stress values for beam Sections I and VI respectively. The positions of the points in these figures describe, in general, typical longitudinal stress distributions near the ends of a pretensioned beam[19].

It can be seen that the Whittemore instrumentation used in the first beam test was successful to some extent in checking the operation of strainometers at release. A determination of strainometer accuracy having thus been made, it was felt that further use of this instrumentation would be of little value. Therefore, it was decided not to include Whittemore instrumentation in the second beam test.

5. THE SECOND BEAM TEST

5.1 GENERAL INFORMATION

The second beam test was conducted over the four day period from August 15 to August 19, 1963. The test beam used was a non-skewed, full size highway bridge beam (PDH Project P-5357) with a length of 57'-2". The beam had the same four feet by three feet cross section as the first test beam; however, 34, 7/16 in. diameter high strength (Roebling 270k) strands were included in its construction as compared to the 46 lower strength strands used in the earlier test. Each of the high strength strands had a larger steel area (0.115 sq. in.) and allowed a higher working load (21.7 kips) than the strands used earlier.

Figure 13 gives a description of the second test beam, including a table of properties for the internally instrumented Sections I and II, and for a typical section through the middle part of the beam span. Note that all of the numerical values for section properties given are the same as those shown for corresponding sections of the first test beam in Fig. 6. As in the first test, the second test beam was cast after the other beams in the bed, and it was located nearest the tensioning end of the same pre-stressing bed that was used for the first beam test. The left end of the beam as it is shown in Fig. 13 was nearest the tensioning end of the bed. Including the test beam, four identical beams were cast in the bed, making a total length of concrete cast approximately 229 ft.

The beam used in the second beam test was selected primarily because of the similarity of its cross section to that of the first test

beam, and because, like the first beam, it was not skewed. It was felt that these similarities would provide a better chance for comparison of the results of strain and temperature data taken prior to prestress release in each beam test. Since, however, the design prestress force was smaller in the second beam, the stress distributions caused by prestress release in each beam test would not be directly comparable.

5.2 INSTRUMENTATION

After completion of the first test, six additional dynamometers became available so that 12 of the devices were used to measure prestressing strand forces in the second beam test. Also, 60 instead of 59 strainometers were used in the second test, and the 24 point temperature measuring equipment used earlier was again installed and operated by PDH Laboratory personnel during the second beam test. For reasons discussed earlier, Whittemore instrumentation was not used in this test.

The 12 strands on which dynamometers were placed are shown circled in Fig. 13. The devices were placed, as in the first beam test, symmetrically with respect to the center line of the beam cross section. In Fig. 14, the tensioning end of the prestressing bed is shown with the dynamometers installed for the second beam test.

All of the strainometers in the second test were located in the beam's left end block, and most of the devices were placed in two transverse sections while three were centered near the surface of the left end face of the beam. Figure 15a shows the strainometer location in the end face and

Section I of the second test beam, and Fig. 15b describes their location in Section II. Unlike the strainometer placement in the first test beam, most of the devices shown in Fig. 15 are spaced over one entire cross-section and several are oriented vertically and transversely as well as longitudinally in the beam.

Also shown in Fig. 15 are the locations of 21 of the 24 thermocouples employed in the test. As shown, these devices were placed so that the temperature in the vicinity of each strainometer could be determined. The three thermocouples not shown in Fig. 15 were used to measure, respectively, ambient temperature, steam curing temperature at the top surface near the left end of the test beam, and the temperature at Section II of the prestressing strand shown instrumented in Fig. 13 with dynamometer No. 12. The thermocouple was attached to this particular strand to provide data for a separate investigation being conducted by the PDH Laboratory involving the development of a strand force measuring device.

5.3 DESCRIPTION OF SECOND BEAM TEST

Table 6 gives a chronological record of the more important phases of the second beam test from the completion of strand tensioning to the final strainometer readings taken after prestress release.

Strand tensioning was completed on the afternoon of August 15, and immediately afterward the four hydraulic jacks were replaced with mechanical holding jacks. The two holding jacks for the near side of the prestressing bed may be seen at the right in Fig. 14. Unlike the first beam test, however, the effect of this exchange on the prestress force

was checked by taking dynamometer readings immediately after the jack replacement had been completed. Additional dynamometer readings were taken at short time invervals throughout the test until completion of prestress transfer.

The strainometers were installed in the second test beam by first wiring specially prepared frames to the deformed bar reinforcement, which were made of the same 1/8 in. rod material that was similarly used in the first beam test. Two of these frames were placed in each of the Sections I and II, and the strainometers to be positioned near the top and side surfaces in these sections were then wired to the frames. Additional 1/8 in. rods were then placed in Section II forming a grid to which the strainometers for the interior of that section were attached. The strainometers in the left end face of the test beam were positioned by suspending them with wire from the adjacent deformed bar reinforcement. After all of the strainometers were in position, the thermocouples were placed in the test beam.

Figure 16a shows the near side of the left end of the second test beam with the strainometers and thermocouples in place. The side forms were not positioned at the left end of the beam until after installation of the internal instrumentation was completed. This installation and the subsequent connecting of wires to external equipment was finished just prior to the first placement in the test beam. Figure 16b is a top view at the left end of the test beam prior to concrete placement.

Initial strainometer readings were taken just after test beam casting, and additional readings were taken at two to four hour intervals during the first 30 hrs., and at longer intervals from then until after

transfer of prestress. Only two strainometers failed to give readings during the test. The temperature measuring equipment, which was put into operation as soon as it was installed, was operated continuously until completion of the test.

The ambient temperatures in the second beam test were higher than those occurring in the earlier test, the variation being from 62 to 84 F. Because of these higher air temperatures relatively little vapor condensation occurred, and there was none of the fog which was present during fabrication of the first test beam. Consequently, the external electrical instrumentation remained dry throughout the second test.

As in the first beam test, the concrete strength was checked during the second test by periodically testing cylinders which were cured along with the second test beam. The cylinders were formed by using waxed paper molds instead of the metal molds used in the first test. Five groups of three cylinders were tested using the machine at the beam fabricating plant. Listed in Table 7 are average values of initial tangent elastic modulus and ultimate strength for the cylinders tested. The fact that concrete strengths shown in Table 7 are lower than the corresponding first beam test values in Table 2 may be partly attributed to the use of different types of cylinder molds in the two tests. It has recently been shown[20] that waxed paper cylinder molds can cause steam cured cylinders to exhibit significantly lower strengths than when metal molds are used. This, however, was not known at the time of casting the second test beam.

Prior to transfer of the prestress force, the beam side forms, instead of being removed, were loosened all along the bed and moved slightly

away from the beam surfaces to facilitate beam movement at release. Also the top covering tarpaulins were left in place until after release, and were moved only enough to allow loosening of the forms and inspection of beam surfaces for cracks. This is in contrast to the complete removal of beam forms and top coverings which occurred before prestress transfer in the first beam test. Prestress transfer was completed on the morning of August 19, after which the final dynamometer and strainometer readings were taken, completing the test.

5.4 RESULTS AND CONCLUSIONS

Table 8 and Fig. 17 give the results from the dynamometer instrumentation for the second beam test. This information is presented similarly to that given earlier in Table 3 and Fig. 10, respectively, for the first beam test.

The average initial tensioning force for the second test beam, as determined from the 12 instrumented strands, was approximately 22.0 kips per strand, and the maximum initial force measured was 22.5 kips as given in Table 8. The latter value represents approximately 72.5 per cent of the ultimate force for the high strength strands used.

The substitution of holding jacks for the tensioning jacks at the live end of the prestressing bed caused a slight decrease in prestress force in the instrumented strands as shown in Table 8 and Fig. 17. The average prestress loss thus occurring was approximately 100 lb per strand, which represents less than one percent of the tensioning force. Because of this, it can be assumed that jack substitution, when carefully done,

does not significantly reduce initial strand tension.

By comparing Fig. 17 with Fig. 10, it can be seen that the prestress force changed with time and strand temperature in approximately the same way during both beam tests up until the time that steam application was reduced. From that time, however, the rate of change in the prestress force did not increase in the second beam test as it did in the first. This can no doubt be attributed to the prevention of shrinkage and cooling which was afforded in the second test by leaving the forms and tarpaulins in place until after prestress release. As a result, and in contrast to the first test, concrete surface stresses in the second test beam did not become large enough to cause noticeable cracking prior to release. The prestress force transferred to the beams, as seen in Table 8, was approximately 20.8 kips per strand, which is less than the prescribed force of 21.7 kips by approximately 4.2 percent based on the latter value.

Results from the temperature data taken from the second test beam are given in Table 9 and in Figs. 18 and 19. Table 9 gives the concrete temperatures at the times when strainometer readings were taken during the test. Temperatures at thermocouple locations were determined directly; however, temperatures for the remaining points in the beam were approximated almost entirely by using the Sterling interpolation method. The interpolated values in Table 9 are in parentheses.

Figure 18 shows the temperature variation with time along vertical lines A and E of Section I, and Fig. 19 shows the corresponding temperature curves for the vertical and horizontal grid lines comprising Section II. Each temperature curve in these figures is denoted by a number which is an

approximate value of the elapsed time in hours since completion of test beam casting. More precise elapsed times are given with the corresponding temperature data in Table 9. The interpolated temperature values in Table 9 are shown enclosed by squares in Figs. 18 and 19, while the thermocouple data are denoted by circled points.

In order to determine the temperatures at the points where thermocouples were not located, temperature curves were first derived for the vertical and horizontal grid lines containing three thermocouples. In Section II, the three interpolated values in any line were then used to derive curves which were checked with the two measured temperature values in the same line. Significantly, the temperature differences occurring at like points on orthogonal curves were within 4F except at elapsed times of 2.5 and 4.5 hrs. This shows that during most of the beam curing period the temperature variation was smooth across Section II, and that the interpolation method used gave results which were probably quite accurate. The curves in Figs. 18 and 19 for the elapsed times of 2.5 and 4.5 hrs., were, in general, determined by trial using drafting curves.

Figures 18 and 19 show that the concrete temperature increased rapidly in Sections I and II during the first 8 to 12 hrs after beam casting, and that it then decreased slowly until release of the prestress force. The curves in these figures are comparable to the corresponding curves from the first beam test as shown in Fig. 11 in that the highest temperatures were reached between the top and mid-depth of the beam, and that the concrete near the bottom surface of the beam was least affected by steam curing. Figure 18 shows that the temperature near the bottom of Section I of the second test beam reached only 114F during fabrication.

Because of this, there is not only reason to believe that concrete strengths were not uniform throughout the test beam, but it is probable that the concrete strength at strand level near the left end of the beam was lower than elsewhere[17]. Since both beam tests disclosed probably inadequate curing in this region, it is reasonable to conclude that insufficient concrete tensile strengths may have been contributory to the occasional beam end face cracking described in Fig. 1.

The results from strainometer data taken throughout the second test are presented in Tables 10 and 11, and in Figs. 20 through 26. Table 10 gives apparent longitudinal strains, and Table 11 gives the apparent vertical and transverse strains occurring in the test beam. All strain values shown in these tables have been corrected for temperature induced errors, and for errors at prestress release caused by material differences. Each strainometer is signified in Tables 10 and 11 according to position and orientation in the beam. For example, strainometer A3V in Section II is located at grid coordinates A,3, and is oriented in the section to indicate vertical strains. Strainometers A5L in Section I and C1T in Section II were rendered inoperative during beam casting. Figures 20 through 24 show the apparent longitudinal and vertical strains which occurred during the test, and Figs. 25 and 26 show, respectively, the longitudinal and vertical stresses caused by prestress transfer. These stresses were determined by using the average elastic modulus of the cylinders tested just before prestress release (see Table 7).

As shown in Figs. 20a and 20b, and more definitely in Figs. 21a and 21b, the apparent longitudinal strain curves for outside vertical lines A and E are quite comparable in each beam section. In addition, except for

changes brought about by prestress transfer, these figures are comparable to one another, and also to the corresponding curves for Section I of the first test beam seen in Fig. 11a. The five sets of curves comprising these figures indicate that stresses occurring longitudinally in the side surfaces of both test beams were nearly always compressive prior to prestress release.

As discussed earlier, in order for these surface compressive stresses to be present, predominantly tensile stresses must have existed farther inward in the beams. Fig. 21c, which shows the apparent longitudinal strains for vertical line C of Section II, indicates that tensile stresses were indeed present throughout the full depth of the second test beam at the centerline of the section. In addition, the horizontal views of the longitudinal strains at Section II provided by Figs. 21d through 21g show the variation from external compressive to internal tensile strains across the section. The only longitudinal surface tensile strains indicated were near the centerline at Section II in the top and bottom fibers of the beam. The presence of tensile as well as compressive strains, and the general regularity in these strain distributions tend to confirm the validity of longitudinal strainometer data taken prior to release.

The curves of apparent vertical strain prior to release at Sections I and II shown in Figs. 22 and 23, respectively, are similar to the longitudinal strain curves in that they display more or less regular strain patterns, and that surface strains were compressive while the greatest tensile strains were near the center of the beam end block.

Figure 24 shows that, prior to release, apparent compressive strains occurred above mid depth in the end face, and tensile strains

were present nearer the bottom of the beam. Also, Table 11 shows that the transverse strains near the top surface at Section II were tensile prior to prestress transfer. These surface strains, and the longitudinal tensile surface strains prior to release in Fig. 23 are the only indications that surface tensile stress was present in the second test beam before prestress transfer. Since no longitudinal cracks have been observed in the top surfaces of beams, transverse surface tension is probably not important. On the other hand, longitudinal top surface tension and vertical tension in the lower part of beam end faces would tend to combine with effects of prestress transfer to possibly cause cracking. However, since it is not possible to determine the magnitude of the surface stresses occurring prior to prestress release, it cannot be said to what extent they influence beam cracking.

Although the relative strain distributions caused by prestress transfer are included among the curves of Figs. 20 through 24, the stresses induced by prestress release are shown in Figs. 25 and 26. Fig. 25 shows the longitudinal transfer stress distributions at beam Sections I and II, and Fig. 26 shows the corresponding vertical stress curves for the two sections and for the left end face of the beam. In Figs. 25 and 26c the points describe smooth stress distributions; therefore, they were connected by curved lines instead of straight line segments. Since no longitudinal strainometers were included at coordinates B3 and D3 in Section II, longitudinal transfer stresses are not known for these points. Therefore, the curves for vertical lines B and D in Fig. 25b are shown as dashed lines between horizontal levels 2 and 4,

and line 3 in Fig. 25c is shown dashed over the whole beam width to indicate that their locations are estimated.

Figures 25a and 25b show typical longitudinal transfer stress distributions for sections near the ends of prestressed beams except for the stress variation across the beam at Section II. As seen in Fig. 25b and more clearly in Fig. 25c, the longitudinal stress varied as much as 380 psi at line 4 across Section II. This variation cannot be readily explained; however, the smoothness of the individual distributions, and their horizontal symmetry about the longitudinal centerline of the beam as shown in Fig. 25c, tend to confirm the accuracy of the curves. The maximum longitudinal stresses in Sections I and II caused by prestress release are seen to have been 1170 psi compression in the outside bottom fibers of Section II, and 140 psi tension in the outside top fibers of the same section.

Figure 26 shows that tensile vertical stresses were caused by prestress release in the left end face and at Section I of the second test beam, and that primarily compressive stresses were induced at Section II. As in the case of the longitudinal transfer stresses, the vertical stresses were symmetrical with the vertical centerline of both Sections I and II, and two of the vertical stress distributions across Section II shown in Fig. 26c were smooth enough to allow curves to be drawn through the stress points. The dashed line was used, as before, to show an estimated distribution.

The maximum vertical transfer stresses were 150 psi tension in the end face of the beam, and 128 psi compression at Section II. Neither the vertical nor longitudinal tensile stresses were of sufficient magnitude

to alone cause concrete cracking; however, as mentioned earlier, beam cracks may be caused by a combination of effects.

If elastic prestress losses are taken into consideration, the maximum theoretical flexural stresses that could have occurred in the second test beam after prestress release are calculated to be 525 psi tension in the top fibers, and 2220 psi compression in the bottom fibers of the beam. These stresses represent, respectively, 10.7 and 45.0 percent of the ultimate concrete strength at prestress transfer given in Table 7, and are within the range of maximum stresses allowed by PDH specifications.

It is important to consider that, although maximum allowable stress requirements are met, the majority of PDH bridge beams probably experience some cracking, even if the cracks are very fine, because of excessive tensile fiber stresses induced by prestress transfer. It has been shown that the ratio of concrete strength in tension to that in compression decreases with increasing compressive strength, and that the value of this ratio is approximately 0.08 for 5000 psi concrete[21]. Also, other investigators have shown[15,17] that tensile strengths for concrete used in prestressed members are consistently lower than 9 percent of the corresponding compressive strengths. Because of this it is felt that cracks occur at release of the prestress force, the widths of which are initially determined by the amount and location of deformed bar reinforcement, and which quite possibly increase in width with time because of subsequent concrete creep.

In regard to this, it has been suggested that the maximum concrete tensile stress allowed by PDH specifications may be excessive, and

that by lowering this stress limit a probable source of beam cracking would be eliminated. In contrast to PDH requirements, the 1961 AASHO Specifications[22] require that "temporary tensile stresses before losses due to creep and shrinkage in members with nonprestressed reinforcement sufficient to resist tensile force in the concrete without cracking" shall be limited to $6\sqrt{f'_{ci}}$. If f'_{ci} is 5000 psi, this allowable tension is approximately 0.085 f'_{ci}, or about 71 percent of the corresponding PDH maximum allowable tensile stress. The difference in these stresses is significant, and the possibility that the PDH requirements are inadequate is worthy of consideration.

6. CONCLUSIONS FROM ENTIRE INVESTIGATION

The exact cause of the beam cracking problem outlined in Section 1.1 was not determined in this investigation. However, knowledge was gained which pointed to probable causes, and it is hoped, that this, along with other information obtained in the research, may be helpful in reducing beam cracking. The principal conclusions from the investigation are summarized below. In evaluating these conclusions, it should be remembered that a good deal of the information obtained from this study may be pertinent only to rectangular beams, and to only one end of the last beam in prestressing bed. Stress conditions in I-sections and at locations other than the ends of beams may be sufficiently different to make some of the results of this investigation non-representative.

1. Results from the internal strain measuring instrumentation cannot be used to determine the magnitudes of stress occurring prior to prestress release in the test beams. However, assuming that the apparent strain curves resulting from internal strain data are qualitatively correct, significant concrete tension may occur longitudinally near beam ends along the longitudinal center line of the top and bottom surfaces, and vertically in beam end faces near the vertical center line and below mid-depth.

2. Steam curing, as it was observed in this investigation, is not applied evenly over the full depth or length of beams. As a result concrete strengths probably are not uniform throughout a beam, and may be significantly lower at strand level near beam ends. Consequently, inadequate concrete strength in this region may be contributory to beam end face cracking.

3. Shrinkage or a combination of shrinkage and rapid cooling of beam surfaces can cause cracking. Although surface cracks attributable to shrinkage often disappear upon release of the prestress force, concrete inelastic action after release may cause them to re-open. This, it is felt, is a possible source of cracks observed near the top surface of beams after fabrication.

To reduce this problem, beam forms and top coverings should not, if possible, be removed after cessation of steam curing and before prestress release. If forms and top coverings must be removed, exposed beam surfaces should be kept wet and should not be allowed to cool rapidly. Prestress release should be completed as quickly as possible after termination of steam curing.

4. Cracks, even if quite fine, probably occur in the top fibers near the ends of a majority of bridge beams at release of prestress because of the large temporary tensile stress allowed in that region by PDH specifications. Because of this it is reasonable to conclude that many of the typically occurring transverse cracks in the top fibers near beam ends, as seen in Fig. 1, may originate from the effects of prestress transfer, and later become visible after widening due to the influence of concrete creep. It is felt that a review of the PDH specification concerned is worth consideration.

7. NOMENCLATURE

SYMBOL	DEFINITION
A_c	Area of concrete in a beam cross section
A_s	Area of prestressed strands in a beam cross section, or cross sectional area of a single strand
A_t	Transformed area of a beam cross section
C.G.C.	Centroid of a beam cross section determined without consideration of steel areas
C.G.S.	Centroid of prestressed strand areas in a beam cross section
E_c	Initial tangent elastic modulus of concrete
E_s	Elastic modulus of steel
e	Distance of C.G.S. from C.G.C. or N. A.
F	Fahrenheit degrees
FM	Fineness Modulus
F_i	Total initial prestress force before transfer
f_c	Compressive stress in concrete
f_t	Tensile stress in concrete
f'_{ci}	Ultimate compressive concrete stress at time of transfer
f'_s	Ultimate strength of prestressing strand
I_c	Moment of inertia of beam cross section considering concrete area only
I_t	Moment of inertia of transformed beam cross section
N.A.	Centroid of a transformed beam section
n	Modular ratio E_s/E_c
Y_b	Distance from C.G.C. or N.A. to bottom fibers of beam
Y_s	Distance from C.G.C. or N.A. to strainometer
Y_t	Distance from C.G.C. or N.A. to top fibers of beam

SYMBOL	DEFINITION
Z_b	Ratio $\frac{I_t}{Y_b}$ or $\frac{I_c}{Y_b}$
Z_t	Ratio $\frac{I_t}{Y_t}$ or $\frac{I_c}{Y_t}$
α_c	Coefficient of thermal expansion for concrete
α_s	Coefficient of thermal expansion for steel
ΔT	Change in temperature
ν_c	Poisson's ratio for concrete

8. APPENDIX I

CONCRETE MIX AND AGGREGATE GRADATION DATA

CONCRETE MIX DATA

Materials

Cement: Lonestar type "D" high early strength cement

Sand: PDH type "A" refractory sand

Coarse Agg.: PDH type "A" crushed limestone, 40-60 per cent combination of PDH types 1B and 2B, respectively

Sika Plastiment

Mix Proportions

Water - cement ratio:	0.382 by wt.
Design slump:	1-3/4 in.
Cement factor:	8.5 sacks per cu yd
Calc. unit wt.:	147 lb/cu ft with 4 per cent air

Quantities per cubic yard

Cement	799 lb
Sand (dry)	901 lb
Coarse Agg. (dry)	1896 lb
Water	305 lb
Plastiment	1.06 lb

AGGREGATE GRADATION DATA

Square Screen Analysis - Per Cent Passing

Screen Sizes	100	50	30	16	8	4	3/8	3/4	1	FM
Sand	6.5	17.9	35.7	58.6	87.8	97.6				2.96
Coarse Agg.					1.4	7.3	44.0	96.4	100	

9. APPENDIX II

CONCRETE CYLINDER STRESS-STRAIN CURVES

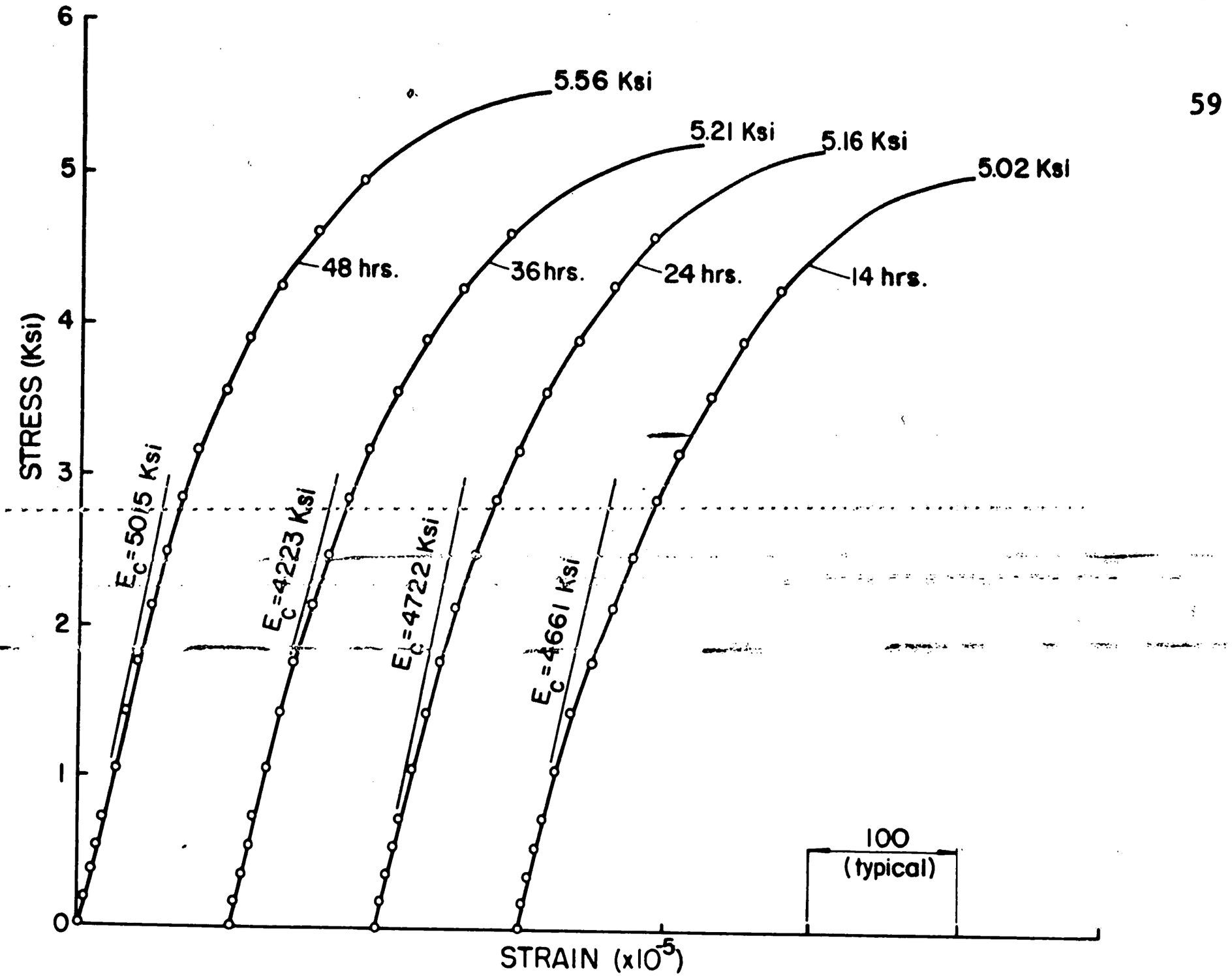

CONCRETE CYLINDER STRESS-STRAIN CURVES- FIRST BEAM TEST

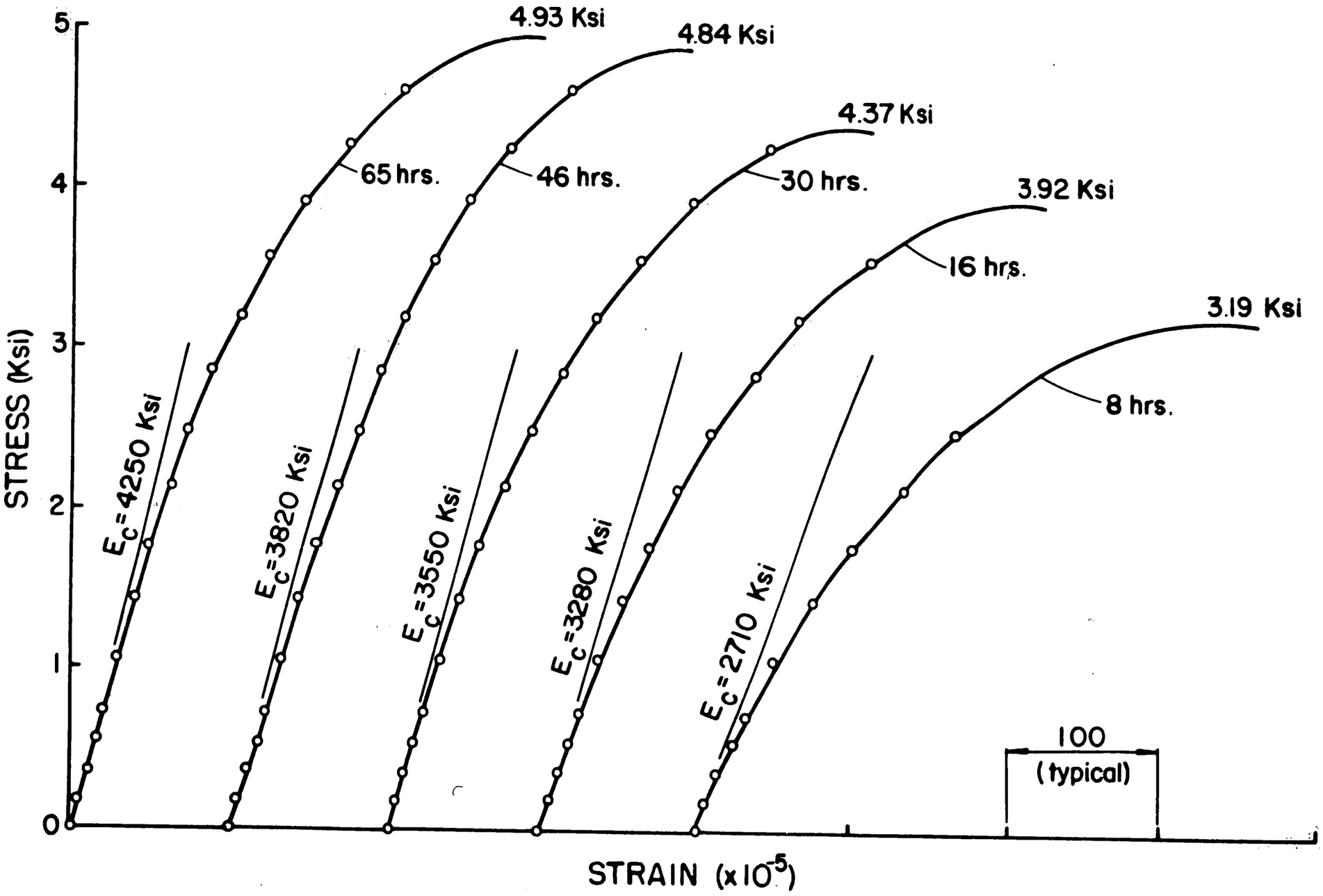

CONCRETE CYLINDER STRESS-STRAIN CURVES- SECOND BEAM TEST

10. TABLES

Table 1 Principal Phases of First Beam Test

Phase of Test		Date and Time	
①	Began Strand Tensioning	23 Oct 62	9:50 PM EDST
②	Completed Strand Tensioning		10:55 PM
③	First Concrete Placed for Bridge Beams	24 Oct 62	8:20 AM
④	Began Casting Test Beam		6:10 PM
⑤	Finished Casting Test Beam		7:40 PM
⑥	Applied Steam Curing		9:35 PM
⑦	Steam Reduced - Beams Still Covered	26 Oct 62	1:00 PM
⑧	Top Covering of Beams Removed		1:45 PM
⑨	Completed Removal of Test Beam Forms		2:30 PM
⑩	Completed Removal of All Forms		3:55 PM
⑪	Completed Transfer of Prestress		4:50 PM
⑫	Final Strainometer Readings Taken	29 Oct 62	4:00 PM EST
⑬	Final Whittemore Readings Taken	16 Nov 62	1:40 PM

Table 2 Concrete Cylinder Data - First Beam Test

Age of Cylinders (hrs)	Initial Tangent Elastic Modulus (ksi)	Ultimate Strength (ksi)
14	4,660	5.02
24	4,720	5.16
36	4,220	5.21
48*	5,020	5.56

*Age at prestress transfer was approximately 45 hrs.

Table 3 Prestress Data - First Beam Test

Date and Time of Reading	Elapsed Time (hrs)	Prestress Force Per Strand (kips)						
		1	2	3	4	5	6	Ave.
23 Oct 62 10:55 PM	0	19.81	20.28	18.80	21.05	19.63	20.60	20.03
24 Oct 62 5:25 PM	18.50	19.30	19.95	18.74	20.70	19.52	20.05	19.71
8:25 PM	21.50	18.78	19.60	18.78	20.30	19.10	19.50	19.34
10:00 PM	23.08	18.05	18.78	18.15	19.80	18.40	18.75	18.65
25 Oct 62 7:45 AM	32.84	16.03	16.50	17.80	18.04	16.60	16.20	16.86
11:15 AM	36.33	16.25	16.83	17.85	18.37	16.85	16.60	17.12
1:30 PM	38.58	16.50	16.97	17.61	18.56	16.91	16.85	17.23
4:05 PM	41.17	16.67	17.30	17.41	18.84	17.10	17.15	17.41
6:40 PM	43.75	17.15	17.40	17.70	19.15	17.57	17.40	17.73
11:00 PM	48.08	17.15	17.90	18.10	19.15	17.47	17.90	17.94
26 Oct 62 7:00 AM	56.08	17.65	18.00	18.63	19.10	18.13	17.95	18.24
12:15 PM	61.33	17.84	18.10	18.60	19.66	18.17	18.05	18.40
26 Oct 62 4:00 PM	65.08	18.80	19.40	19.65	20.54	19.20	19.40	19.50

Table 4 Results from 5-inch Whittemore Gage Readings - First Beam Test

Date and Time	Gage Line	Strains Relative to 4:20 P.M. October 26, 1962 ($\times 10^{-6}$)																	
		1-2	2-3	3-4	4-5	5-6	6-7	7-8	8-9	9-10	11-12	12-13	13-14	14-15	15-16	16-17	17-18	18-19	19-20
October 26, 1962 4:55 P.M.-6:05 P.M.	A	-20	-20 (60)	0	0	20	40	20	-20 (160)	0	20	-40 (20)	60	0	40	--	--	--	--
	B	-40	-20	-40	0	-60	-20	-40	-60	X	-40	-40	0	0	-40	-20	--	--	--
	C	--	--	--	--	--	--	--	--	--	--	--	--	--	--	--	--	0 (X)	-200
	D	--	--	--	--	--	--	--	-120	-100	--	--	--	--	--	--	--	--	--
	E	-20	-40	-100	-140	-180	-140	-160	-40	-200	-200	-200	-140	-180	-140	-120	-40	-20	-20
	F	40	-40 (-160)	-140	-240	-240	-240	-280	-300 (-300)	-320	-200	-240 (X)	-340	-240	-260	-200	-60	-40 (X)	-40
	G	-20	X	X	-320	-380	-360	-280	-240	-380	-300	-340	-220	-320	-200	-200	-200	-180	-120
	H	-40	-200	-480	-540	-400	-460	-400	-420	-440	-160	-160	-420	-400	-380	X	-300	-340	-180
	J	0	-420 (-180)	-500	-600	-580	-540	-360	-540 -520	-460	-460	-340 (X)	-400	-440	-440	-500	-400	X (X)	-220
October 26, 1962 6:45 P.M.-8:50 P.M.	A	-20	-20 (80)	0	20	20	40	20	20 (100)	0	20	0 (140)	60	40	120	--	--	--	--
	B	-60	-20	-40	-20	-60	-40	-60	-60	X	-60	-20	-20	20	-40	40	--	--	--
	C	--	--	--	--	--	--	--	--	--	--	--	--	--	--	--	--	20 (X)	-220
	D	--	--	--	--	--	--	--	-140	-140	--	--	--	--	--	--	--	--	--
	E	0	-40	-140	-140	-200	-160	-140	-40	-160	-260	-220	-160	-160	-100	-160	20	0	-80
	F	60	-100 (80)	-200	-360	-220	-280	-240	-280 (-200)	-280	-240	-240 X	-240	-200	-200	-200	-60	-20 (X)	-20
	G	-40	X	X	-320	-360	-360	-300	-260	-480	-300	-340	-260	-280	-140	-200	-240	X	-100
	H	-140	-180	-480	-520	-420	-480	-460	-420	-560	-160	-380	-440	-380	-380	X	-260	-380	-120
	J	-80	-400 (-180)	-500	-540	-560	-580	-440	-640 (-560)	-500	-500	-420 (X)	-380	-500	-580	-560	-400	X (X)	-340

Note: Minus signs indicate compressive strains.
Strain values in parentheses apply to far side of beam.
"X" denotes no gage reading due to faulty whittemore targets.

Table 4 (Continued)

Date and Time	Gage Line	Strains Relative to 4:20 P.M. October 26, 1962 ($\times 10^{-6}$)																
		1-2	2-3	3-4	4-5	5-6	6-7	7-8	8-9	9-10	11-12	12-13	13-14	14-15	15-16	16-17	17-18	18-19	19-20
October 28, 1962 5:45 P.M.	A	-100	-200 (-40)	-180	-220	-140	-80	-40	-20 (-100)	-60	-60	-80 (60)	-40	-80	-180	--	--	--	--
	B	-160	-180	-240	-200	-220	-180	-140	-120	X	-160	-120	-100	-100	-220	-200	--	--	--
	C	--	--	--	--	--	--	--	--	--	--	--	--	--	--	--	--	-180 (X)	-320
	D	--	--	--	--	--	--	--	-240	-240	--	--	--	--	--	--	--	--	--
	E	-100	-200	-260	-320	-360	-320	-260	-140	-380	-320	-300	-320	-320	-340	-340	-180	-140	-140
	F	-20	-260 (-100)	-360	-420	-420	-420	-400	-420 (-380)	-460	-380	-320 (X)	-360	-380	-400	-380	-280	-180 (X)	-160
	G	-160	X	X	-540	-500	-540	-440	-480	-580	-500	-480	-380	-460	-360	-460	-400	X	-200
	H	-320	-380	-660	-640	-600	-660	-640	-540	-640	-360	-520	-620	-580	X	X	-560	-520	-340
	J	-120	-520 (-240)	-680	-780	-740	-780	-640	-880 (-620)	-640	-660	-600 (X)	-620	X	X	-760	-600	X (X)	-380
October 29, 1962 4:30 P.M.	A	-180	-220 (-100)	-180	-220	-140	0	-40	-60 (-160)	-60	-60	-120 (60)	-20	-100	-160	--	--	--	--
	B	-180	-180	-200	-220	-200	-120	-200	-180	X	-180	-80	-60	-120	-260	-180	--	--	--
	C	--	--	--	--	--	--	--	--	--	--	--	--	--	--	--	--	140 (X)	-360
	D	--	--	--	--	--	--	--	-180	-200	--	--	--	--	--	--	--	--	--
	E	-100	-180	-260	-300	-400	-280	-240	-120	-280	-300	-340	-300	-320	-320	-340	-120	-200	-140
	F	-80	-300 (-140)	-300	-420	-380	-400	-380	-420 (-400)	-440	-400	-360 (X)	-380	-400	-420	-400	-260	-220 (X)	-180
	G	-140	X	X	-520	-500	-540	-420	-400	-520	-460	-500	-460	-420	-340	-460	-400	X	-220
	H	-220	-340	-720	-660	-600	-740	-640	-540	-600	-360	-540	-660	-580	X	X	-600	-540	-540
	J	X	-520 (-300)	-660	-760	-740	-780	-660	-800 (-840)	-640	-660	-640 (X)	-660	X	X	-800	-620	X (X)	-560

Table 4 (Continued)

Date and Time	Gage Line	Strains Relative to 4:20 P.M. October 26, 1962 ($\times 10^{-6}$)																
		1-2	2-3	3-4	4-5	5-6	6-7	7-8	8-9	9-10	11-12	12-13	13-14	14-15	15-16	16-17	17-18	18-19	19-20
November 16, 1962 1:40 P.M.	A	-340	-180 (160)	20	-480	-220	160	0	320 (160)	-320	220	-100 (X)	-20	-120	-120	--	--	--	--
	B	-220	-720	-380	-280	-220	-80	-100	-120	X	-120	-100	-80	-140	-220	-180	--	--	--
	C	--	--	--	--	--	--	--	--	--	--	--	--	--	--	--	--	340 (X)	-340
	D	--	--	--	--	--	--	--	-240	-220	--	--	--	--	--	--	--	--	--
	E	-120	-240	-240	-420	-380	-320	-260	-160	-300	-340	-380	-340	-360	-360	-540	-440	80	-160
	F	-40	-300 (-200)	-360	-500	-420	-580	-420	-520 (-460)	-480	-440	-460 (X)	-400	-480	-560	-480	-340	-240 (X)	-220
	G	-120	X	X	-600	-580	-580	-480	-460	-600	-560	-580	-500	-500	-440	-560	-300	X	-320
	H	-340	-400	-820	-740	-700	-760	-740	-620	-740	-480	-660	-740	-680	X	X	-680	-660	-400
	J	X	-600 (-300)	-900	-940	-860	-820	-800	-940 (-1400)	-780	-800	-700 (X)	-660	X	X	-960	-740	X (X)	-440

Table 5 Results from 10-inch Whittemore Gage Readings - First Beam Test

Date and Time	Gage Lines	Strains Relative to 4:20 PM, October 26, 1962 ($x10^{-6}$)							
		1-3	3-5	5-7	7-9	12-14	14-16	16-18	18-20
October 26, 1962 5:23 PM - 5:52 PM	A	0	30	80	60	50	90	--	--
	B	-50	-10	40	10	0	40	--	--
	C	--	--	--	--	--	--	--	20
	D	--	--	--	--	--	--	--	--
	E	0	-60	-160	-140	-140	-70	-100	10
	F	-20	-160	-180	-250	-270	-180	-140	-20
	G	X	X	-310	-340	-350	-50	-210	-100
	H	-160	-420	-420	-410	-420	-300	-340	-230
	J	-210	-470	-520	-520	-420	-550	-470	-60

Note: Minus signs indicate compressive strains.
"X" denotes no gage reading due to faulty whittemore targets.

Table 6 Principal Phases of Second Beam Test

Phase of Test		Date and Time	
①	Began Strand Tensioning	15 Aug 63	11:10 AM
②	Completed Strand Tensioning		1:30 PM
③	Completed Placement of Holding Jacks		1:50 PM
④	Began Concrete Placement	16 Aug 63	8:10 AM
⑤	Began Casting Test Beam		3:10 PM
⑥	Finished Casting Test Beam		4:30 PM
⑦	Applied Steam Curing		5:30 PM
⑧	Steam Reduced	19 Aug 63	7:00 AM
⑨	Forms Loosened (Not Removed)		7:45 AM
⑩	Completed Transfer of Prestress		10:30 AM
⑪	Final Strainometer Readings Taken		1:45 PM

Table 7 Concrete Cylinder Data - Second Beam Test

Age of Cylinders (hrs)	Initial Tangent Elastic Modulus (ksi)	Ultimate Strength (ksi)
8	2,710	3.19
16	3,280	3.92
30	3,550	4.37
46	3,820	4.84
65*	4,250	4.93

*Beam age at prestress transfer was 66 hrs.

DATE AND TIME OF READING		ELAPSED TIME (hrs.)	FORCE PER STRAND (KIPS)												
			1	2	3	4	5	6	7	8	9	10	11	12	AVE.
AUGUST 15, 1963	1:40PM	0	22.25	21.60	21.30	21.85	21.60	21.80	21.65	22.40	22.50	22.45	22.10	22.00	21.96
	2:00PM	0.3	22.25	21.45	21.15	21.70	21.45	21.80	21.50	22.30	22.35	22.35	22.00	21.90	21.85
AUGUST 16, 1963	1:30AM	11.8	22.15	21.40	21.10	21.65	21.45	21.60	21.45	22.35	22.30	22.30	21.90	21.80	21.78
	10:00AM	20.3	22.10	21.35	21.05	21.40	21.45	21.50	21.45	22.10	22.15	22.30	21.90	21.65	21.70
	2:00PM	24.3	21.90	21.10	21.05	21.35	21.20	21.10	21.20	22.10	22.00	22.15	21.65	21.45	21.52
	4:00PM	26.3	21.80	20.85	21.05	21.10	21.15	21.25	21.20	21.85	21.95	22.10	21.70	21.35	21.49
	5:00PM	27.3	21.75	20.65	21.05	21.10	21.10	21.10	21.10	21.80	21.85	22.00	21.60	21.20	21.36
	7:00PM	29.3	21.10	20.40	20.70	20.50	20.70	20.60	20.60	21.30	21.40	21.45	21.00	20.80	20.88
	9:00PM	31.3	20.90	20.30	20.40	20.30	20.40	20.30	20.35	20.95	21.00	21.05	20.65	20.50	20.59
AUGUST 17, 1963	12:45AM	35.1	20.50	20.20	19.70	20.00	20.05	20.00	19.95	20.45	20.65	20.80	20.35	20.25	20.24
	9:30AM	43.8	20.55	20.25	19.75	20.05	20.05	20.00	20.00	20.50	20.70	20.85	20.40	20.30	20.28
	12:20PM	46.7	20.20	20.30	19.90	20.05	20.05	20.10	20.05	20.55	20.70	20.85	20.45	20.35	20.30
	4:30PM	50.8	20.65	20.40	20.15	20.05	20.05	20.25	20.05	20.60	20.75	20.90	20.50	20.45	20.40
	9:15PM	55.6	20.75	20.45	20.40	20.30	20.25	20.30	20.15	20.65	20.80	21.00	20.60	20.50	20.51
AUGUST 18, 1963	11:45AM	70.1	20.90	20.60	20.40	20.50	20.30	20.35	20.30	20.80	20.95	21.15	20.70	20.65	20.63
	4:30PM	74.8	21.00	20.60	20.40	20.50	20.30	20.35	20.30	20.85	21.00	21.15	20.70	20.70	20.65
AUGUST 19, 1963	6:40AM	89.0	21.05	20.80	20.55	20.65	20.40	20.50	20.30	20.90	21.10	21.20	20.85	20.85	20.76
	10:30AM	92.8	21.05	20.90	20.60	20.65	20.45	20.55	20.40	21.00	21.15	21.30	20.90	20.90	20.82

Table 8 Prestress Data - Second Beam Test

Table 9 Concrete Temperatures in Second Test Beam

Date and Time	Elapsed Time (hrs)	Temperature (F)												
		Left End Face			Section I									
		a	b	c	A1	A2	A3	A4	A5	E1	E2	E3	E4	E5
16 Aug 63 4:30 PM	0	84	(84)	83	86	(85)	83	(83)	82	84	(83)	82	(83)	83
7:00 PM	2.5	89	(88)	86	96	(93)	88	(86)	83	101	(100)	98	(95)	85
9:00 PM	4.5	107	(105)	102	110	(110)	104	(97)	87	123	(122)	118	(110)	91
17 Aug 63 12:45 AM	8.2	167	(161)	155	144	(150)	143	(129)	109	138	(143)	143	(138)	114
4:30 AM	12.0	165	(162)	159	140	(147)	140	(125)	104	131	(136)	136	(131)	110
9:30 AM	17.0	159	(153)	146	130	(137)	130	(119)	100	127	(129)	128	(122)	103
12:30 PM	20.0	153	(146)	139	128	(134)	128	(117)	100	124	(128)	127	(119)	102
4:30 PM	24.0	147	(140)	132	133	(133)	125	(113)	98	131	(129)	127	(118)	102
9:15 PM	28.8	141	(133)	124	133	(131)	122	(110)	96	131	(128)	124	(117)	100
18 Aug 63 11:45 AM	43.2	125	(118)	110	130	(123)	111	(100)	88	123	(117)	112	(105)	93
4:30 PM	48.0	122	(115)	107	123	(117)	108	(98)	87	120	(115)	110	(104)	92
19 Aug 63 7:00 AM	62.5	114	(106)	98	120	(113)	102	(91)	80	118	(110)	106	(100)	86
10:30 AM	66.0	109	(104)	97	102	(102)	97	(90)	80	98	(100)	100	(96)	83
10:55 AM	66.4	109	(104)	98	102	(102)	97	(90)	80	98	(100)	100	(96)	83
1:45 PM	69.2	103	(98)	92	97	(96)	94	(90)	80	90	(92)	93	(91)	83

Note: Values in parentheses were determined by interpolation

Table 9 (Continued)

Date and Time	Elapsed Time (hrs)	Temperature (F)											
		Section II											
		A1	A2	A3	A4	A5	B1	B2	B3	B4	B5	C1	C2
16 Aug 63 4:30 PM	0	86	(86)	85	(84)	83	(85)	84	(84)	83	(84)	83	(84)
7:00 PM	2.5	99	(102)	99	(93)	85	(95)	90	(92)	90	(86)	90	(90)
9:00 PM	4.5	127	(121)	112	(102)	92	(121)	112	(110)	106	(94)	115	(112)
17 Aug 63 12:45 AM	8.2	144	(151)	149	(140)	123	(161)	178	(176)	164	(139)	166	(185)
4:30 AM	12.0	142	(149)	148	(136)	119	(162)	180	(176)	165	(137)	168	(188)
9:30 AM	17.0	133	(138)	137	(128)	113	(151)	166	(162)	150	(129)	156	(179)
12:30 PM	20.0	130	(134)	133	(124)	112	(148)	158	(156)	143	(124)	152	(164)
4:30 PM	24.0	135	(131)	130	(120)	108	(146)	150	(146)	135	(118)	148	(154)
9:15 PM	28.8	134	(126)	125	(115)	104	(143)	143	(137)	127	(111)	145	(145)
18 Aug 63 11:45 AM	43.2	125	(114)	113	(104)	94	(130)	127	(122)	112	(103)	131	(129)
4:30 PM	48.0	125	(111)	110	(101)	93	(128)	124	(116)	108	(99)	127	(125)
19 Aug 63 7:00 AM	62.5	122	(106)	105	(96)	87	(123)	116	(109)	100	(93)	122	(116)
10:30 AM	66.0	102	(101)	100	(94)	88	(113)	118	(110)	100	(91)	115	(117)
10:55 AM	66.4	102	(101)	100	(94)	88	(113)	118	(110)	100	(91)	115	(113)
1:45 PM	69.2	92	(97)	96	(91)	85	(109)	110	(104)	98	(89)	110	(111)

Table 9 (Continued)

Date and Time	Elapsed Time (hrs)	Temperature (F)												
		Section II												
		C3	C4	C5	D1	D2	D3	D4	D5	E1	E2	E3	E4	E5
16 Aug 63 4:30 PM	0	84	(84)	84	(84)	83	(84)	85	(84)	84	(84)	83	(83)	83
7:00 PM	2.5	90	(88)	86	(94)	90	(93)	89	(88)	100	(103)	96	(100)	90
9:00 PM	4.5	109	(104)	94	(107)	111	(111)	106	(95)	118	(122)	119	(108)	96
17 Aug 63 12:45 AM	8.2	187	(175)	144	(162)	183	(180)	167	(140)	147	(155)	153	(143)	125
4:30 AM	12.0	188	(178)	144	(160)	183	(178)	168	(137)	139	(149)	149	(139)	120
9:30 AM	17.0	175	(159)	134	(150)	169	(166)	153	(129)	132	(138)	137	(128)	112
12:30 PM	20.0	164	(152)	128	(147)	161	(157)	145	(124)	129	(136)	134	(125)	112
4:30 PM	24.0	152	(139)	121	(145)	152	(147)	136	(119)	134	(134)	130	(122)	110
9:15 PM	28.8	142	(132)	115	(143)	145	(141)	127	(111)	133	(133)	129	(119)	108
18 Aug 63 11:45 AM	43.2	123	(113)	103	(129)	129	(121)	112	(102)	124	(123)	117	(108)	99
4:30 PM	48.0	118	(109)	100	(125)	125	(117)	109	(99)	121	(119)	115	(106)	97
19 Aug 63 7:00 AM	62.5	109	(101)	93	(121)	117	(109)	102	(92)	119	(114)	109	(100)	91
10:30 AM	66.0	109	(102)	92	(112)	116	(107)	101	(91)	103	(105)	103	(97)	89
10:55 AM	66.4	109	(102)	92	(112)	116	(107)	101	(91)	103	(105)	102	(97)	87
1:45 PM	69.2	105	(98)	91	(107)	112	(106)	100	(90)	99	(103)	100	(95)	87

Table 10 Apparent Longitudinal Strains Occurring in Second Test Beam

Date and Time	Elapsed Time (hrs)	Apparent Longitudinal Strain ($\times 10^{-6}$)										
		Section I									Section II	
		A1L	A2L	A3L	A4L	E1L	E2L	E3L	E4L	E5L	A1L	A2L
16 Aug 63 4:30 PM	0	0	0	0	0	0	0	0	0	0	0	0
7:00 PM	2.5	-10	-6	-16	-12	-6	-10	-7	-7	8	-9	-14
9:00 PM	4.5	-29	-22	-41	-39	-24	-18	-25	-16	1	-15	-91
17 Aug 63 12:45 AM	8.2	-27	-31	-47	-41	-48	-32	-50	-33	-33	-18	-87
4:30 AM	12.0	-36	-39	-61	-46	-49	-45	-58	-51	-47	-22	-90
9:30 AM	17.0	-46	-53	-74	-57	-49	-52	-60	-58	-50	-22	-96
12:30 AM	20.0	-50	-64	-83	-78	-39	-55	-63	-64	-65	-26	-105
4:30 PM	24.0	-50	-79	-92	-73	-54	-59	-58	-57	-51	-76	-105
9:15 PM	28.8	-52	-86	-111	-88	-54	-62	-63	-53	-46	-89	-111
18 Aug 63 11:45 AM	43.2	-67	-86	-127	-89	-41	-58	-65	-61	-56	-80	-100
4:30 PM	48.0	-62	-102	-130	-94	-39	-49	-68	-48	-21	-65	-89
19 Aug 63 7:00 AM	62.5	-71	-95	-134	-98	-37	-42	-53	-42	-11	-53	-66
10:30 AM	66.0	-40	-69	-86	-85	-14	-22	-18	-11	9	-14	-36
10:55 AM	66.4	-45	-69	-106	-136	-4	-22	-31	-56	-71	16	-41
1:45 PM	69.2	-43	-60	-96	-127	-9	-27	-21	-47	-61	32	-20

Note: Minus signs indicate compressive strains

Table 10 (Continued)

Date and Time	Elapsed Time (hrs)	Apparent Longitudinal Strain ($\times 10^{-6}$)											
		Section II											
		A3L	A4L	A5L	B1L	B2L	B4L	B5L	C1L	C2L	C3L	C4L	C5L
16 Aug 63 4:30 PM	0	0	0	0	0	0	0	0	0	0	0	0	0
7:00 PM	2.5	-19	-18	-17	-7	-8	-12	-2	-11	0	8	6	-5
9:00 PM	4.5	-102	-86	-51	-7	-35	-21	-16	-6	6	10	3	2
17 Aug 63 12:45 AM	8.2	-119	-80	-86	-14	-42	-26	-19	-2	16	28	18	-2
4:30 AM	12.0	-110	-88	-95	-11	-37	-17	-24	5	26	45	41	7
9:30 AM	17.0	-115	-92	-93	-2	-25	-3	-18	13	41	54	54	7
12:30 AM	20.0	-106	-100	-106	-4	-11	20	-6	33	66	80	74	20
4:30 PM	24.0	-103	-96	-108	0	1	26	3	67	88	112	113	44
9:15 PM	28.8	-95	-112	-108	-13	-4	34	7	82	99	135	126	76
18 Aug 63 11:45 AM	43.2	-90	-104	-96	-5	4	36	14	90	110	151	135	99
4:30 PM	48.0	-85	-78	-72	3	11	43	10	95	123	167	141	127
19 Aug 63 7:00 AM	62.5	-72	-73	-51	13	21	50	18	119	157	203	174	139
10:30 AM	66.0	-45	-40	-23	23	28	49	10	116	133	161	149	121
10:55 AM	66.4	-91	-185	-298	31	23	-26	-235	121	138	161	94	-114
1:45 PM	69.2	-80	-173	-265	46	36	-21	-223	132	134	163	90	-114

Table 10 (Continued)

Date and Time	Elapsed Time (hrs)	Apparent Longitudinal Strain ($\times 10^{-6}$)								
		Section II								
		D1L	D2L	D4L	D5L	E1L	E2L	E3L	E4L	E5L
16 Aug 63 4:30 PM	0	0	0	0	0	0	0	0	0	0
7:00 PM	2.5	-4	-5	0	-16	-11	-14	-10	-15	-13
9:00 PM	4.5	-9	-13	4	-14	-11	-80	-85	-78	-32
17 Aug 63 12:45 AM	8.2	-11	-19	-7	-22	-14	-75	-109	-83	-73
4:30 AM	12.0	-7	-8	2	-3	-15	-80	-100	-85	-75
9:30 AM	17.0	-7	4	14	9	-15	-80	-95	-86	-77
12:30 AM	20.0	3	24	34	26	-16	-84	-88	-97	-97
4:30 PM	24.0	17	39	45	34	-65	-84	-88	-96	-97
9:15 PM	28.8	26	47	23	46	-75	-94	-106	-111	-106
18 Aug 63 11:45 AM	43.2	51	53	38	58	-68	-86	-98	-104	-90
4:30 PM	48.0	64	57	48	51	-68	-73	-77	-75	-70
19 Aug 63 7:00 AM	62.5	70	70	48	51	-40	-50	-60	-70	-55
10:30 AM	66.0	72	64	52	48	-22	-35	-40	-54	-34
10:55 AM	66.4	82	64	-13	-187	10	-35	-79	-189	-299
1:45 PM	69.2	74	60	2	-183	27	-13	-63	-173	-286

Table 11 Apparent Vertical and Transverse Strains Occurring in the Second Test Beam

Date and Time	Elapsed Time (hrs)	Apparent Vertical and Transverse Strains ($\times 10^{-6}$)										
		Left End Face			Section I						Section II	
		a	b	c	A2V	A3V	A4V	E2V	E3V	E4V	A2V	A3V
16 Aug 63 4:30 PM	0	0	0	0	0	0	0	0	0	0	0	0
7:00 PM	2.5	3	2	0	-6	5	0	-2	-6	-7	-11	-6
9:00 PM	4.5	-2	0	5	-21	-17	-11	-20	-13	-19	-17	-29
17 Aug 63 12:45 AM	8.2	-9	-10	7	-23	-6	-20	-24	-19	-31	-37	-29
4:30 AM	12.0	-15	-16	3	-30	-20	-25	-33	-33	-44	-45	-36
9:30 AM	17.0	-28	-16	11	-38	-24	-30	-41	-28	-35	-92	-71
12:30 PM	20.0	-34	-14	15	-49	-37	-36	-50	-37	-49	-101	-74
4:30 PM	24.0	-40	-14	23	-53	-61	-49	-53	-43	-58	-111	-90
9:15 PM	28.8	-42	-15	18	-66	-84	-67	-58	-50	-59	-126	-100
18 Aug 63 11:45 AM	43.2	-42	-13	25	-73	-106	-82	-56	-59	-64	-116	-111
4:30 PM	48.0	-51	-13	27	-78	-89	-79	-60	-68	-74	-96	-88
19 Aug 63 7:00 AM	62.5	-54	-14	32	-82	-77	-74	-64	-75	-83	-96	-80
10:30 AM	66.0	-60	-14	37	-70	-67	-65	-73	-86	-100	-87	-124
10:55 AM	66.4	-35	35	72	-60	-62	-55	-80	-92	-106	-107	-114
1:45 PM	69.2	-32	40	68	-56	-57	-52	-77	-89	-106	-97	-110

Note: Minus signs indicate compressive strains.

Table 11 (Continued)

Date and Time	Elapsed Time (hrs)	Apparent Vertical and Transverse Strain ($x10^{-6}$)												
		Section II												
		A4V	B3V	B4V	C2V	C3V	C4V	D3V	D4V	E2V	E3V	E4V	B1T	D1T
16 Aug 63 4:30 PM	0	0	0	0	0	0	0	0	0	0	0	0	0	0
7:00 PM	2.5	-7	2	11	-2	-1	12	9	0	-16	-2	7	21	33
9:00 PM	4.5	-20	-8	1	-14	-1	-3	-2	-2	-27	-20	-4	40	50
17 Aug 63 12:45 AM	8.2	-30	-10	-22	-15	-9	-7	-4	-7	-46	-34	-24	39	30
4:30 AM	12.0	-44	-16	-17	-14	5	-24	-8	-19	-55	-49	-44	36	33
9:30 AM	17.0	-59	-20	-31	-13	19	-39	5	-37	-65	-65	-50	42	35
12:30 PM	20.0	-66	-23	-31	-7	75	-40	13	-49	-92	-85	-84	47	36
4:30 PM	24.0	-79	-21	-38	6	72	-30	30	-52	-100	-97	-89	50	36
9:15 PM	28.8	-90	-20	-44	14	72	-22	46	-57	-123	-115	-95	41	26
18 Aug 63 11:45 AM	43.2	-105	-4	-41	14	123	-26	71	-62	-129	-109	-92	36	22
4:30 PM	48.0	-100	-2	-49	22	149	-18	81	-67	-120	-115	-98	36	20
19 Aug 63 7:00 AM	62.5	-110	7	-53	31	163	-13	92	-75	-119	-109	-101	25	18
10:30 AM	66.0	-124	11	-66	24	145	-16	84	-71	-111	-105	-86	25	21
10:55 AM	66.4	-129	6	-91	9	150	-46	84	-96	-131	-120	-91	25	16
1:45 PM	69.2	-121	4	-91	14	155	-51	94	-91	-116	-110	-80	53	41

11. FIGURES

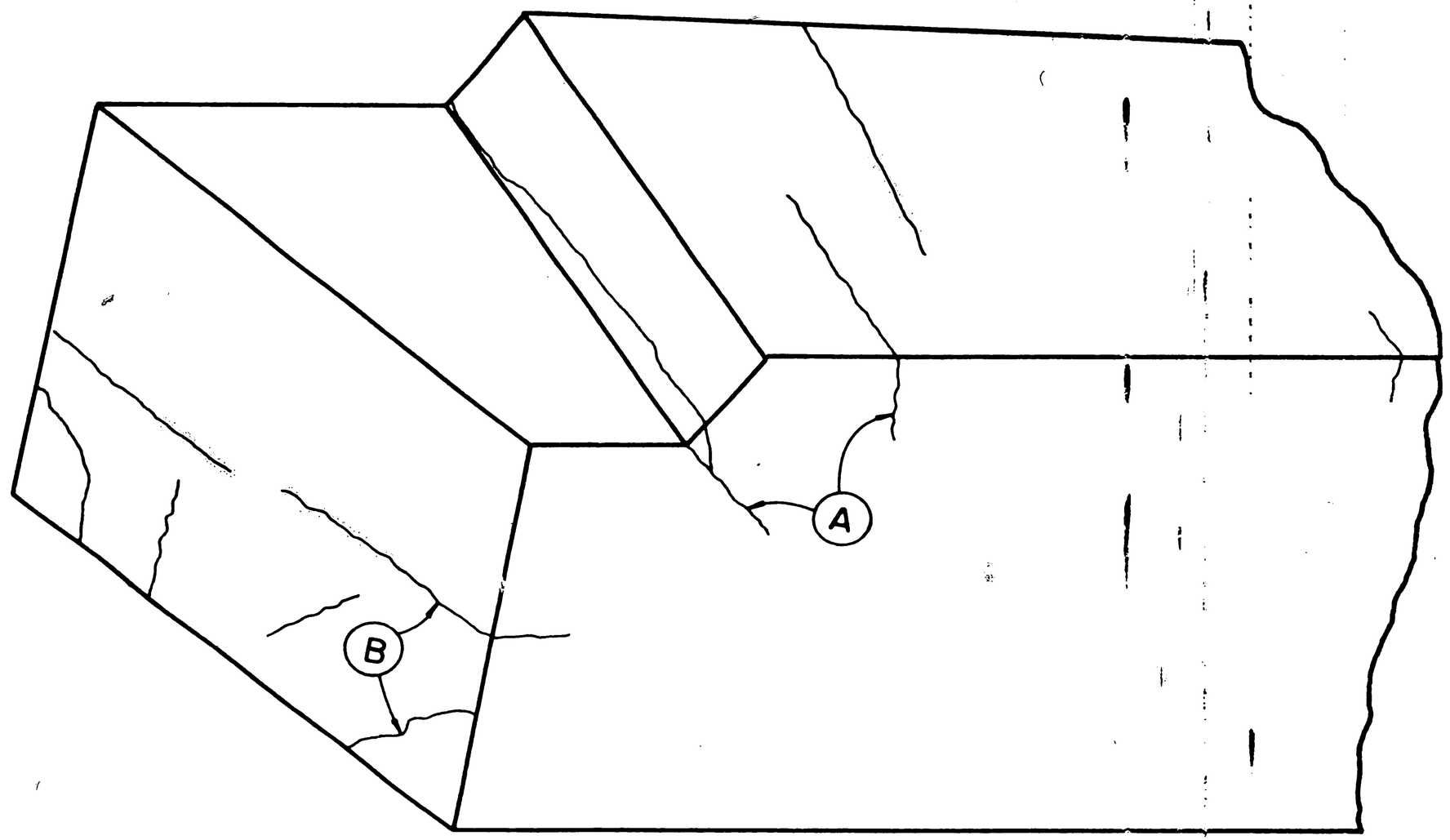

Fig. 1 Typical Cracks in Highway Bridge Beams

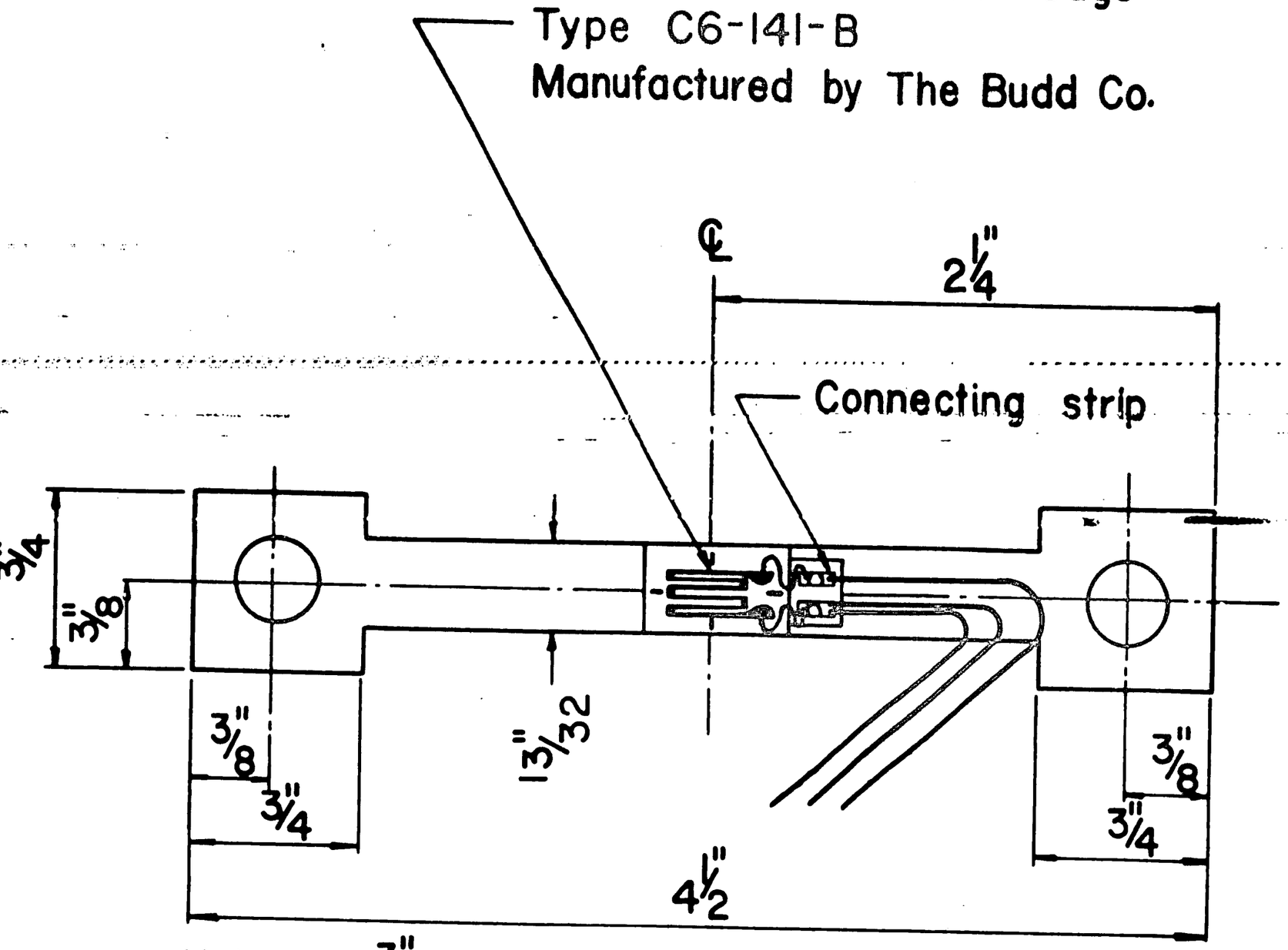

Holes are 3/8" in diameter.

Plate thickness is approximately 0.057 in.

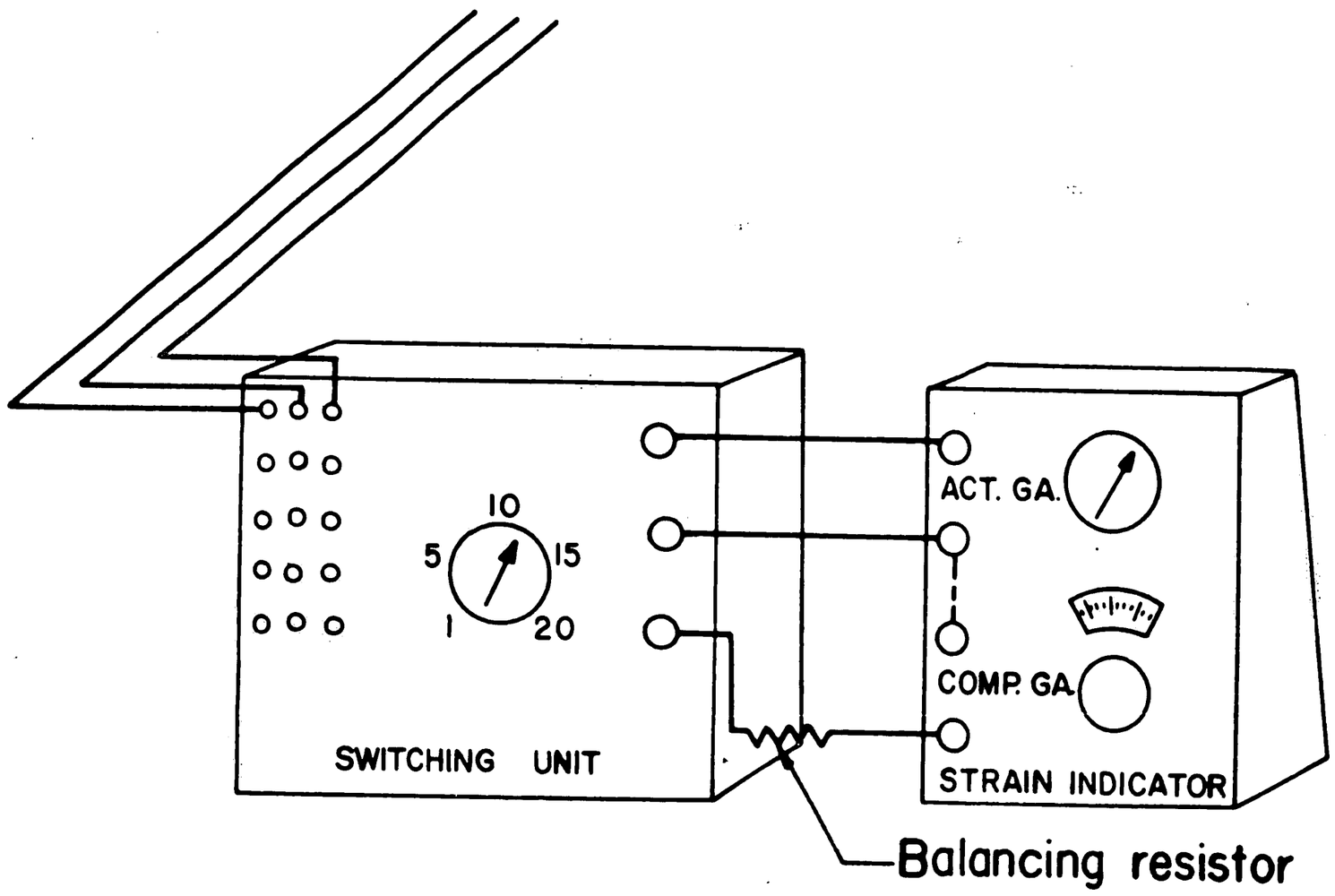

Fig. 2 The Strainometer and Related Instrumentation

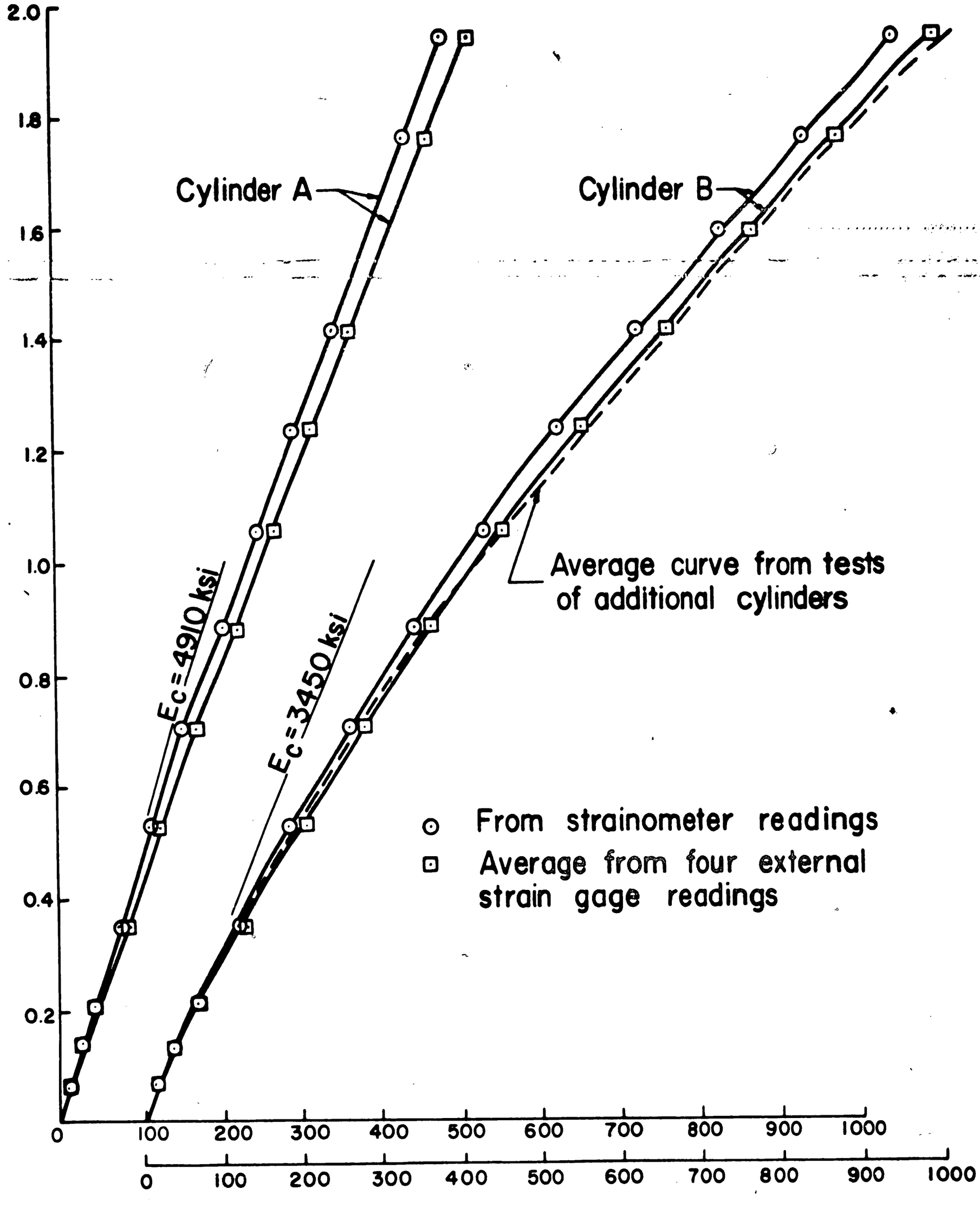

Fig. 3 Stress-Strain Curves for Cylinders with Embedded Strainometers

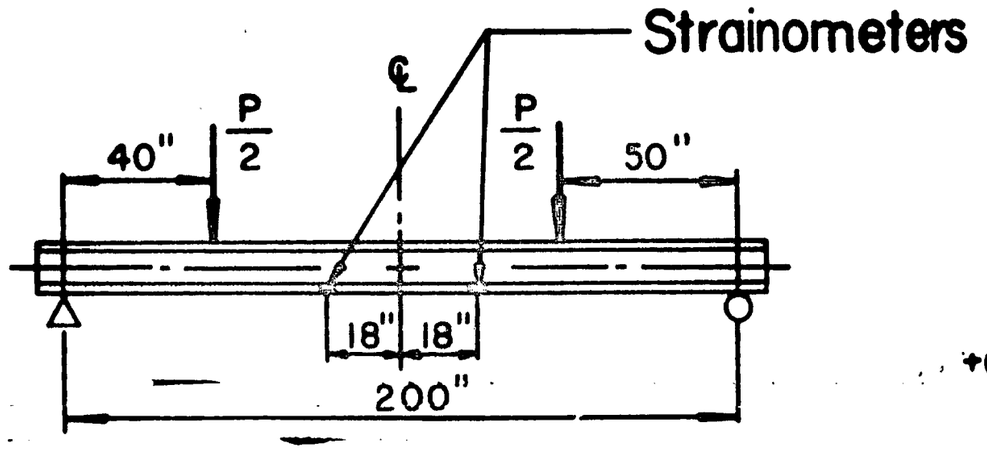

A_t = 105.3 in.^{2} $\quad$ e = 5.02 in.

I_t = 3986 in.^{4} $\quad$ Y_b = 5.22 in.

F_e = 89.8 k $\quad$ E_c = 3970 ksi

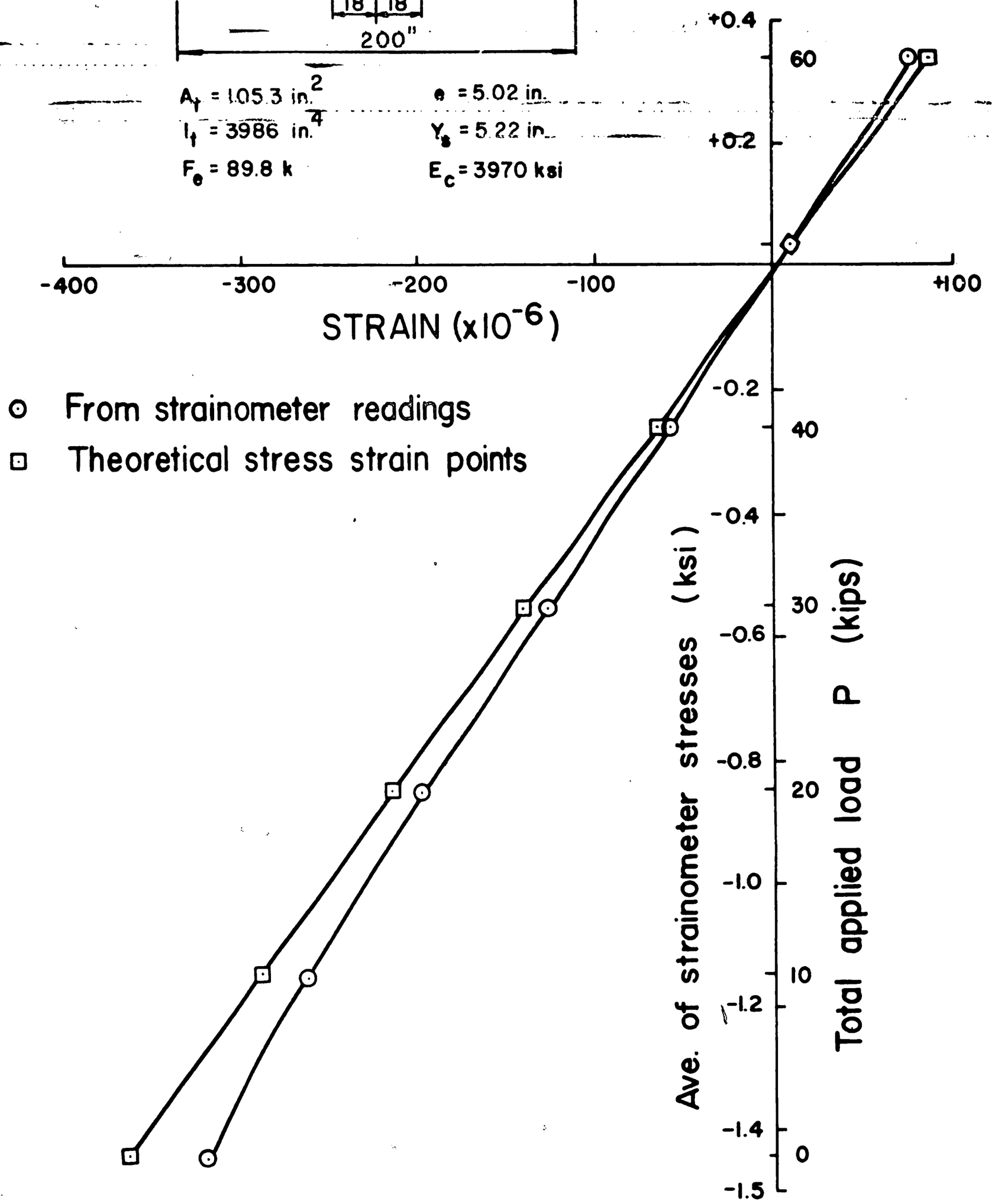

Fig. 4 Results from Strainometer Test using Pretensioned I-Beam

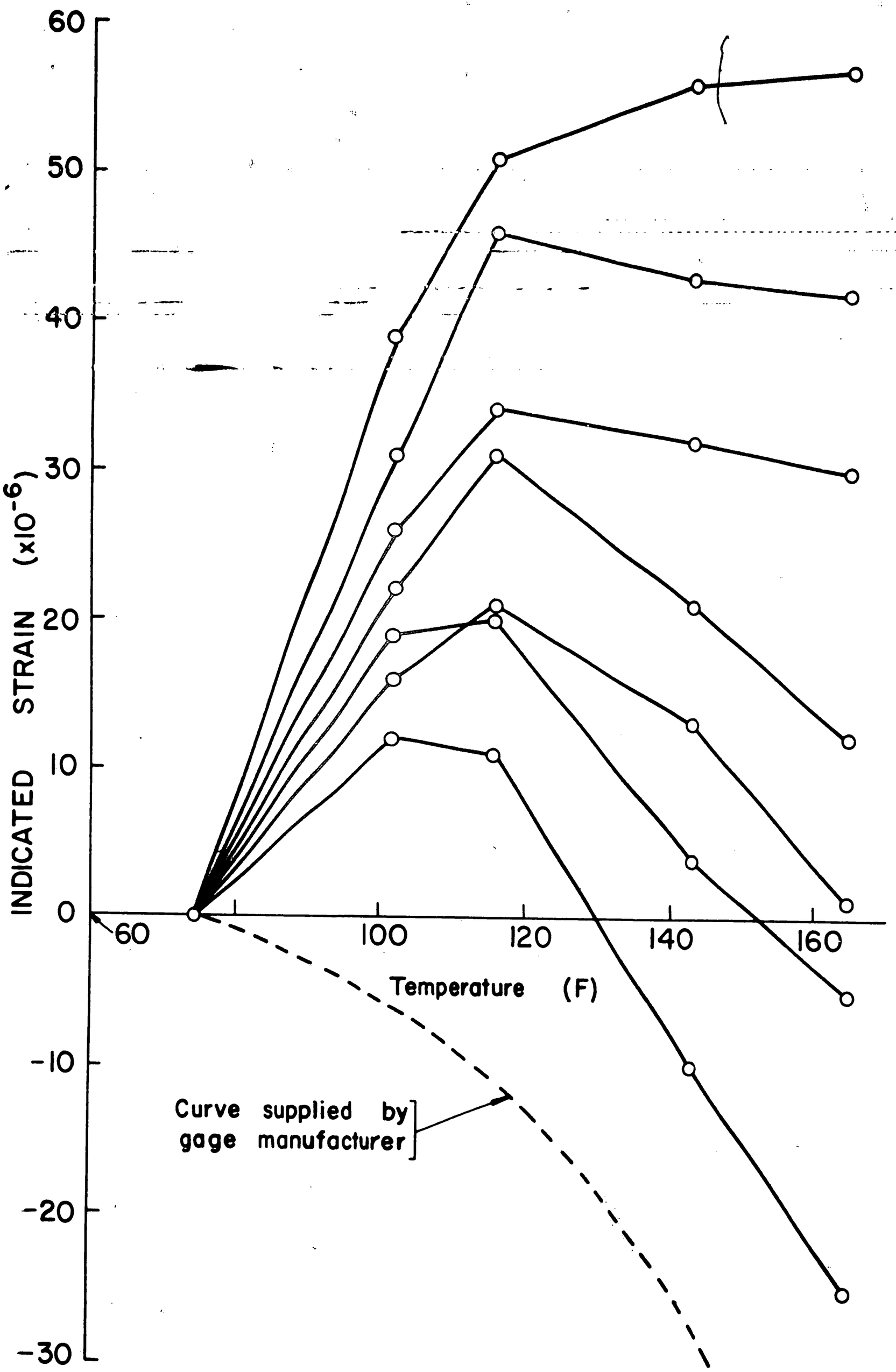

Fig. 5 Typical Temperature Compensation Curves for Strainometers

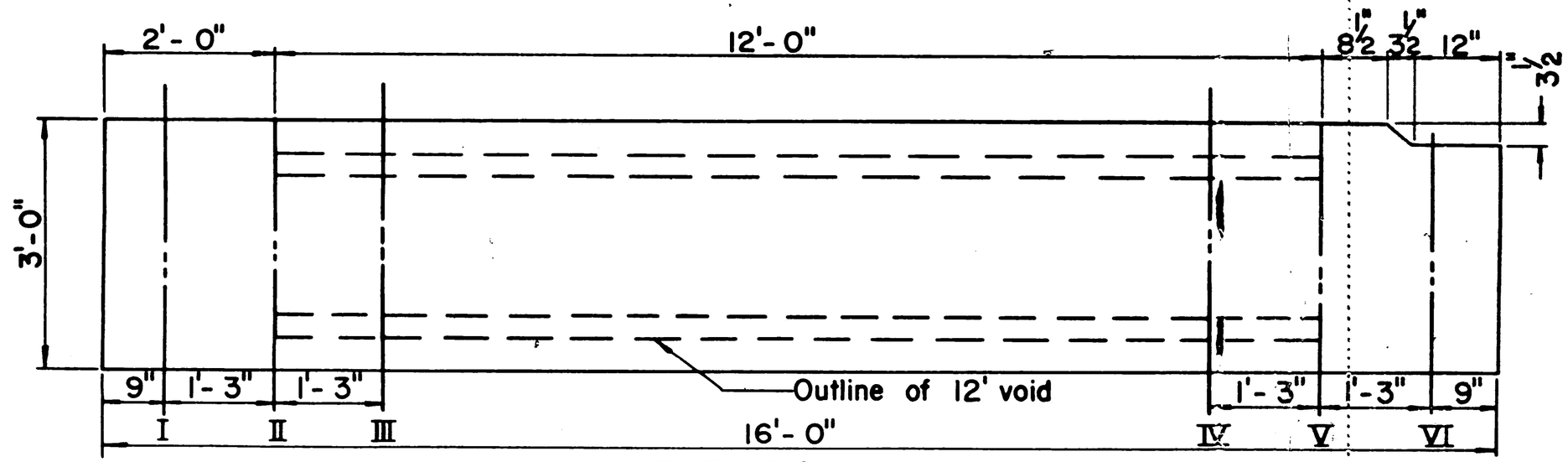

ELEVATION

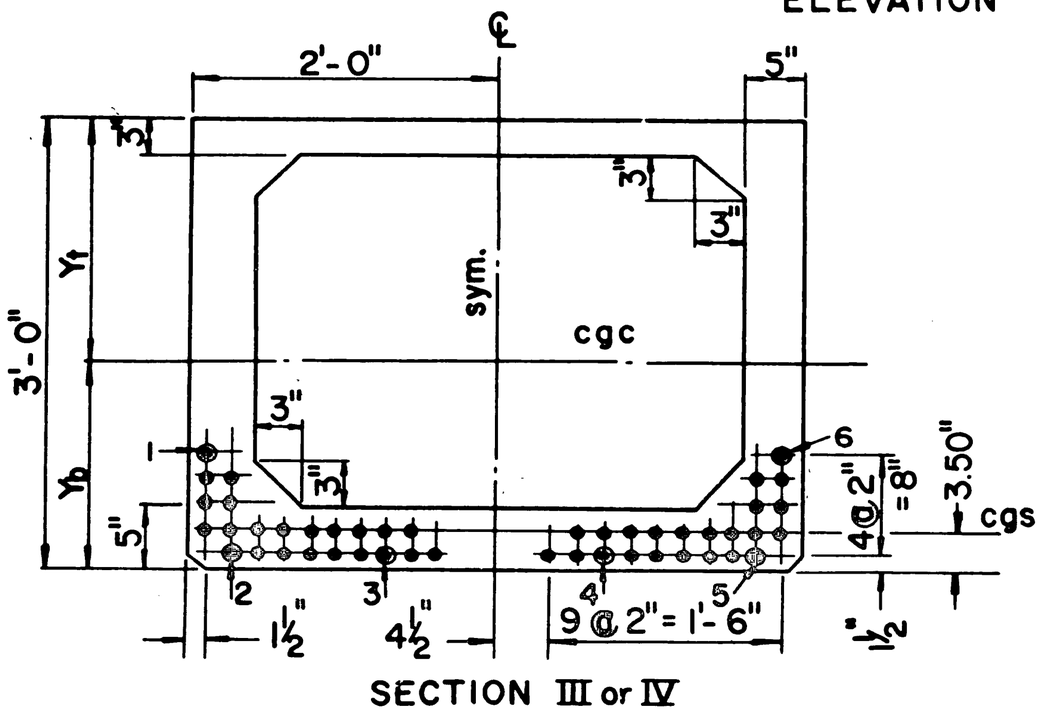

SECTION III or IV

Property	Section I	Section III or IV	Section VI
A (in^2)	1,728	682	1,560
Y_t (in)	18.00	19.53	16.25
Y_b (in)	18.00	16.47	16.25
I_c (in^4)	186,600	117,700	137,300
Z_t (in^3)	10,370	6,027	8,450
Z_b (in^3)	10,370	7,147	8,450

Note: Circled strands were instrumented with dynamometers at live end of bed.

Fig. 6 Description of First Test Beam

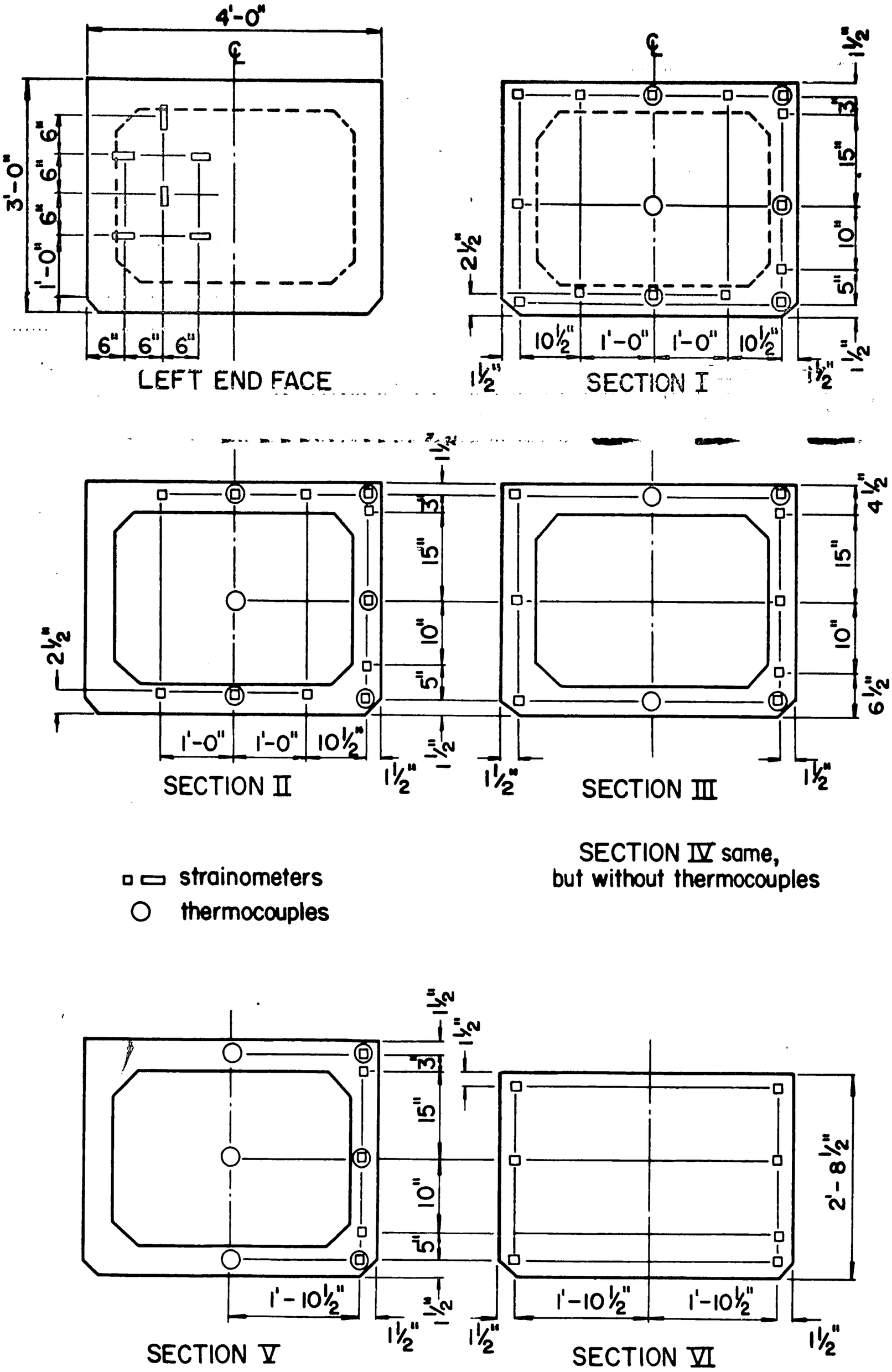

Note: All internal instrumentation is located 1½" from exterior surface except as shown.

Fig. 7 Location of Internal Instrumentation for First Beam Test

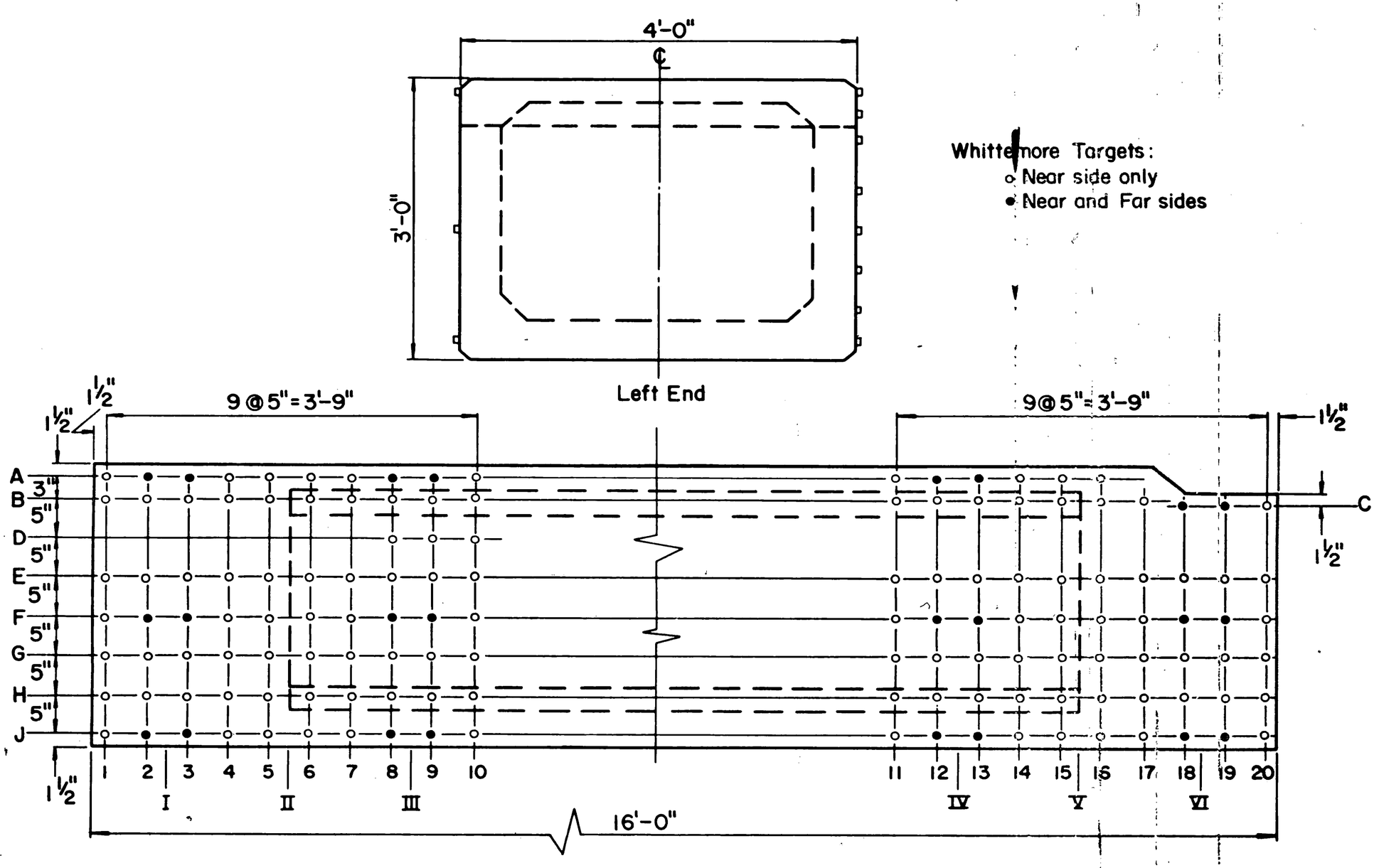

Fig. 8 Whittemore Instrumentation for First Beam Test

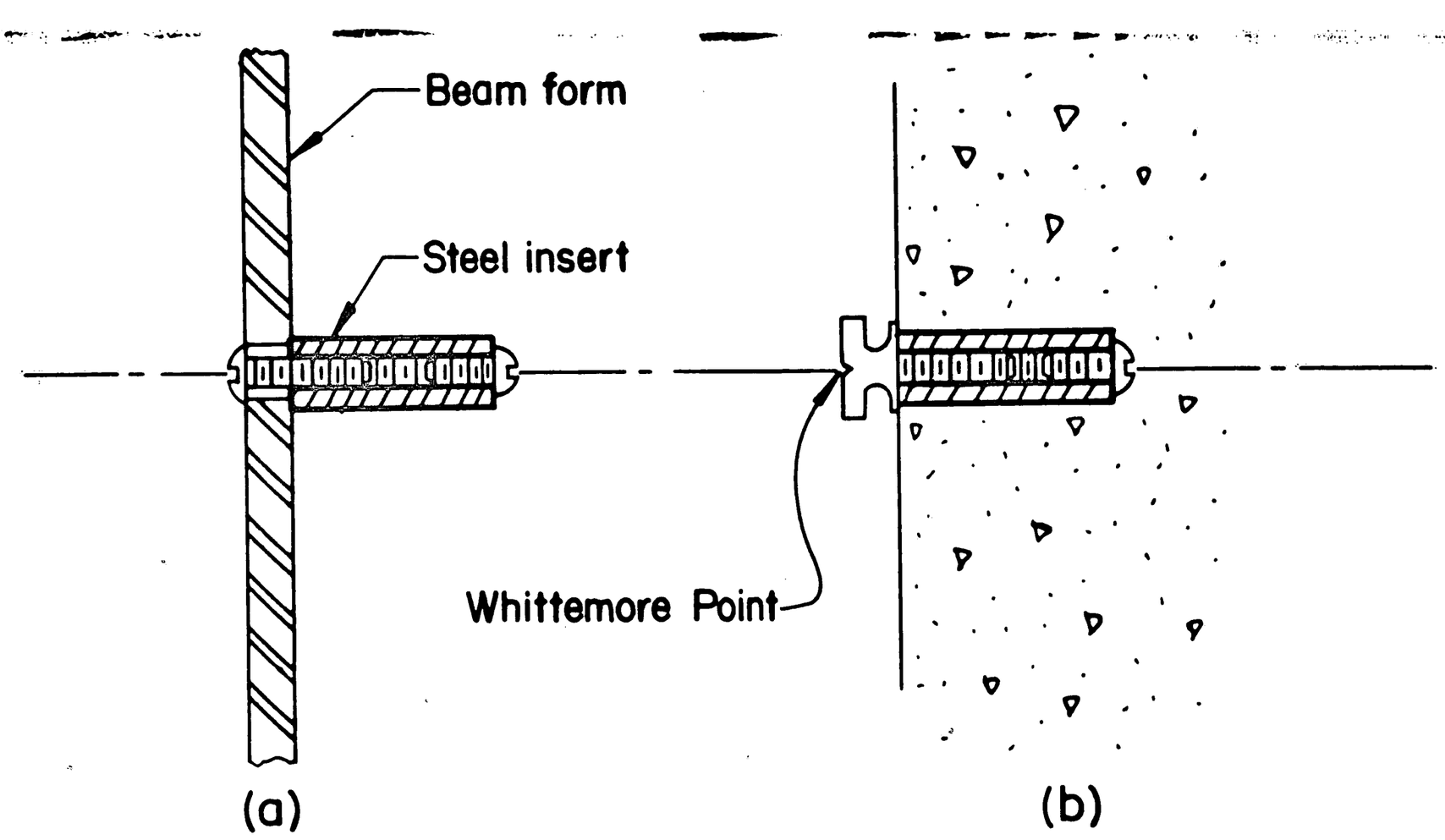

Fig. 9 Description of Whittemore Target used in First Beam Test

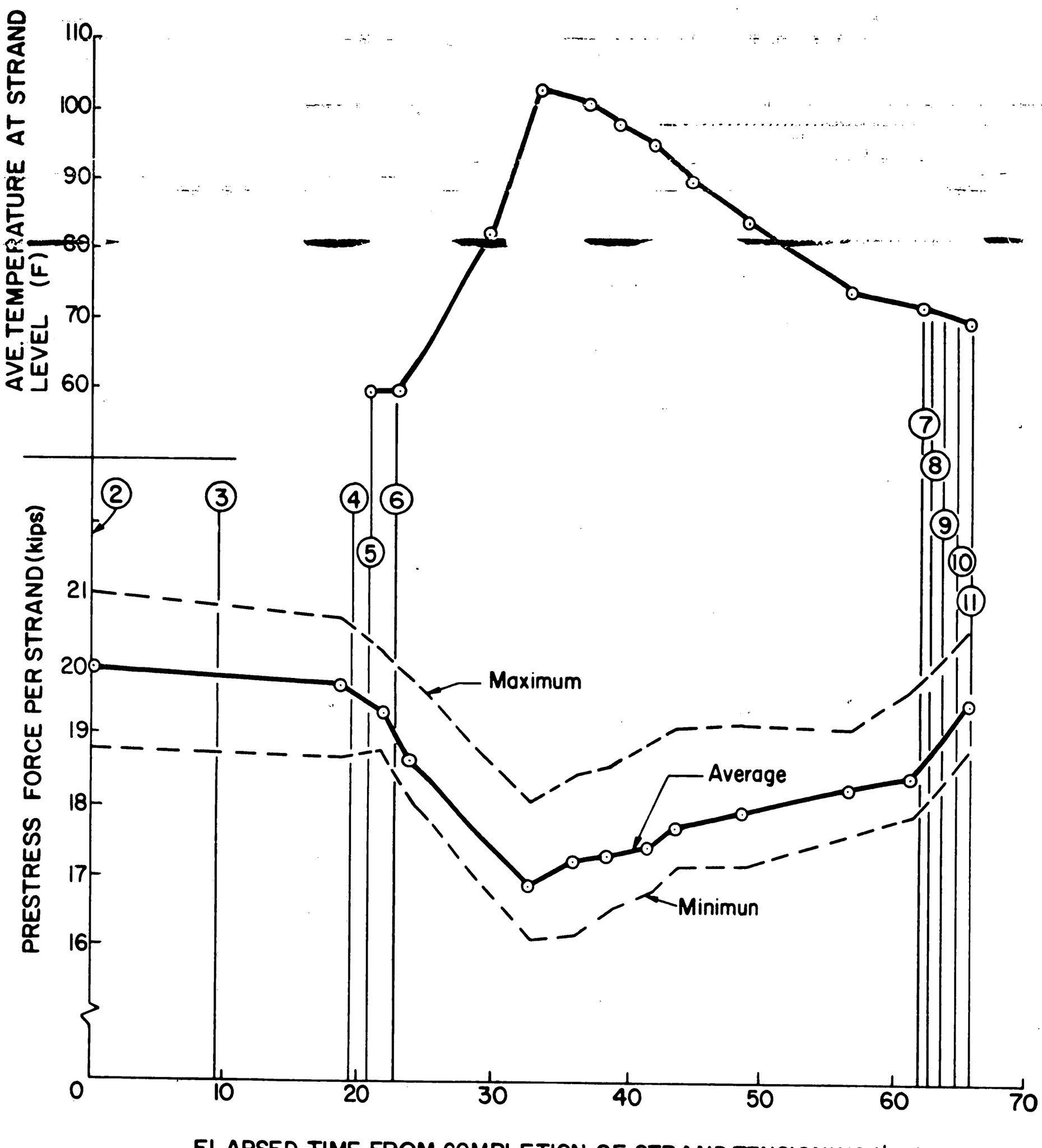

Fig. 10 Variation with Time of Prestress Force and Strand Temperature in First Beam Test

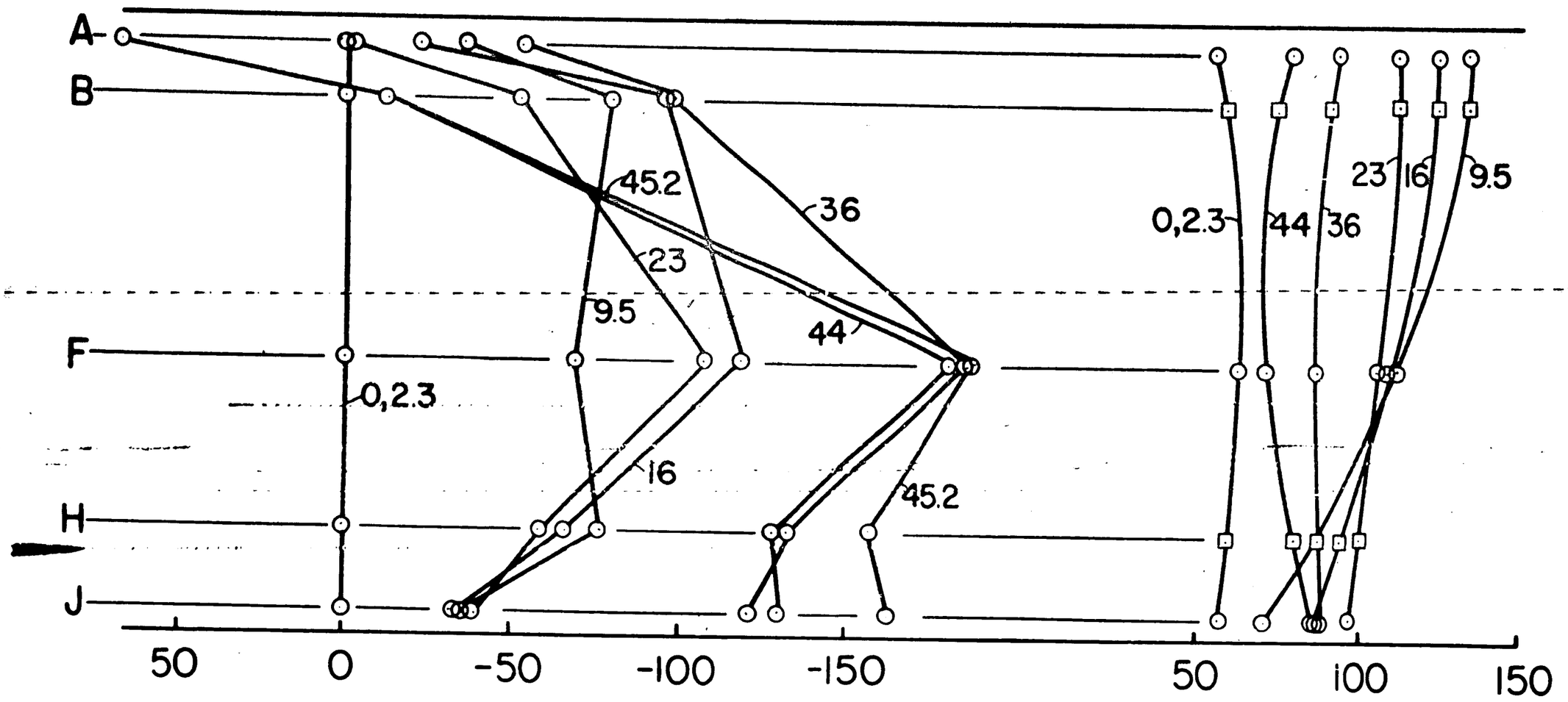

(a) SECTION I

NOTE: 1. Numbers to curves denote elapsed time since beam casting.
2. Temperature values in squares were determined by interpolation.

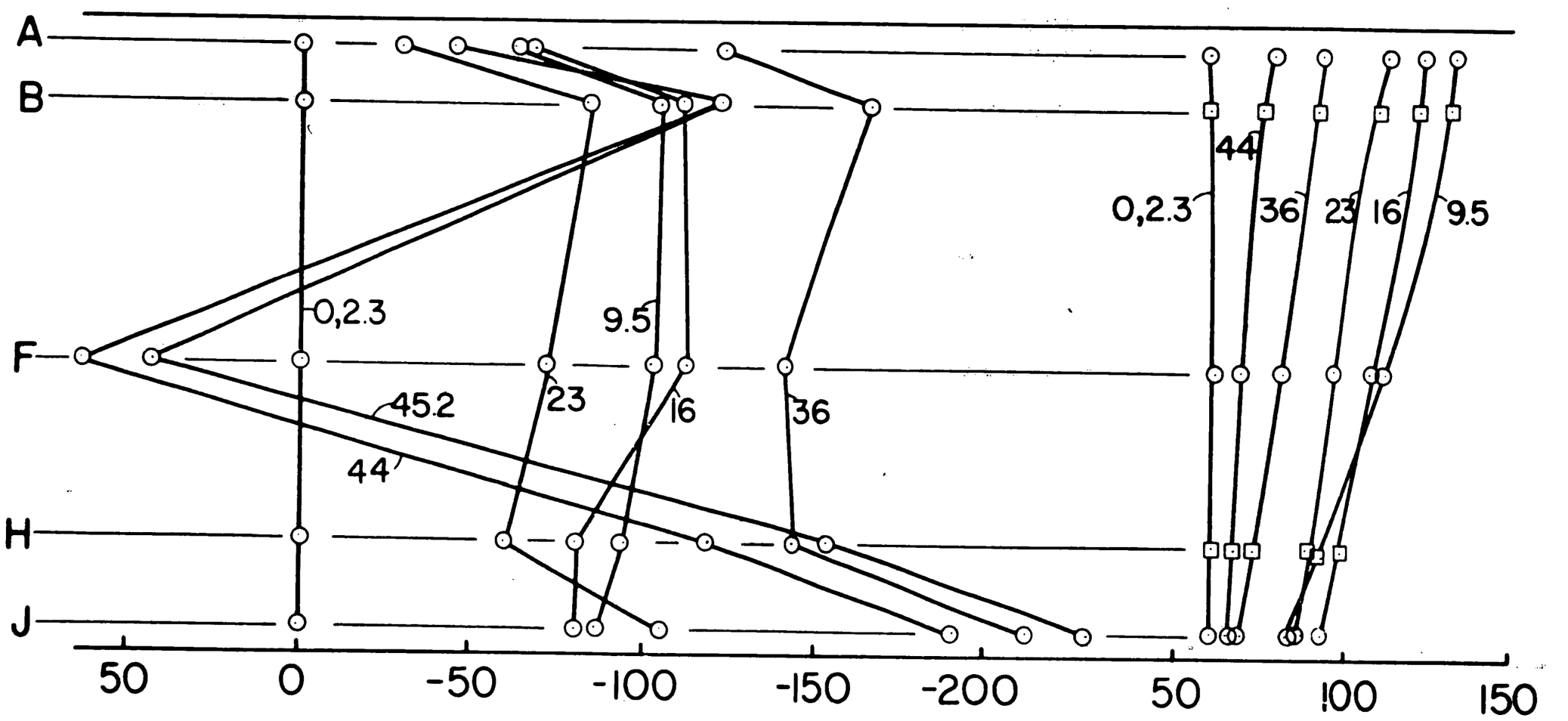

(b) SECTION II

Fig. 11 Variation of Apparent Strain and Concrete Temperature in First Test Beam

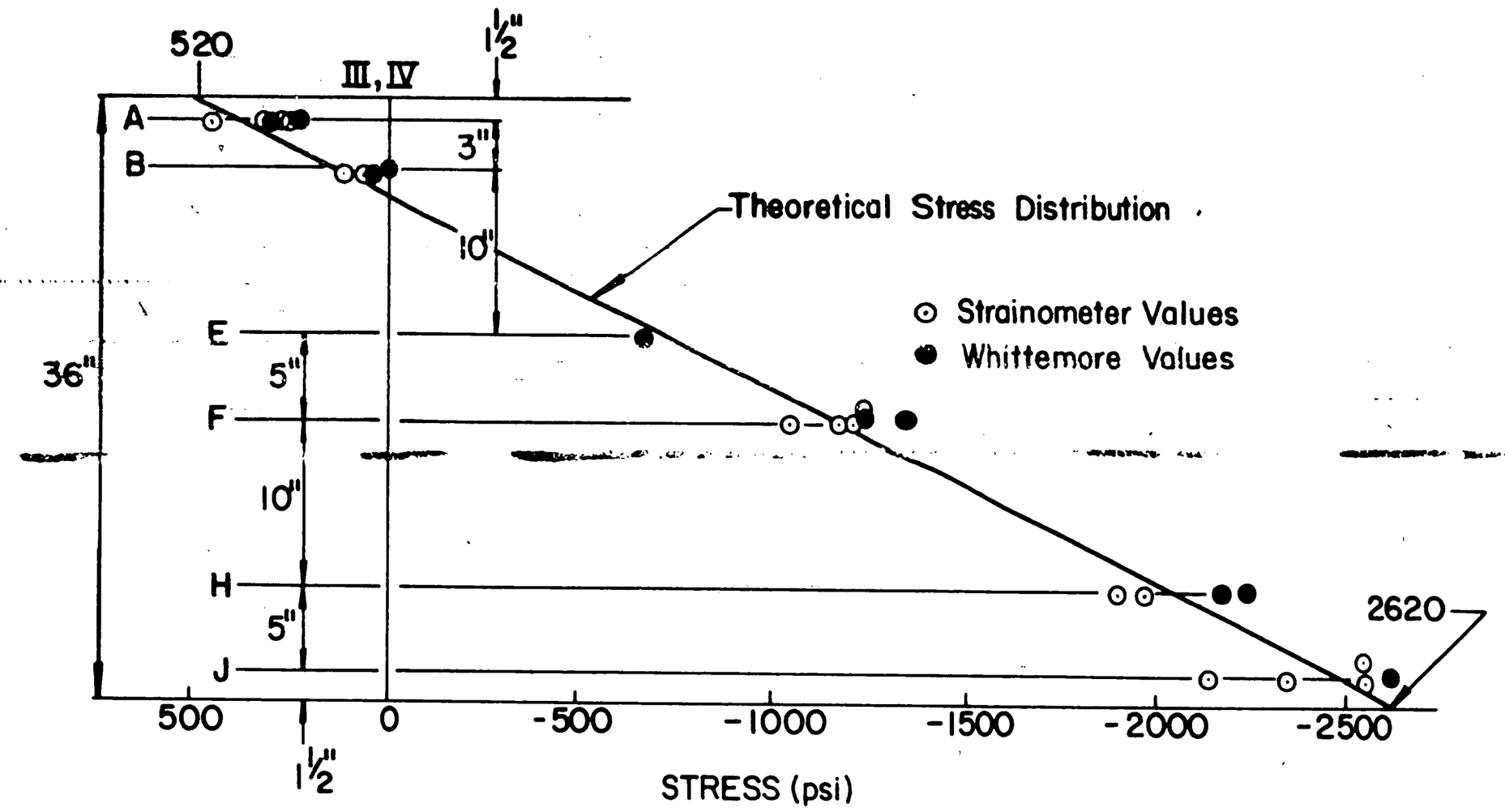

(a) SECTION III, IV

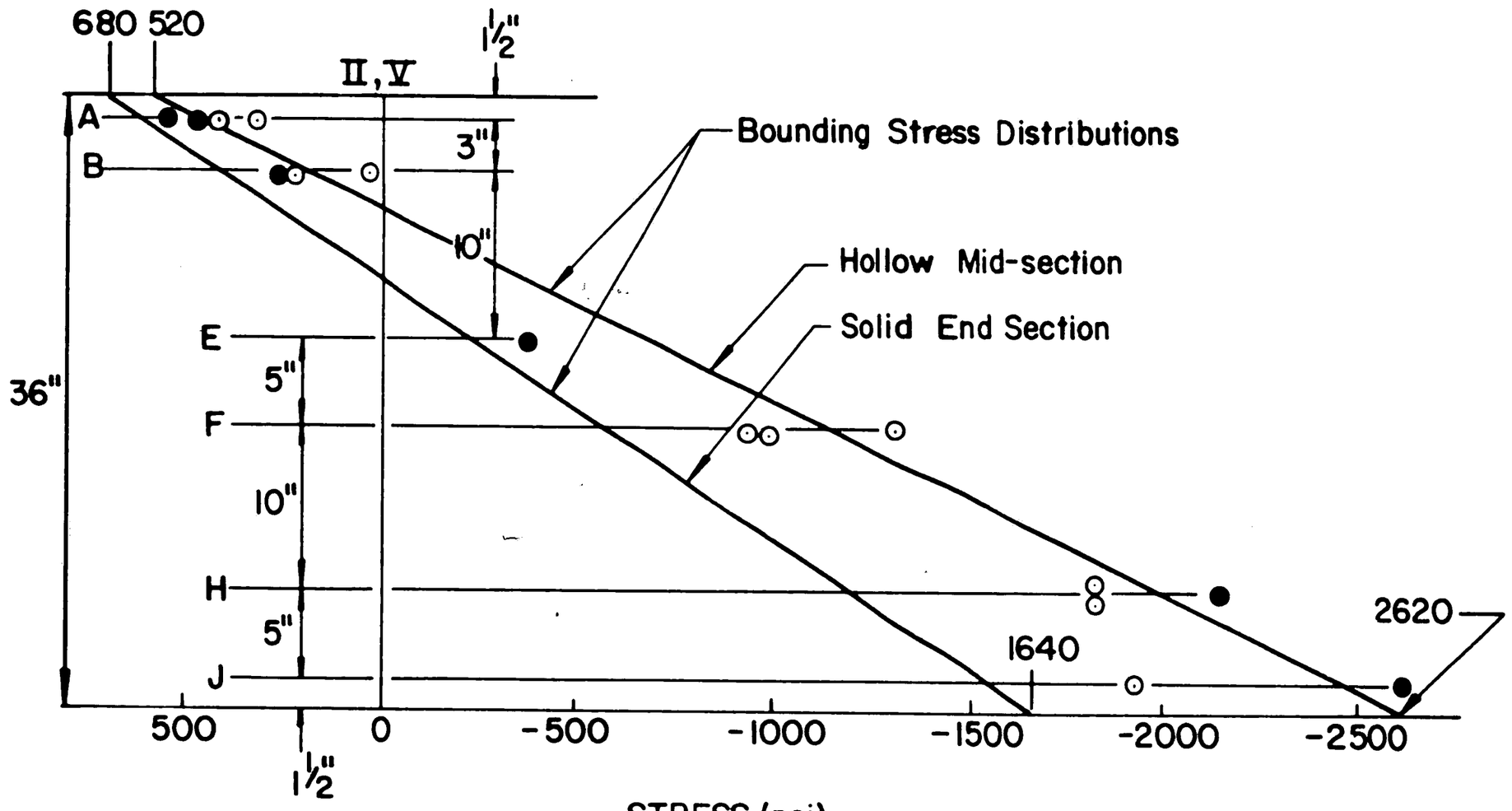

(b) SECTION II.V

Fig. 12 Longutidinal Stresses Caused by Prestress Transfer in First Test Beam

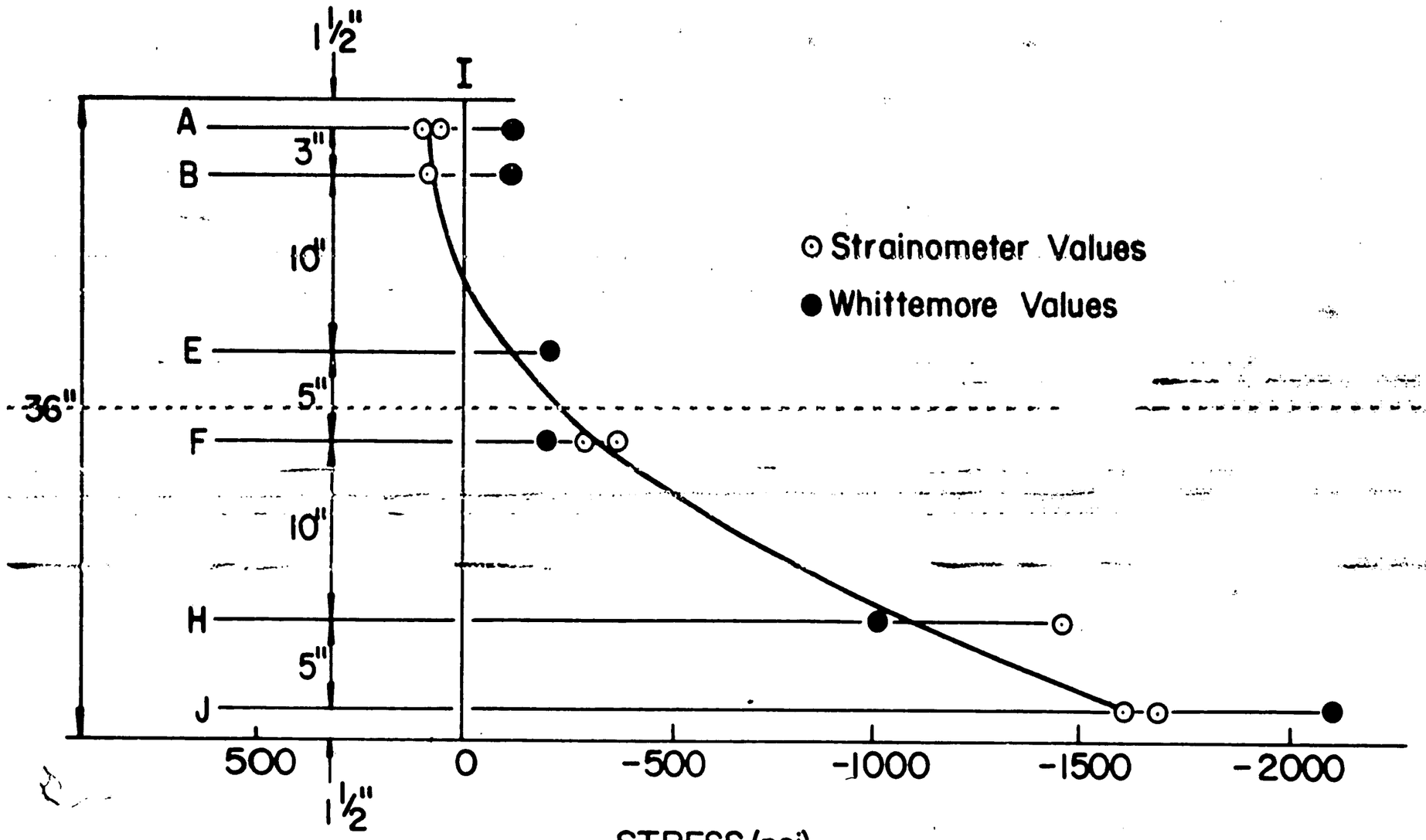

STRESS (psi)

(c) SECTION I

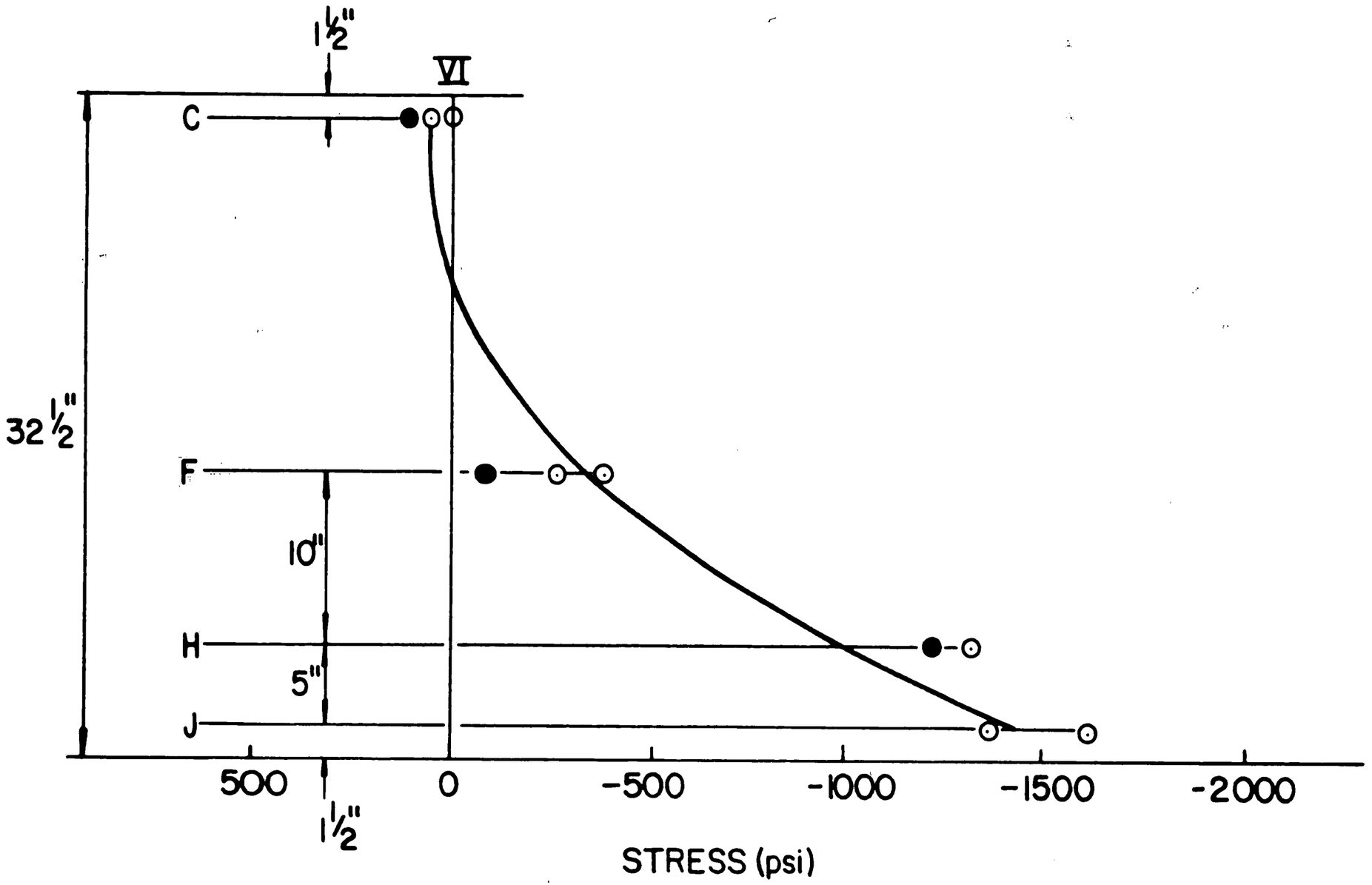

STRESS (psi)

(d) SECTION VI

Fig. 12 (cont'd)

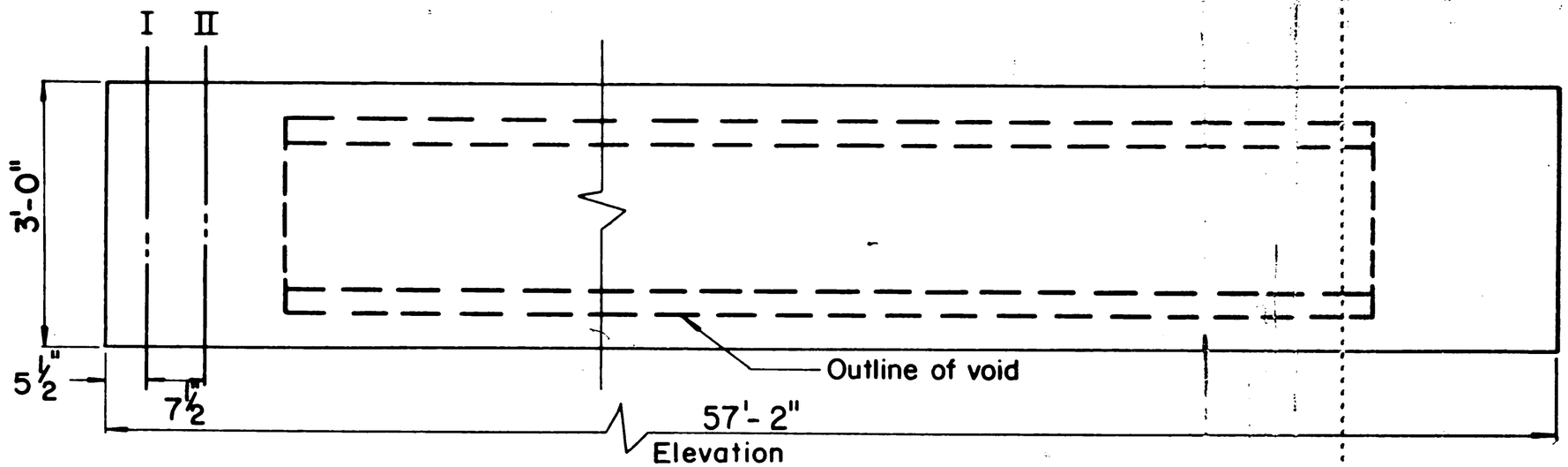

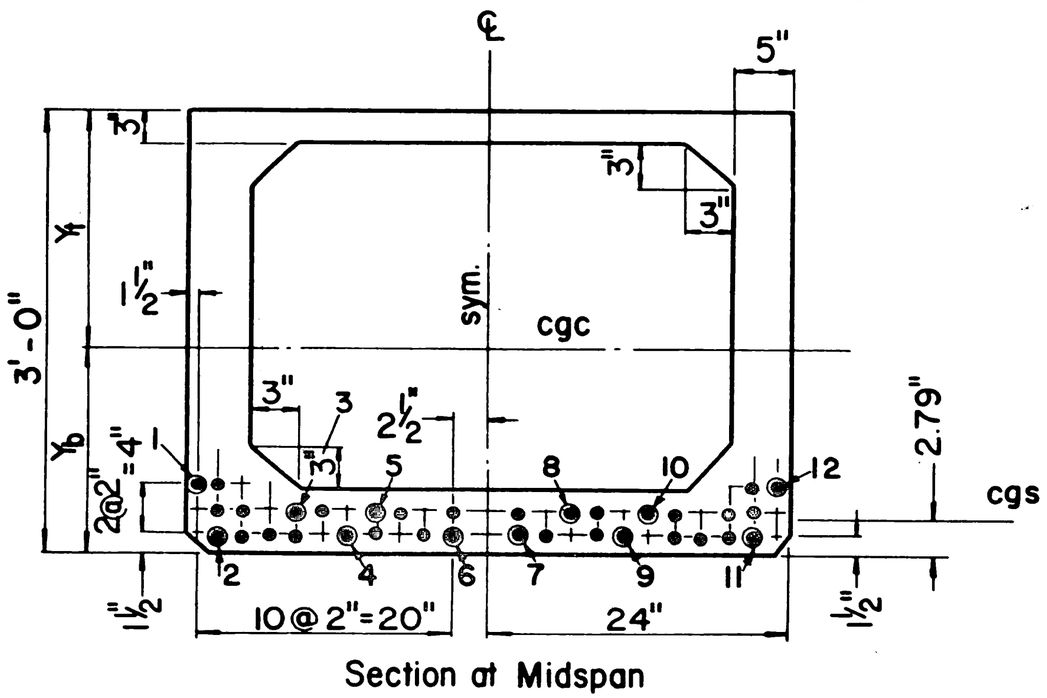

Section at Midspan

Property	Section I or II	Section at Midspan
A (in^2)	1,728	682
Y_t (in)	18.00	19.53
Y_b (in)	18.00	16.47
I_c (in^4)	186,600	117,700
Z_t (in^3)	10,370	6,027
Z_b (in^3)	10,370	7,147

Note: Circled strands were instrumented with dynamometers at live end of bed.

Fig. 13 Description of Second Test Beam

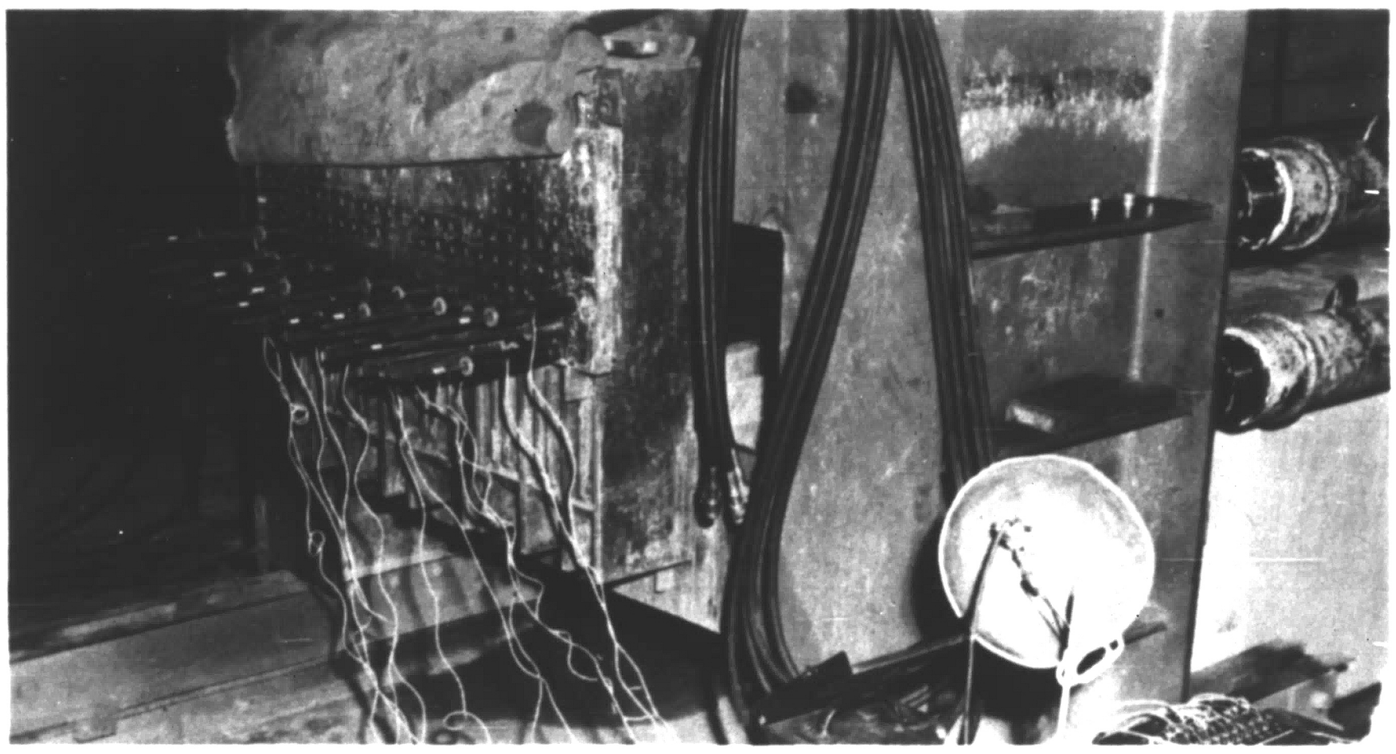

Figure 14 Dynamometer Installation for Second Beam Test

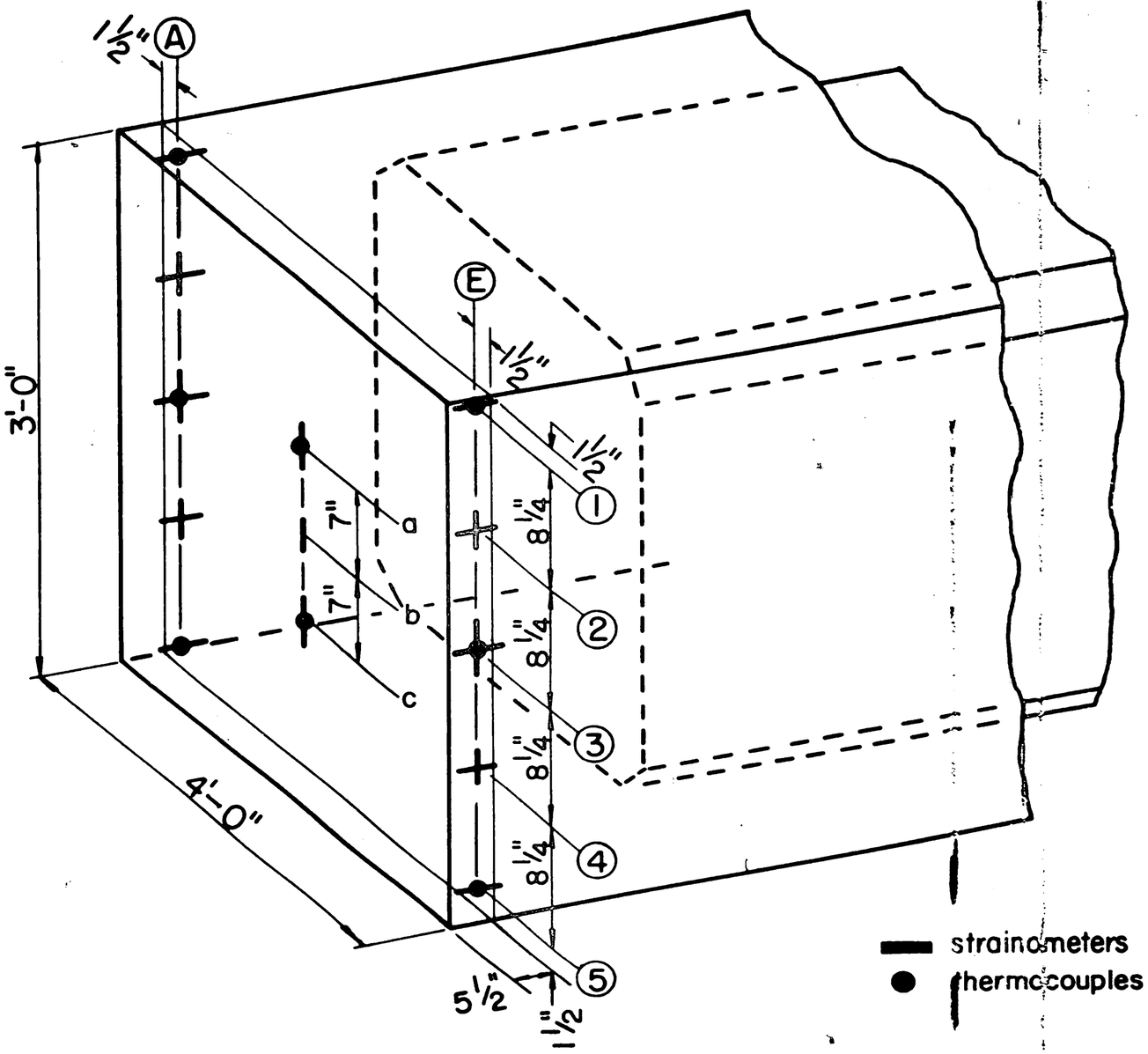

(a) LEFT END FACE AND SECTION I

Fig. 15 Location of Internal Instrumentation for Second Beam Test

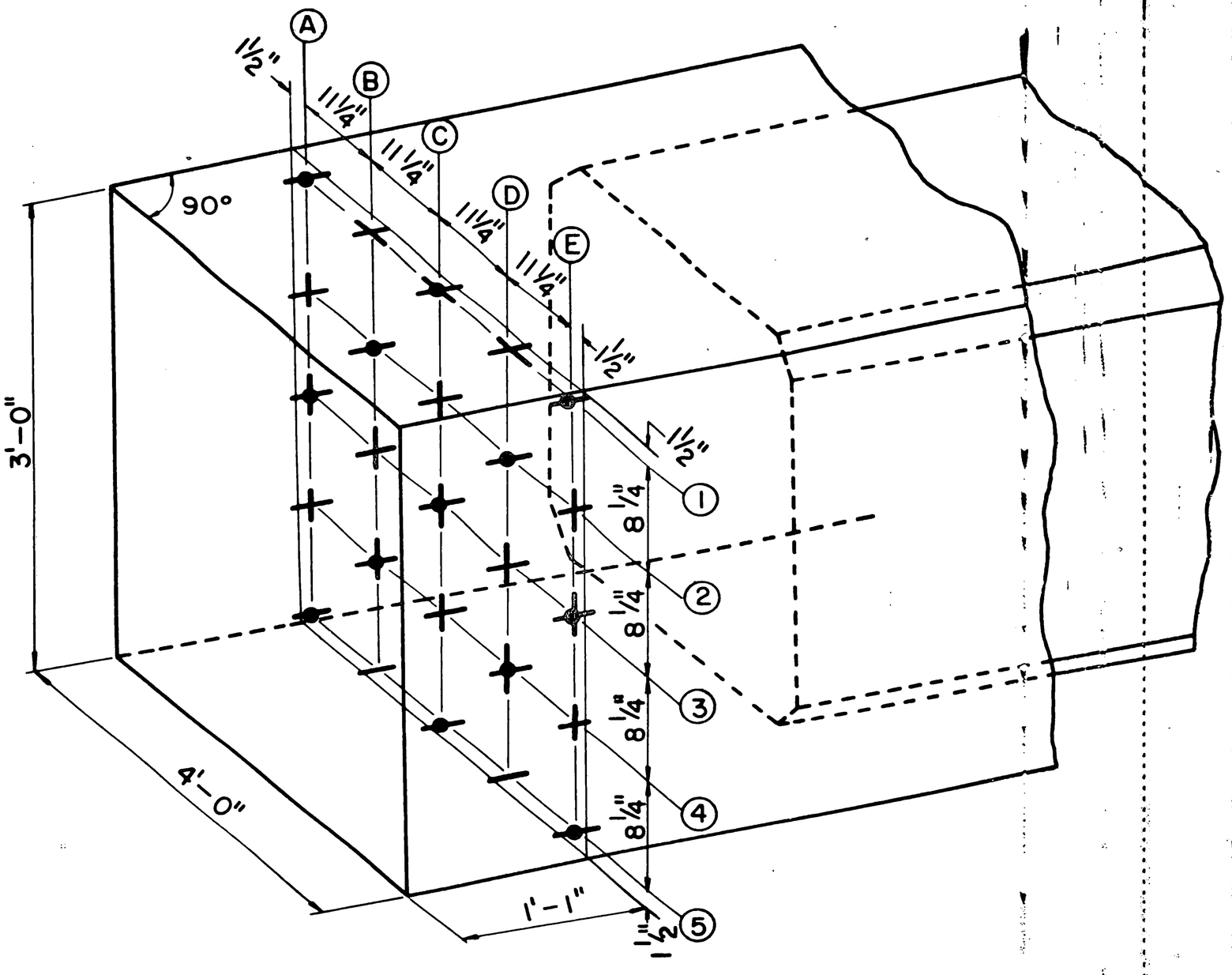

(b) SECTION II

Fig. 15 (cont'd)

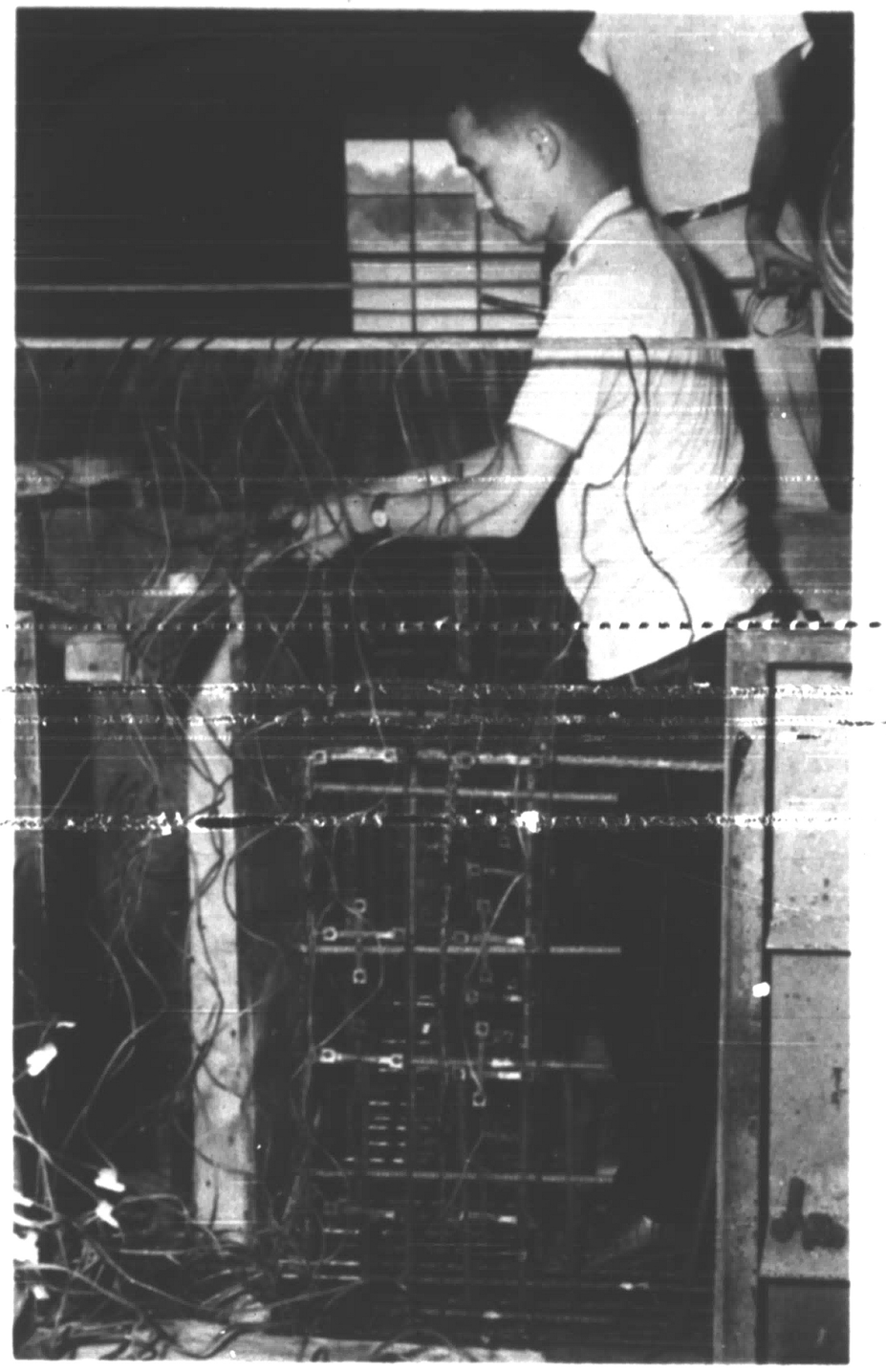

(a) Near Side View

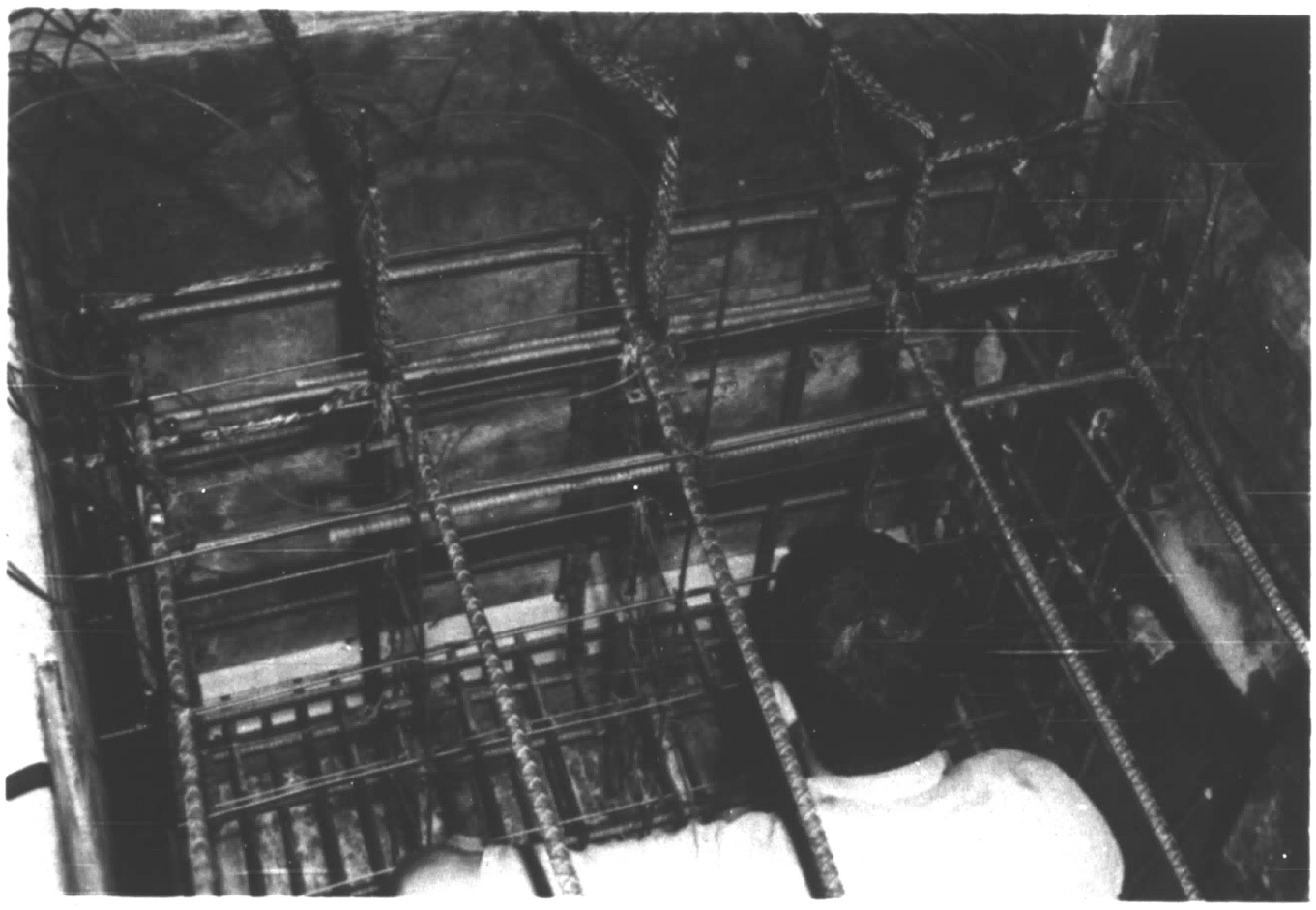

(b) Top View

Figure 16 Strainometers and Thermocouples in Place
Second Beam Test

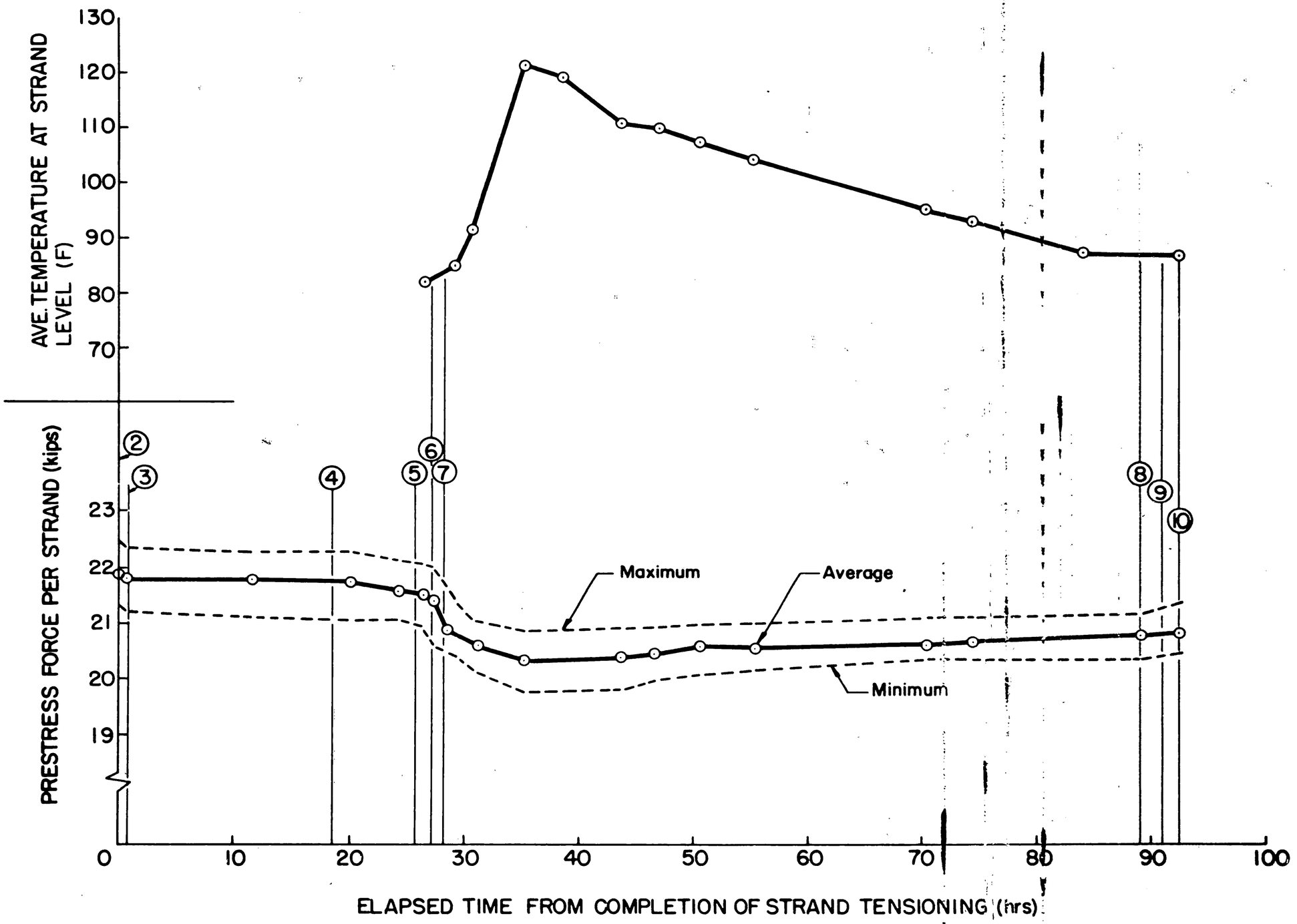

Fig. 17 Variation with Time of Prestress Force and Strand Temperature in Second Beam Test

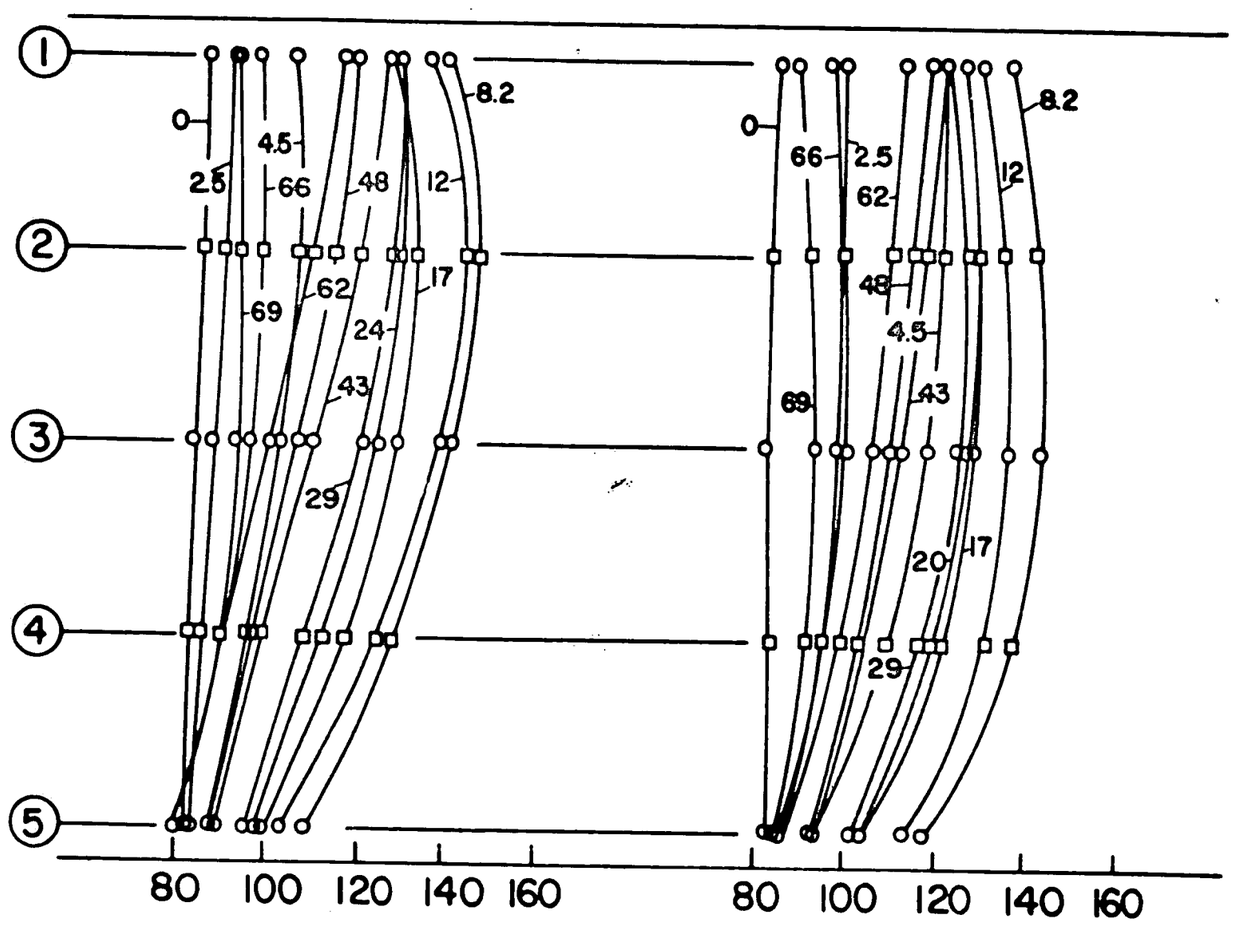

Fig. 18 Temperature Variation with Time in Section I - Second Beam Test

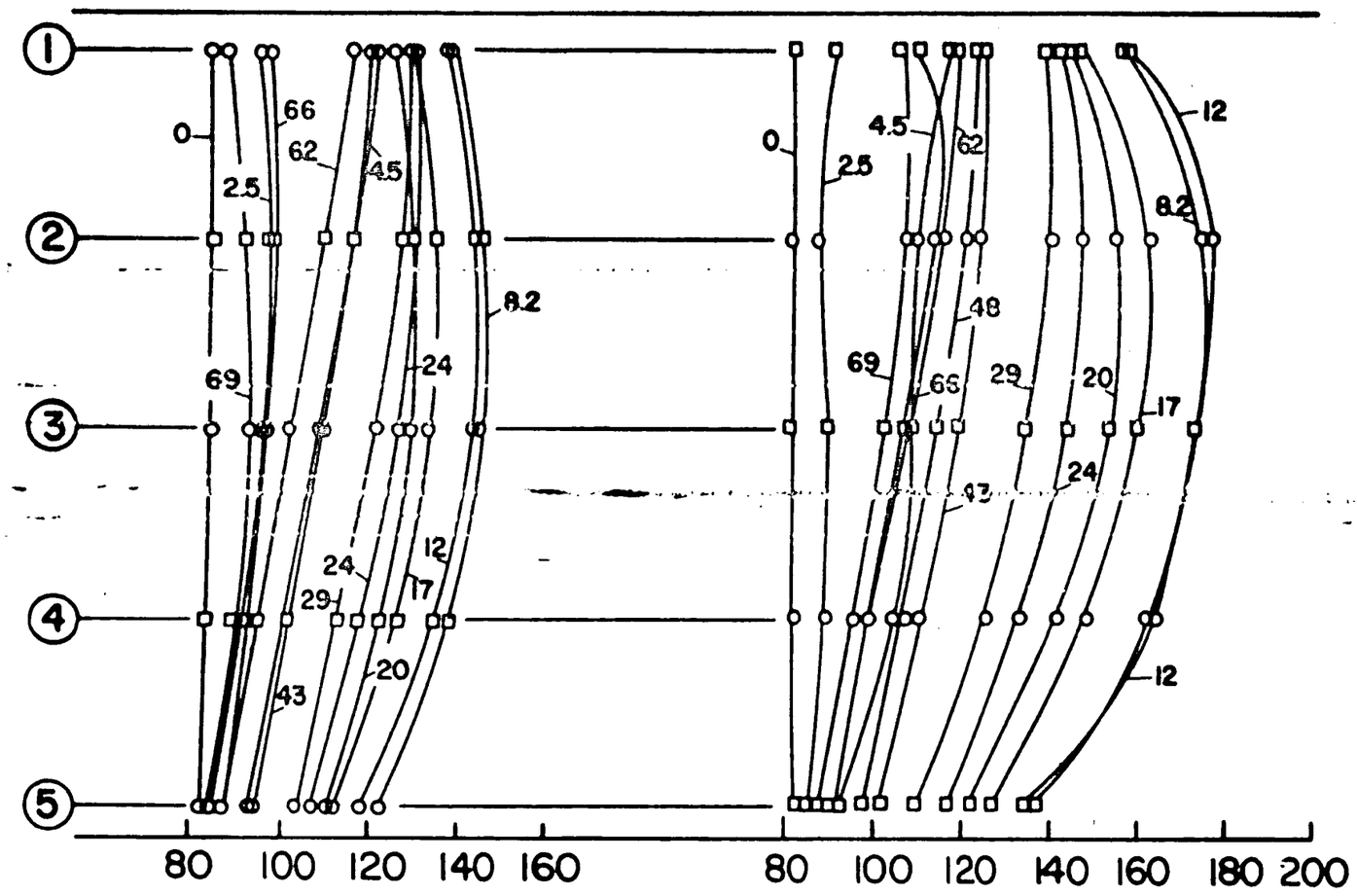

(a) LINE Ⓐ (b) LINE Ⓑ

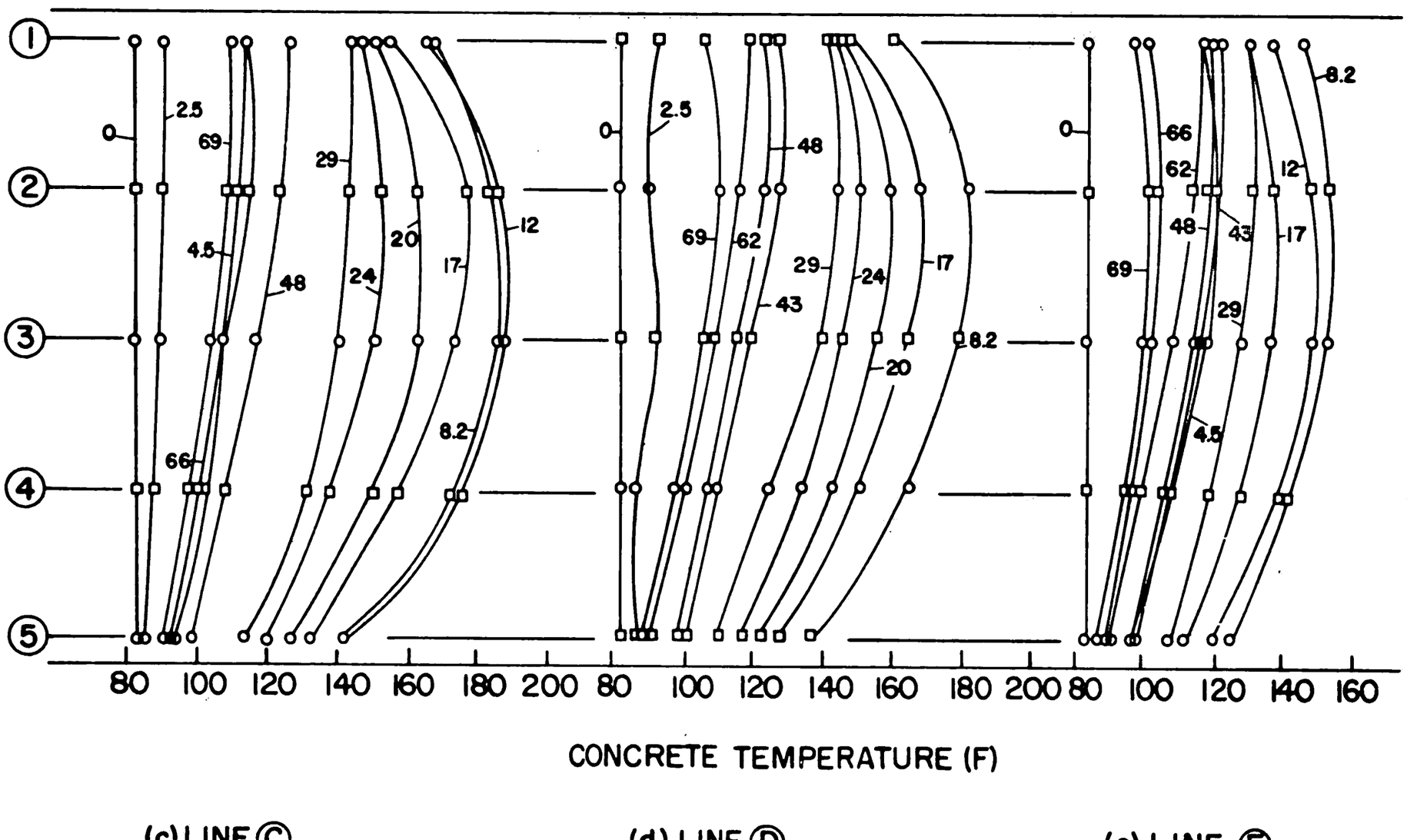

(c) LINE Ⓒ (d) LINE Ⓓ (e) LINE Ⓔ

Fig. 19 Temperature Variation with Time in Section II - Second Beam Test

Note: Numbers to curves designate elapsed time in hours

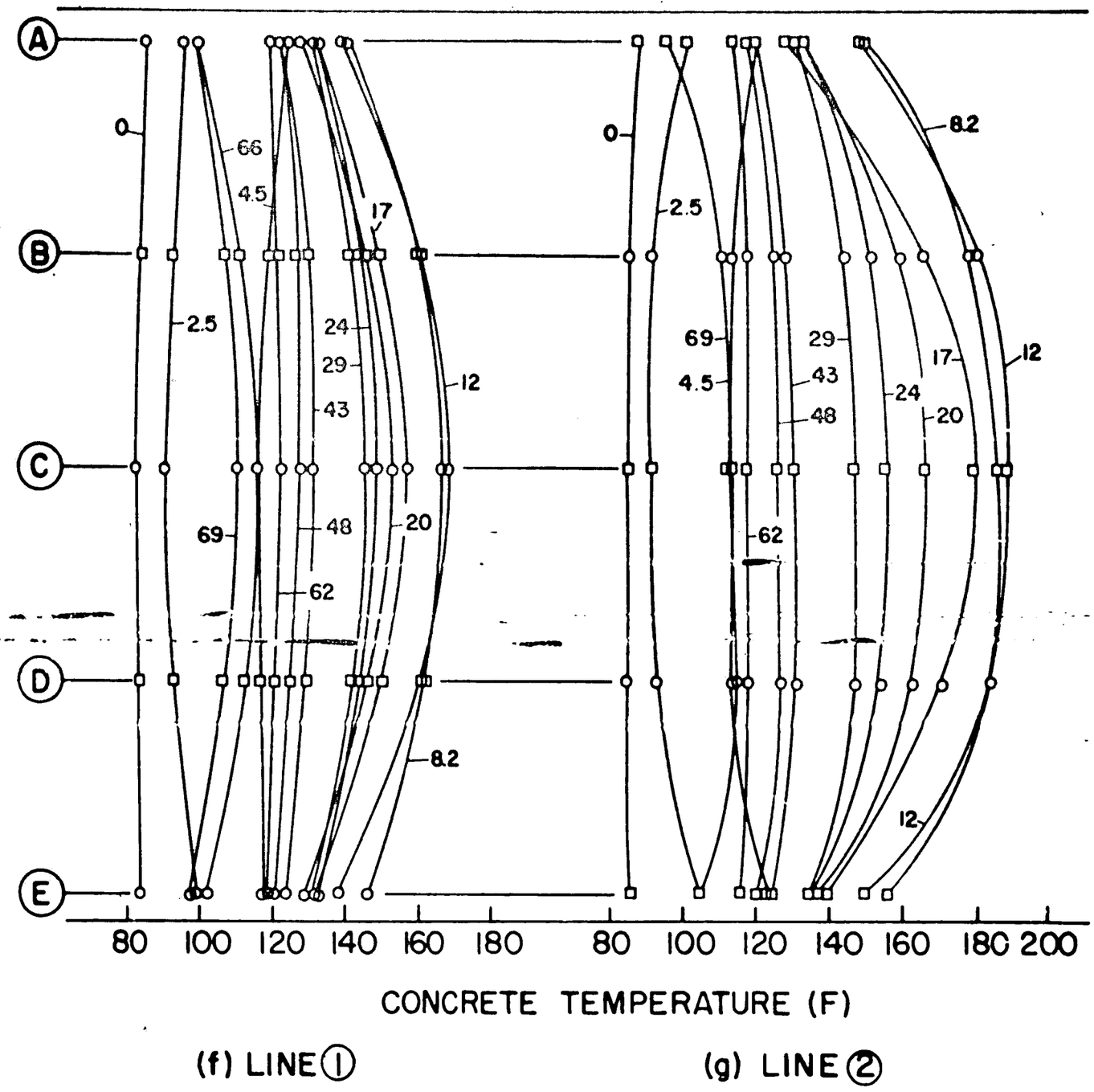
A
B
C
D
E
0
66
4.5
2.5
69
62
24
29
43
48
20
17
12
8.2
80 100 120 140 160 180
CONCRETE TEMPERATURE (F)
(f) LINE ①
0
2.5
69
4.5
62
29
43
48
24
20
17
12
8.2
80 100 120 140 160 180 200
CONCRETE TEMPERATURE (F)
(g) LINE ②

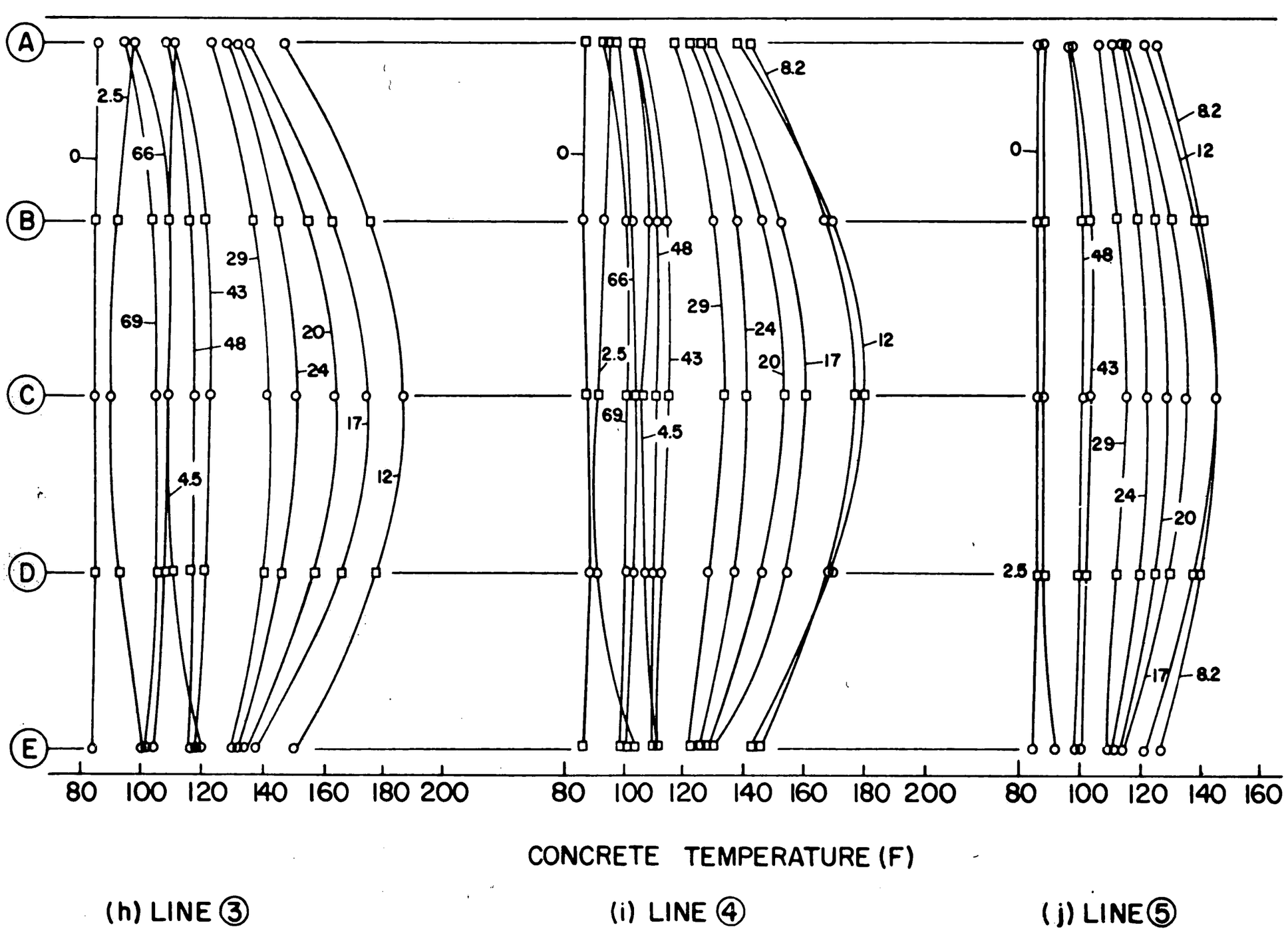
A
B
C
D
E
0
2.5
66
69
4.5
29
43
48
20
24
17
12
8.2
80 100 120 140 160 180 200
(h) LINE ③
0
66
48
2.5
69
4.5
29
24
20
17
12
8.2
80 100 120 140 160 180 200
CONCRETE TEMPERATURE (F)
(i) LINE ④
0
2.5
48
43
29
24
20
17
12
8.2
80 100 120 140 160
(j) LINE ⑤

Fig. 19 (cont'd)

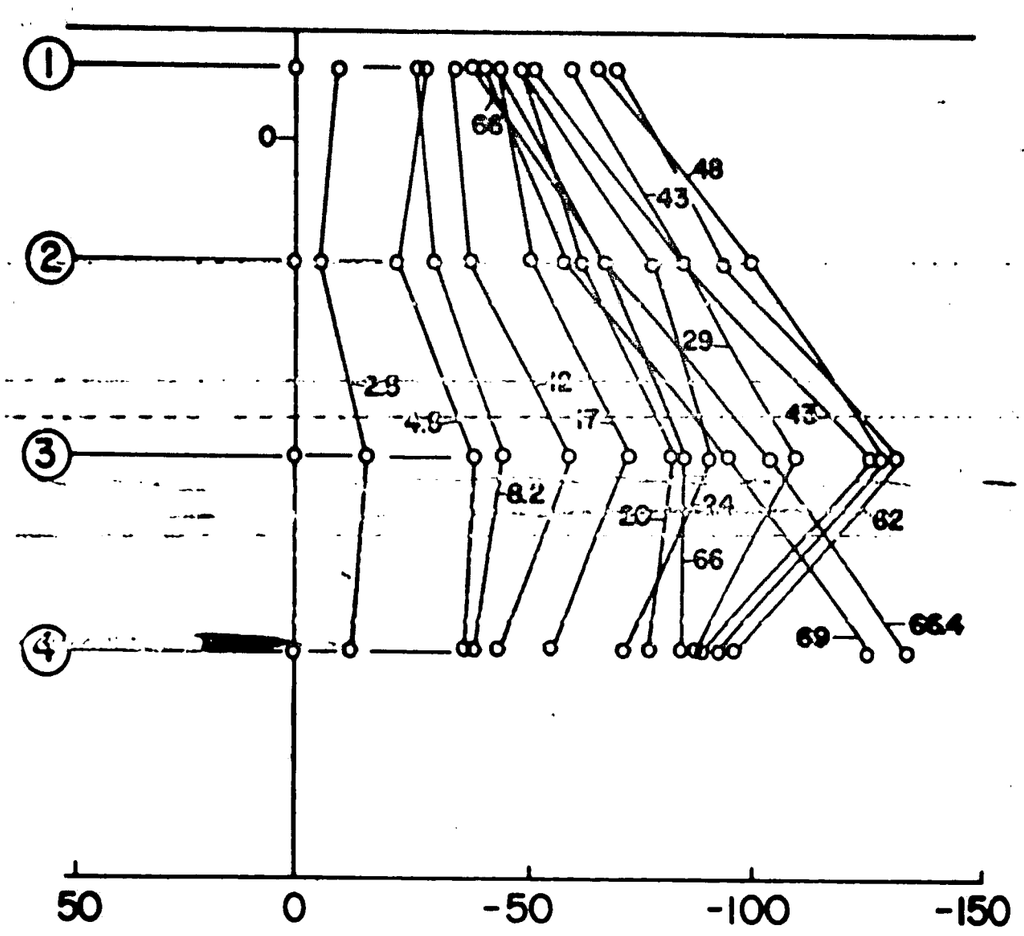

(a) LINE Ⓐ

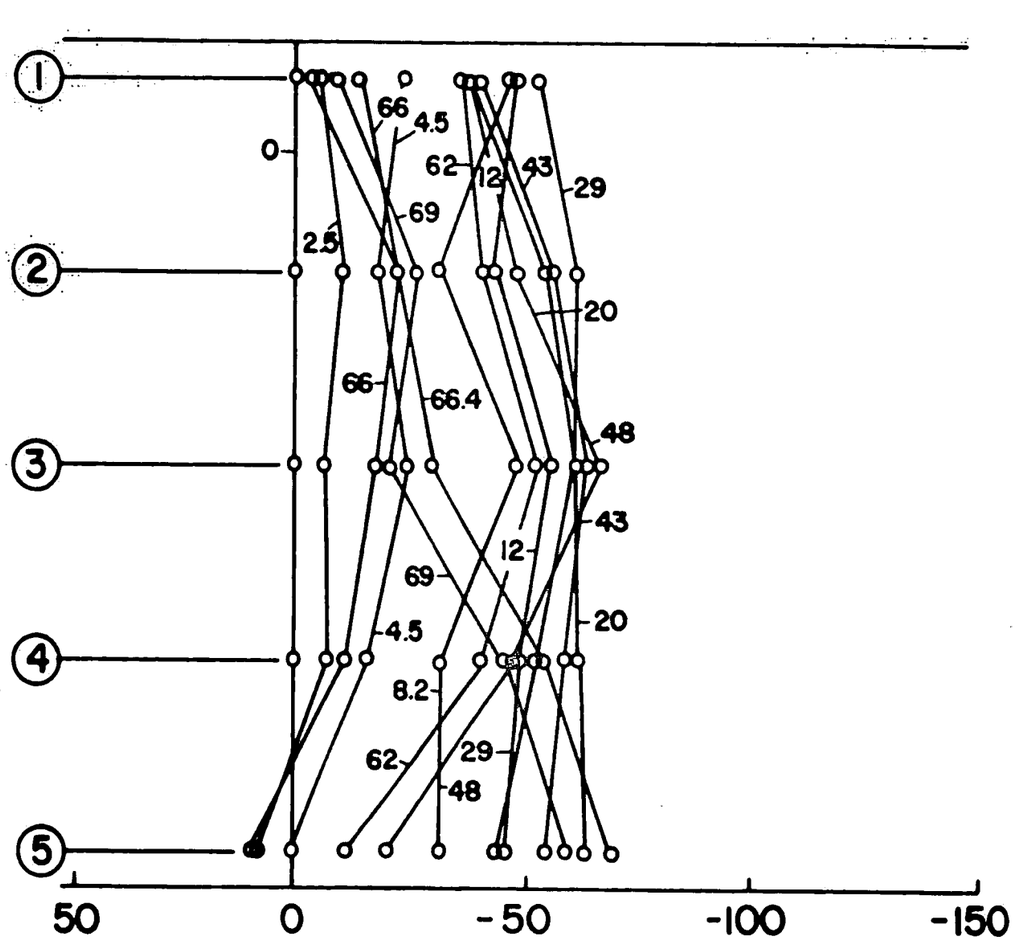

(b) LINE Ⓔ

Fig. 20 Apparent Longitudinal Strain in Section I - Second Beam Test

Note: Numbers to curves designate elapsed time in hours

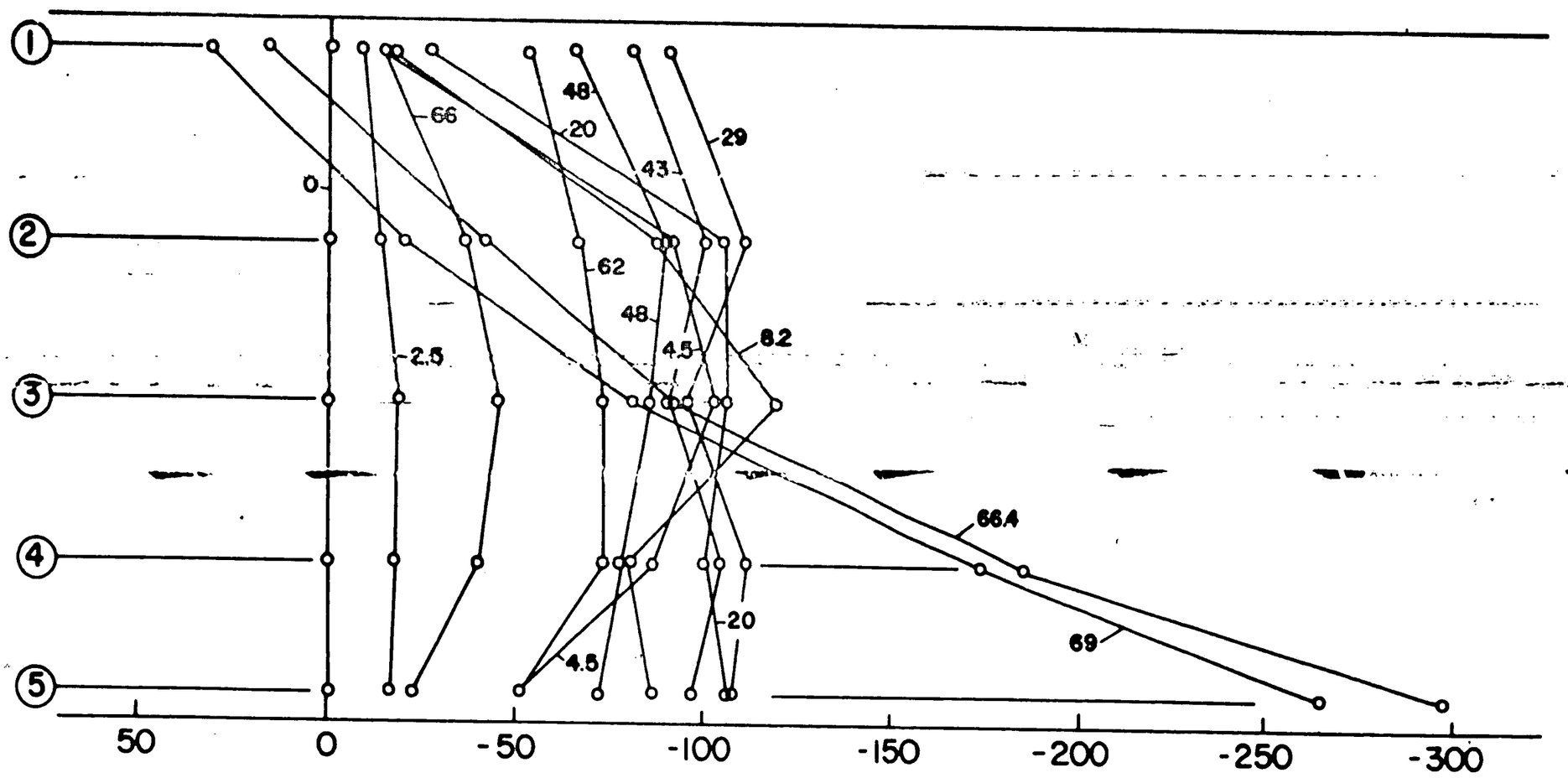

(a) LINE Ⓐ

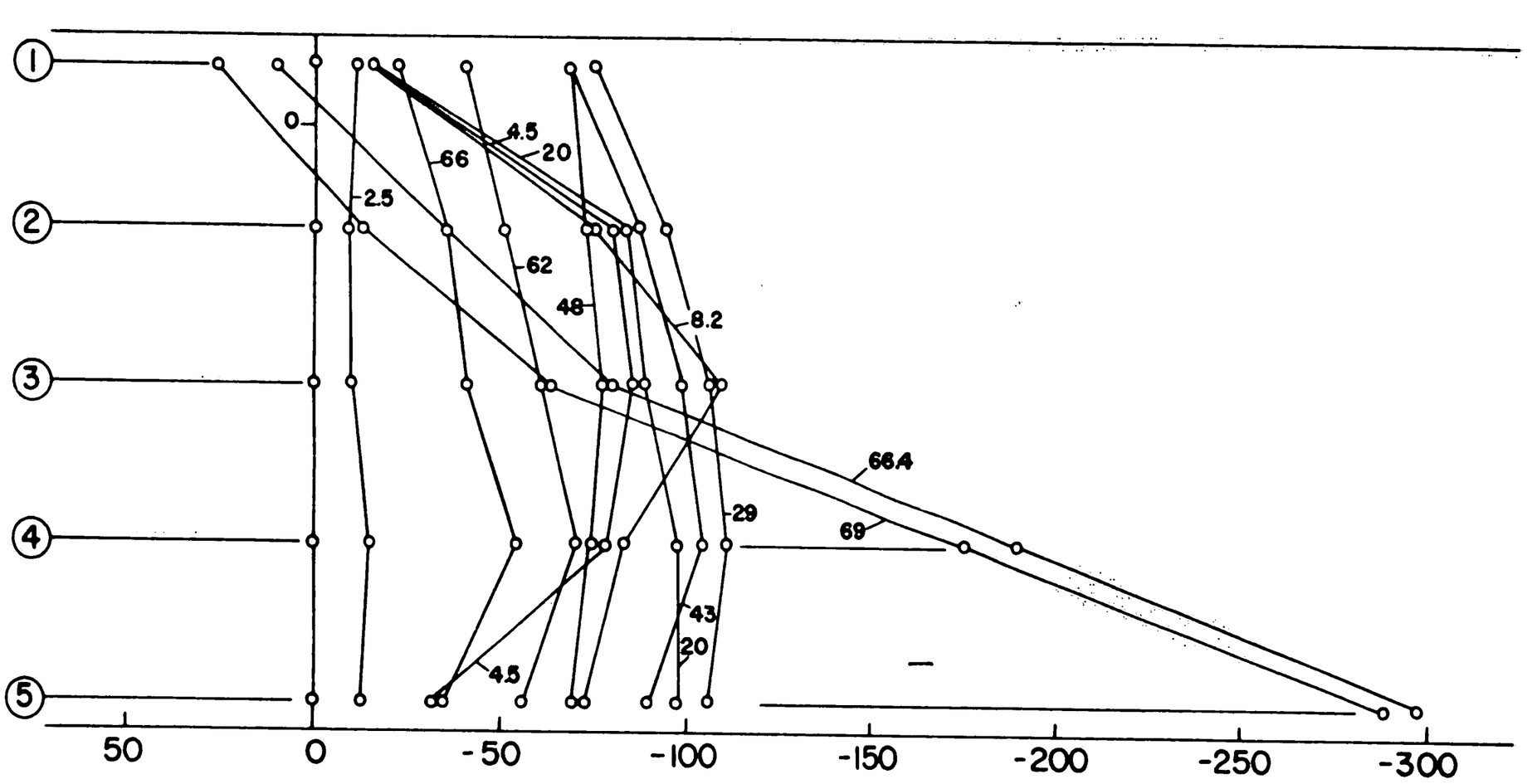

(b) LINE Ⓔ

Note: Numbers to curves designate elapsed time in hours

Fig. 21 Apparent Longitudinal Strain in Section II - Second Beam Test

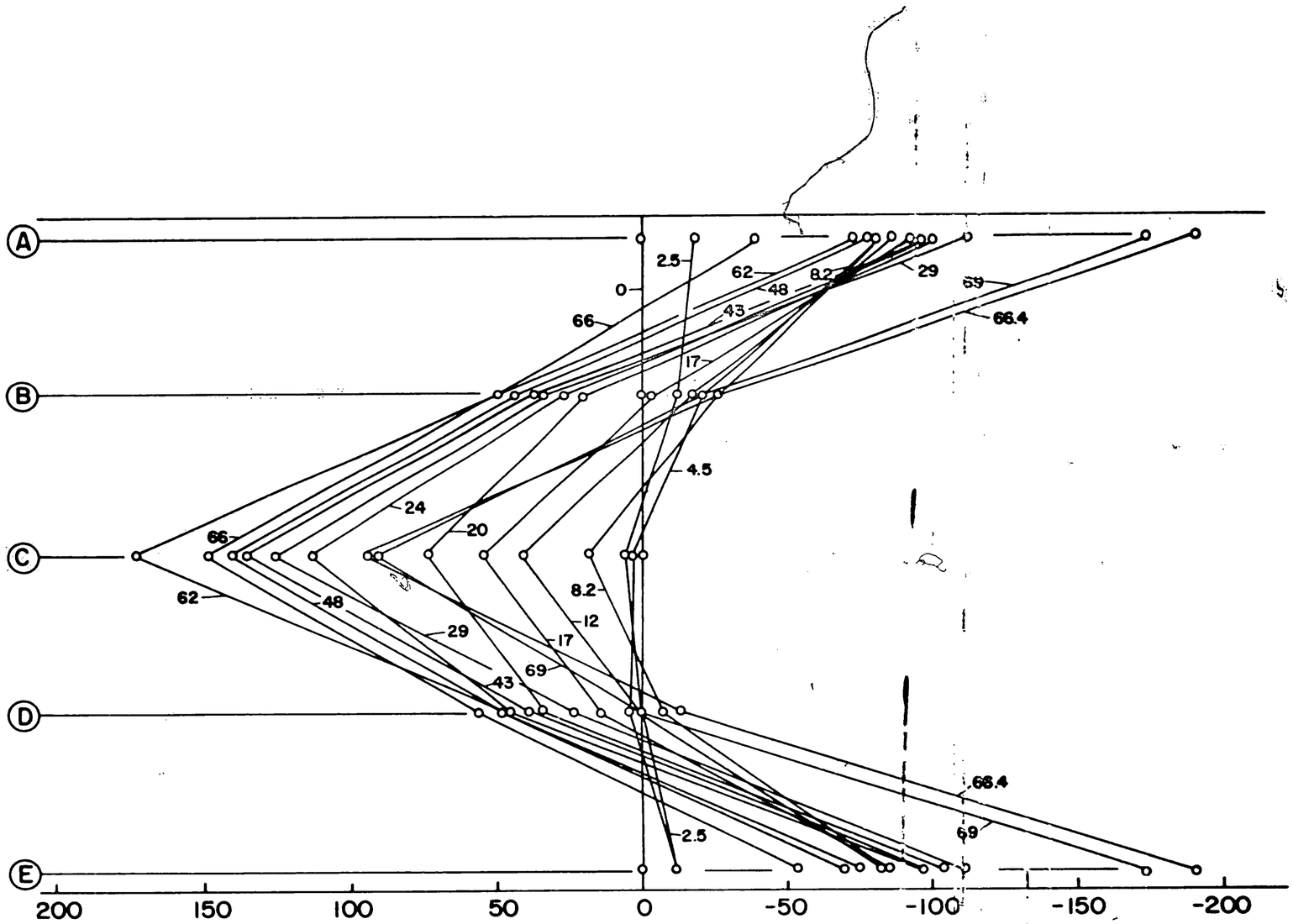

(f) LINE ④

Fig. 21 (cont'd)

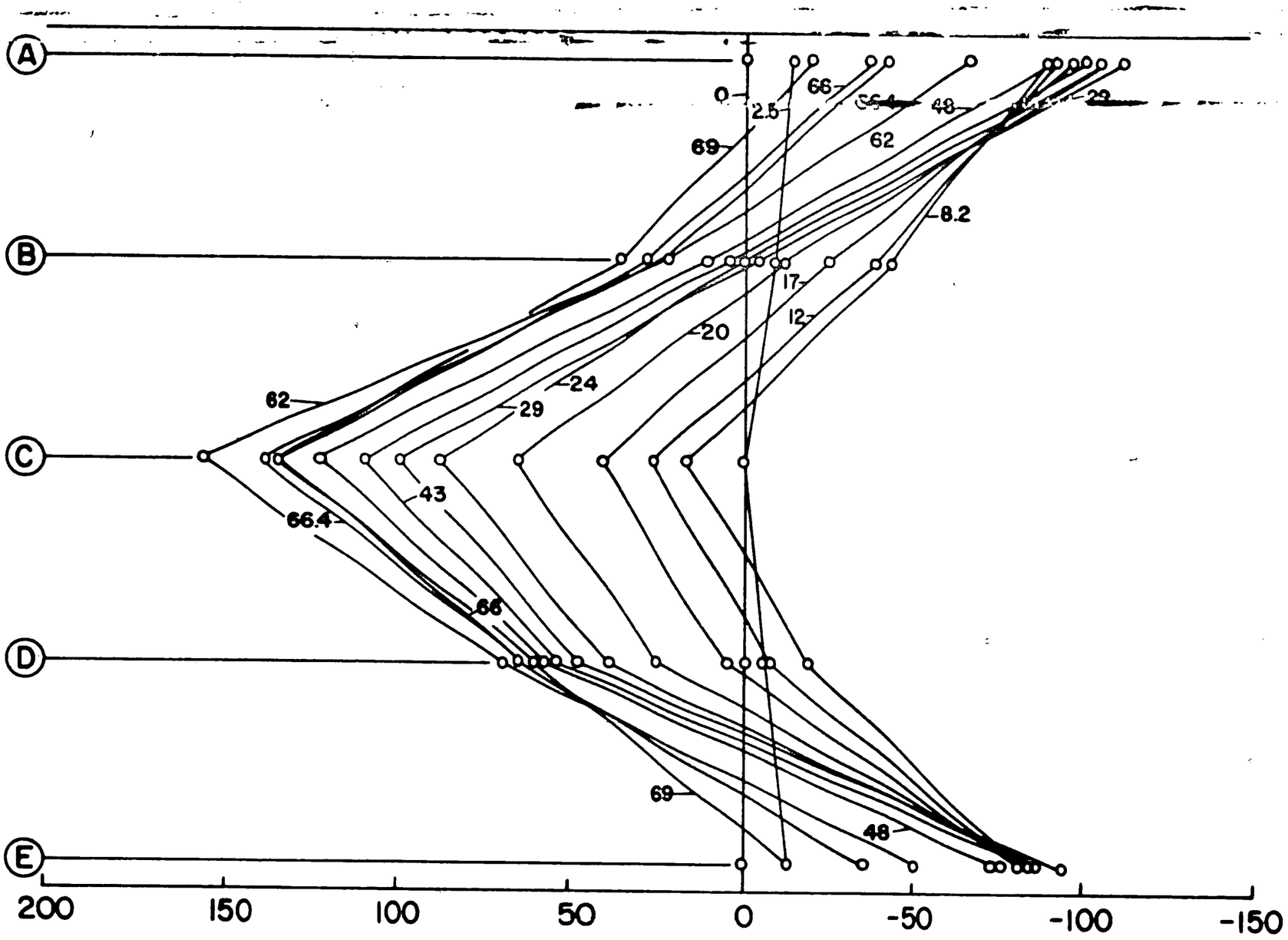

(e) LINE ②

Fig. 21 (cont'd)

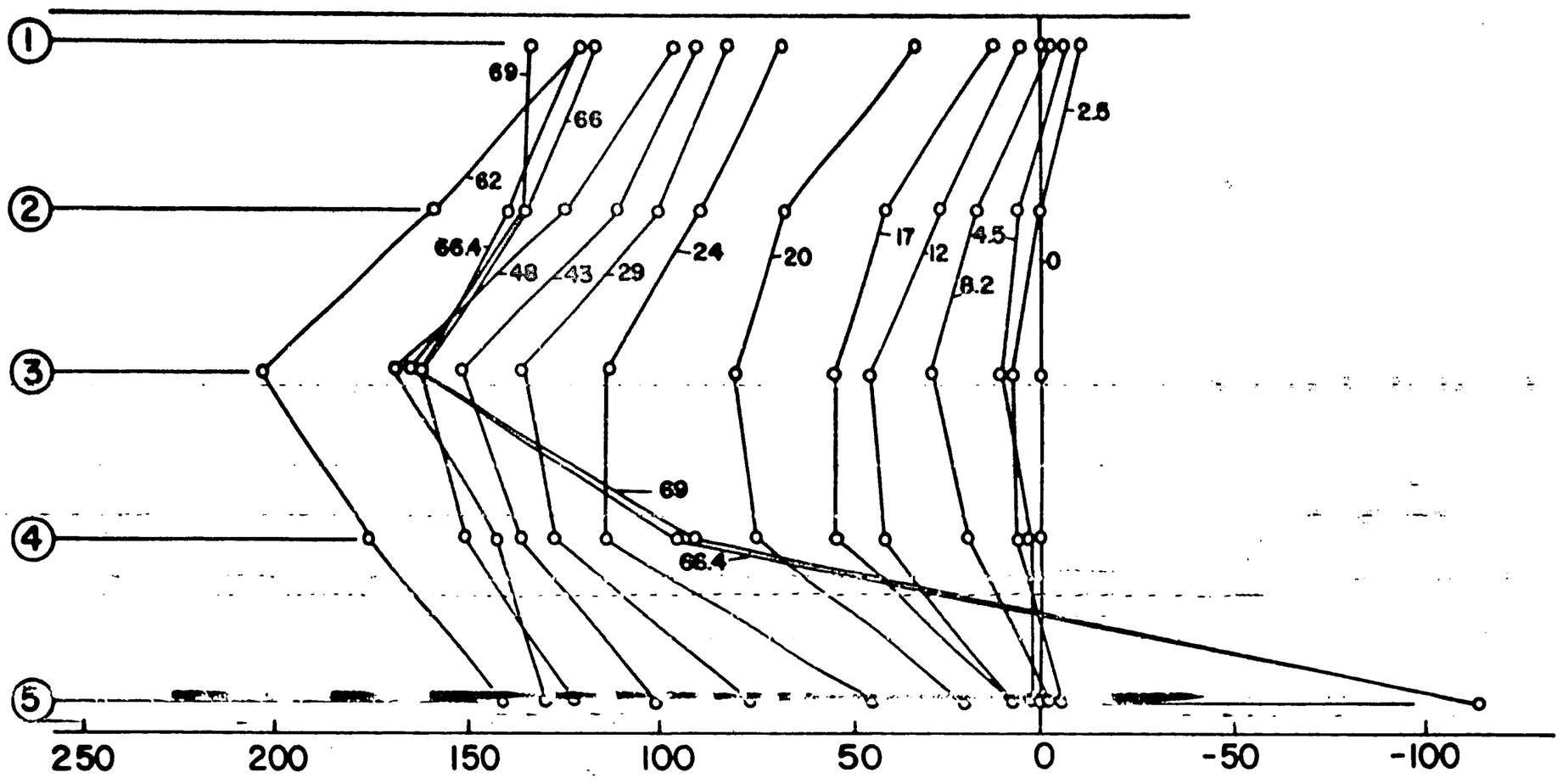

(c) LINE Ⓒ

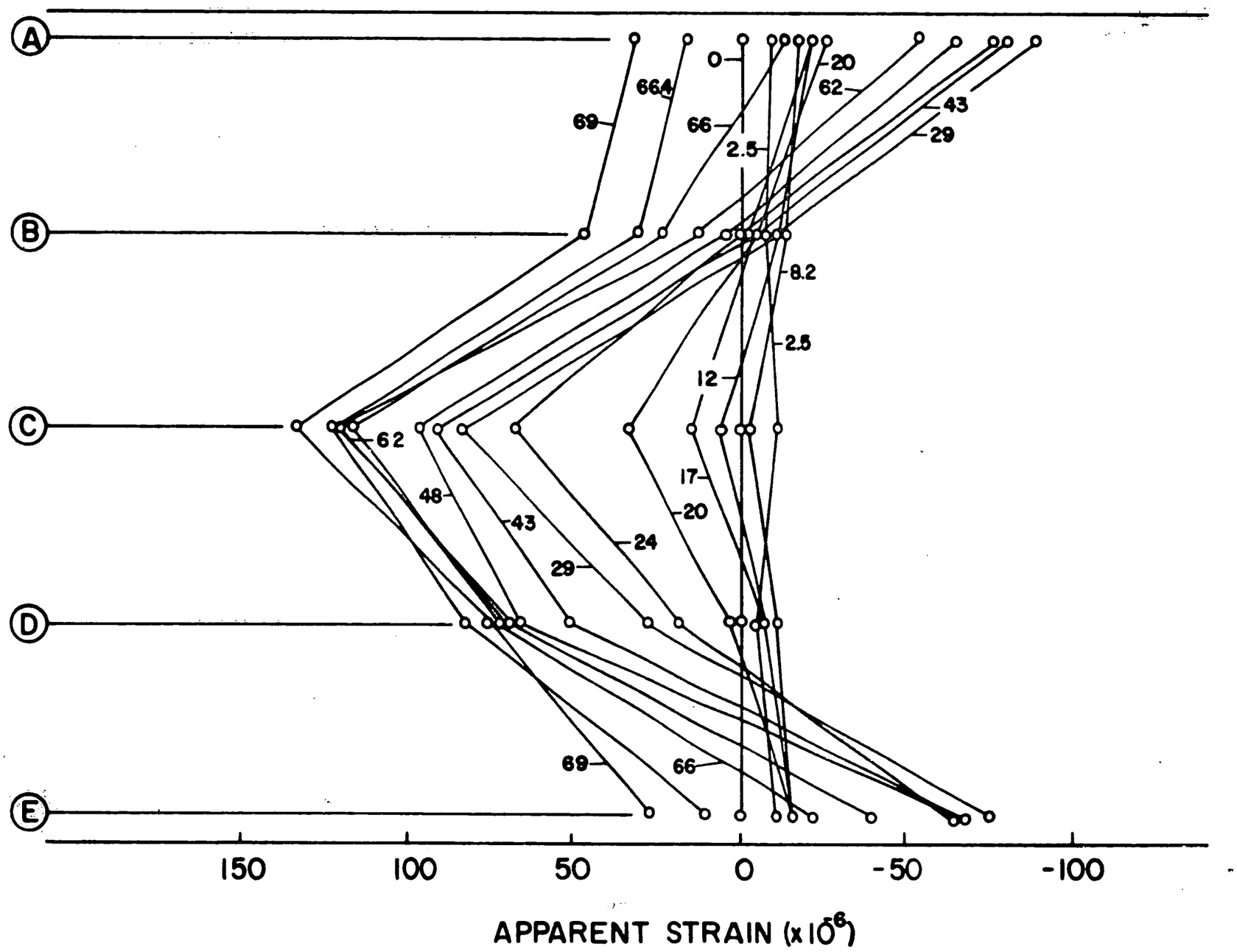

(d) LINE ①

Fig. 21 (cont'd)

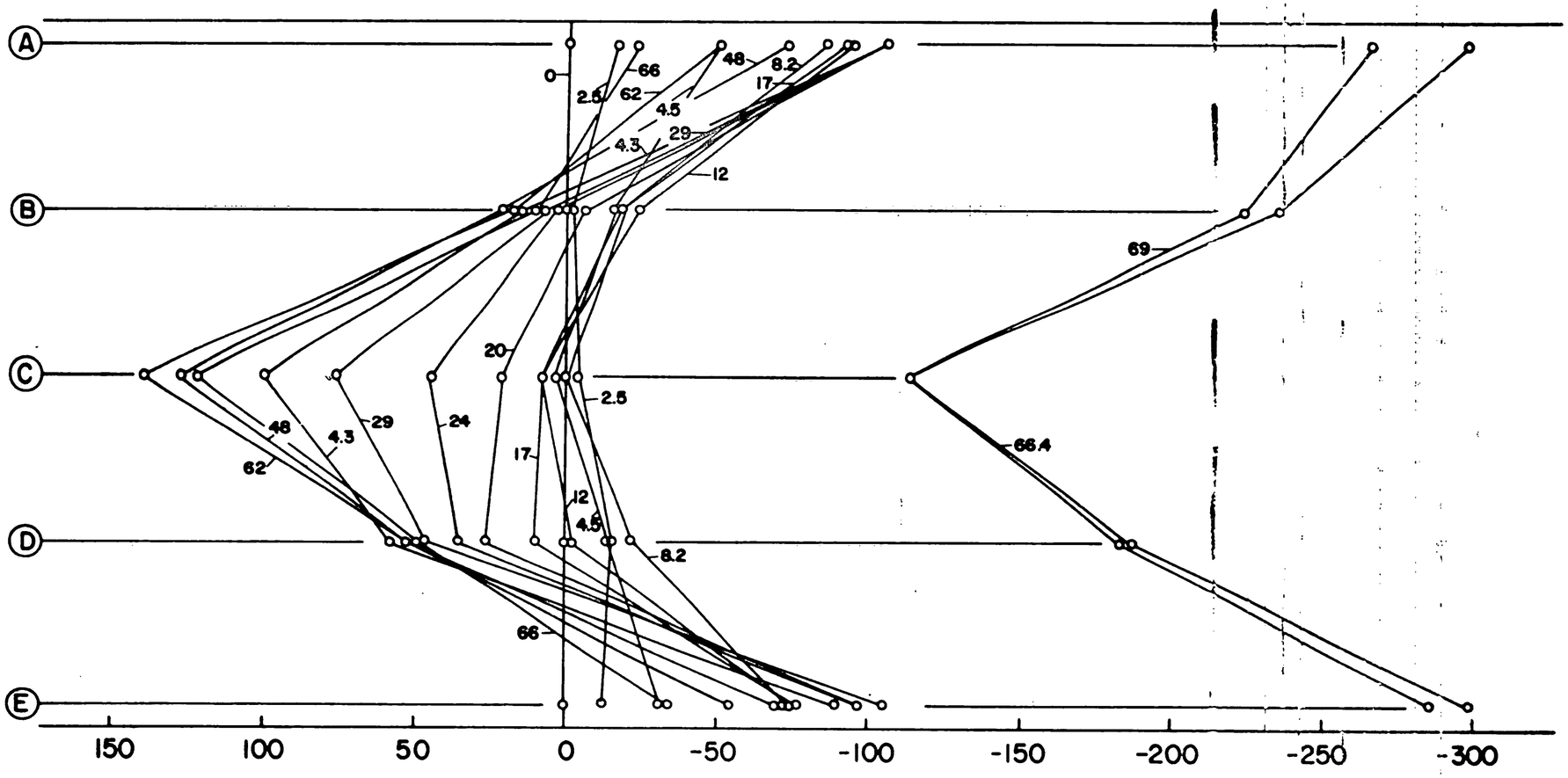

(g) LINE ⑤

Fig. 21 (cont'd)

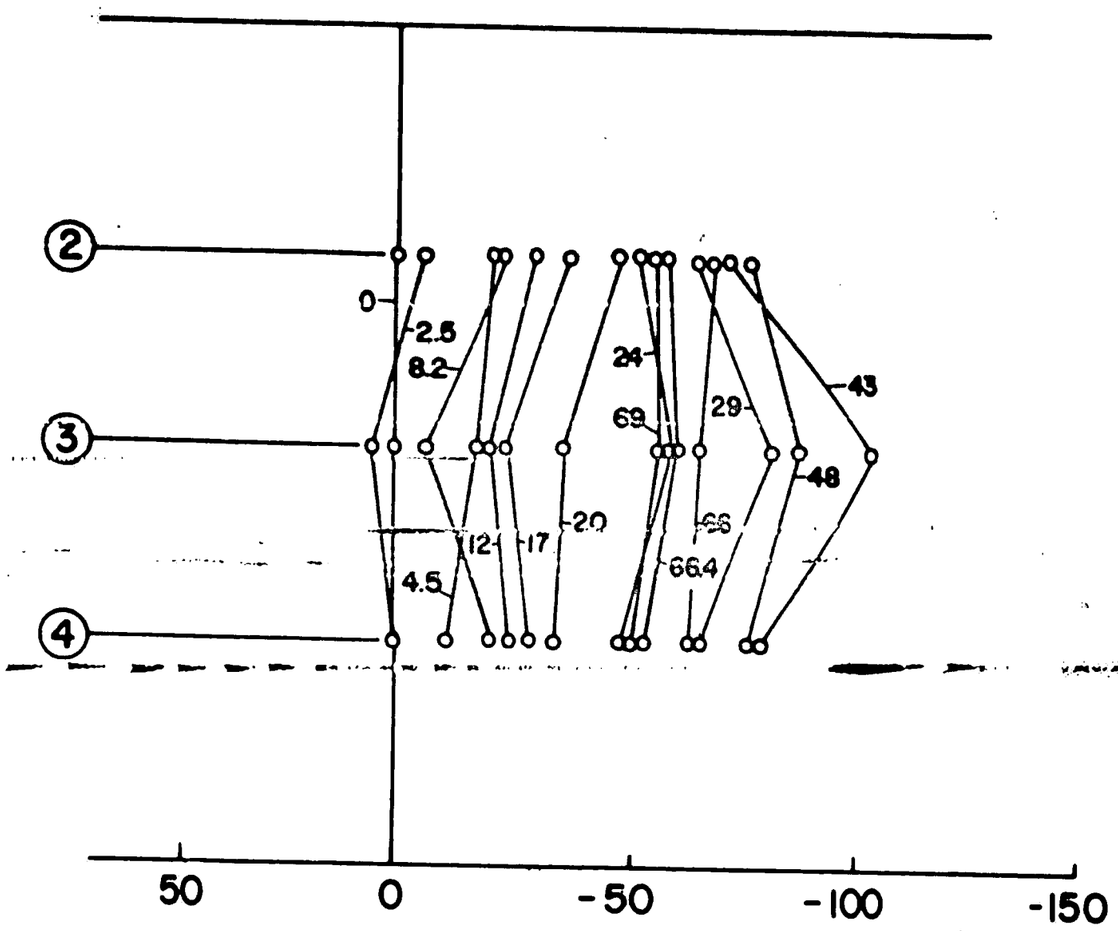

(a) LINE Ⓐ

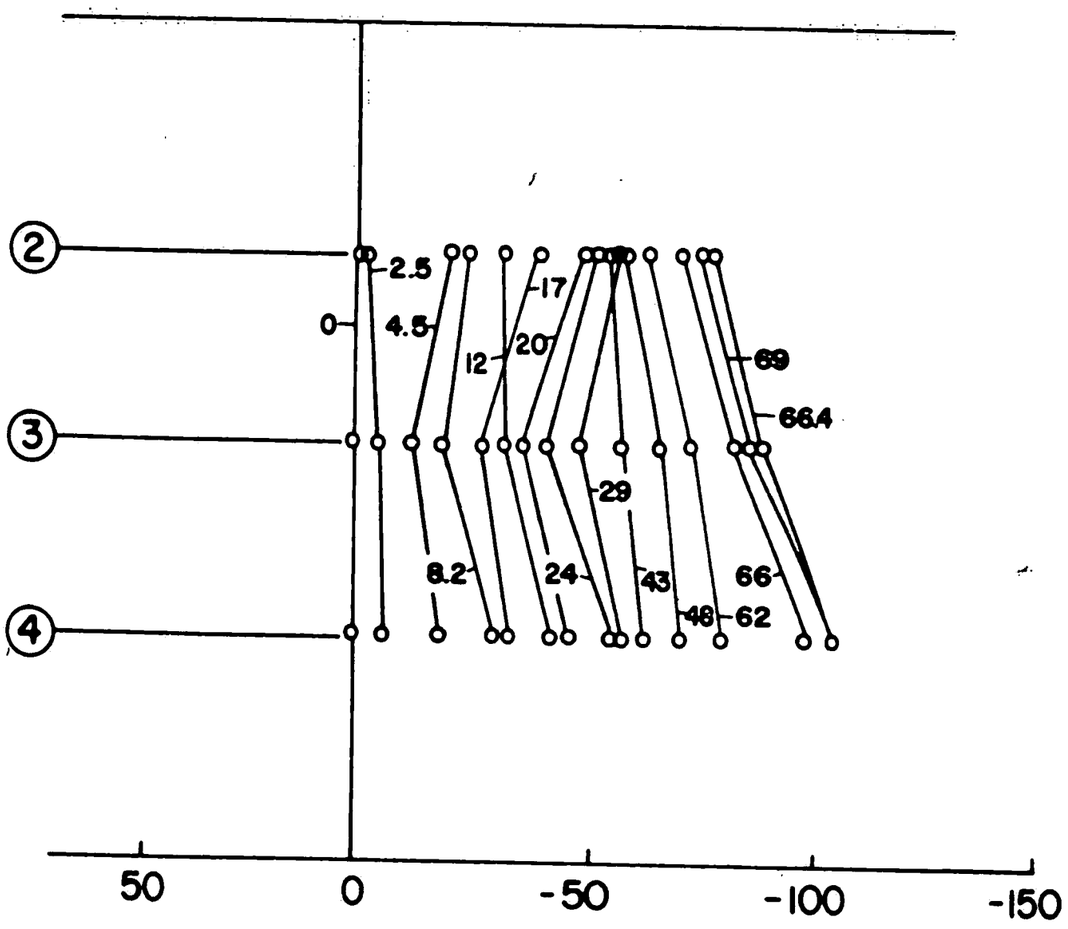

(b) LINE Ⓔ

Fig. 22 Apparent Vertical Strain in Section I - Second Beam Test

Note: Numbers to curves designate elapsed time in hours

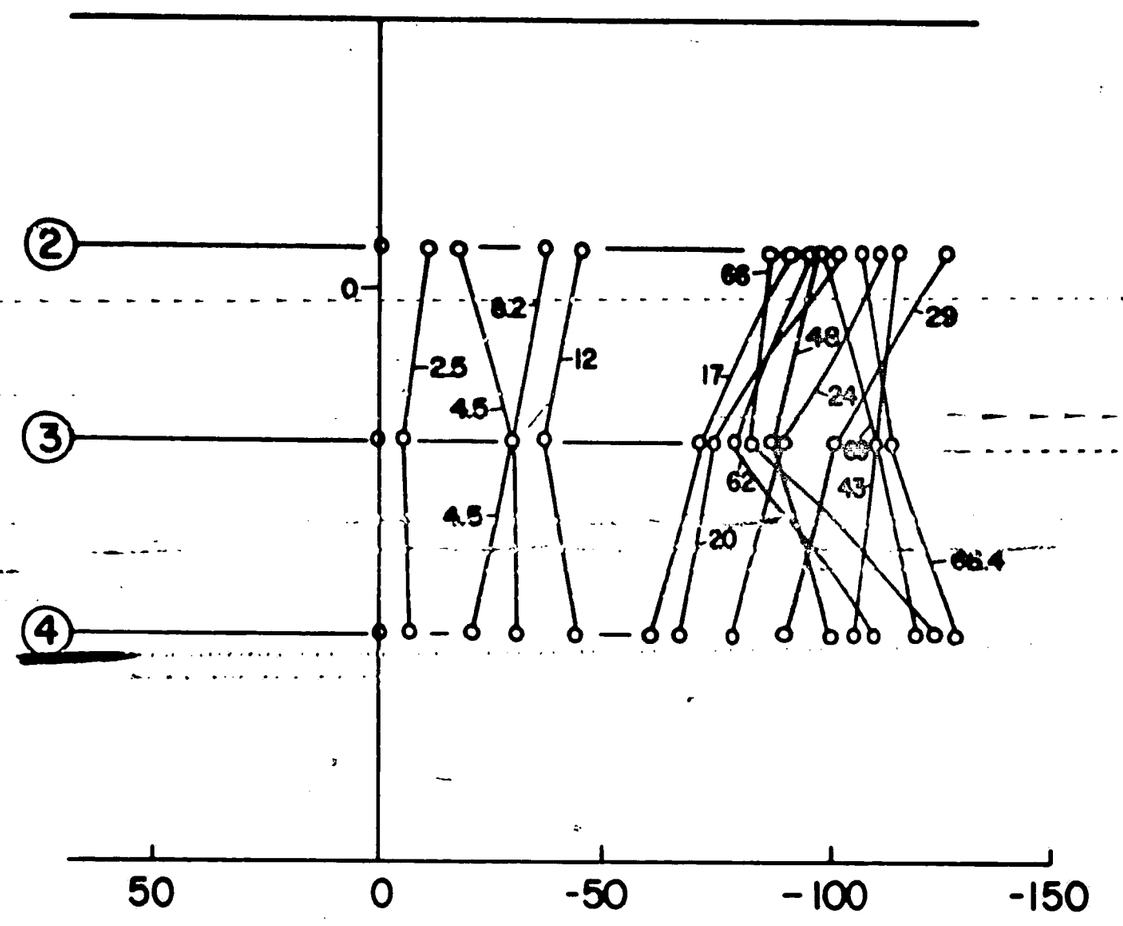

(a) LINE Ⓐ

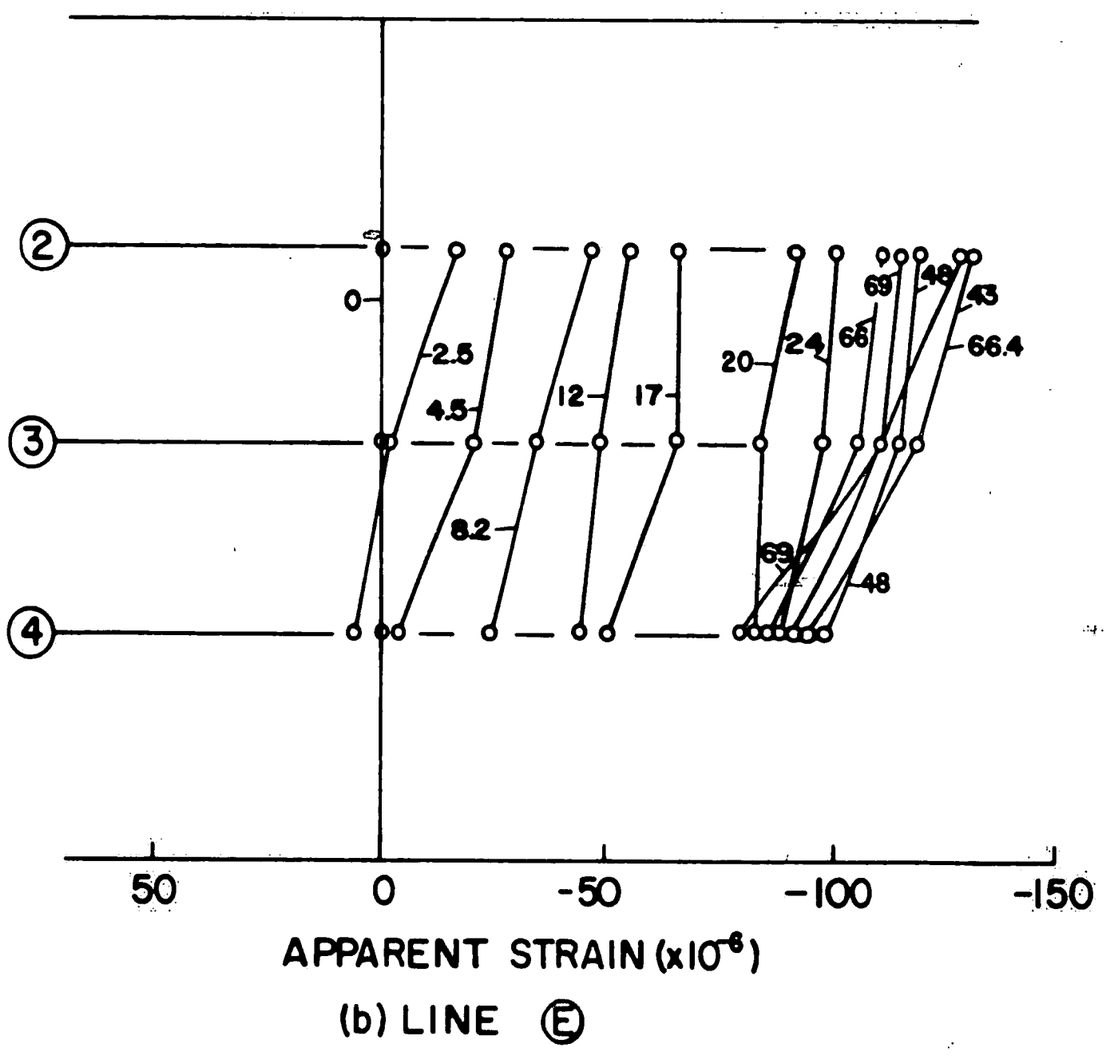

(b) LINE Ⓔ

Fig. 23 Apparent Vertical Strain in Section II - Second Beam Test

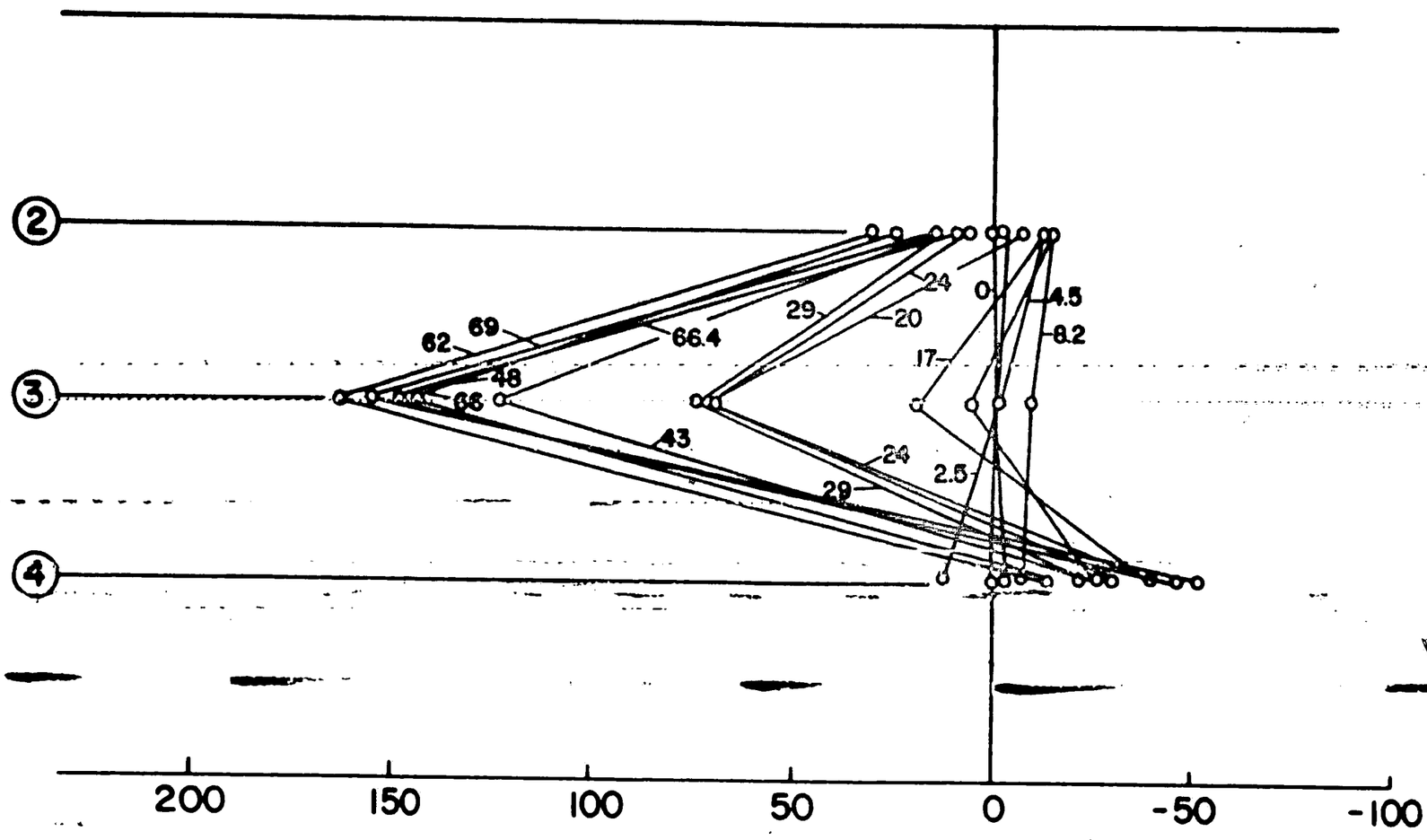

APPARENT STRAIN ($\times 10^{-6}$)

(c) LINE ©

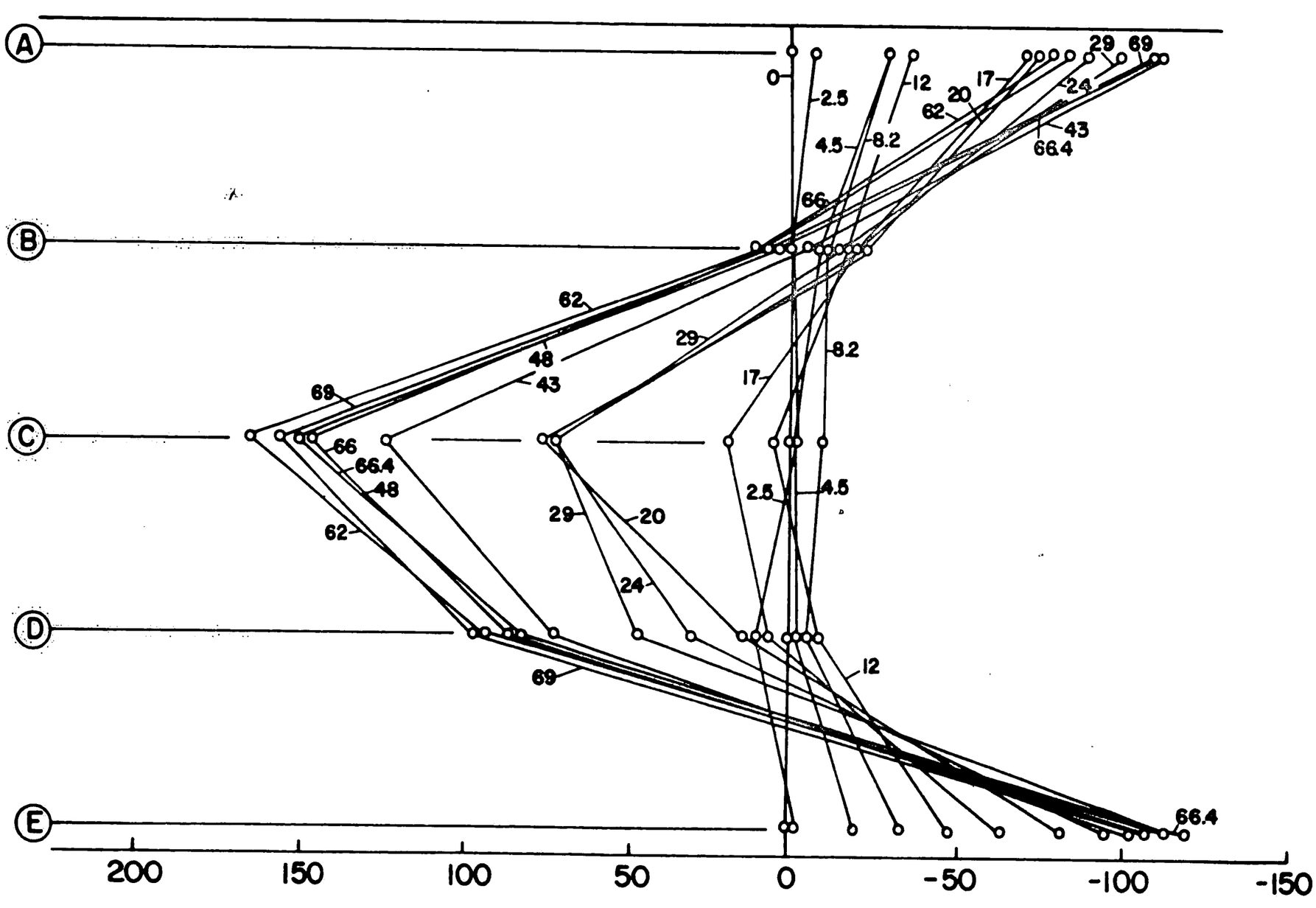

APPARENT STRAIN ($\times 10^{-6}$)

(d) LINE ③

Fig. 23 (cont'd)

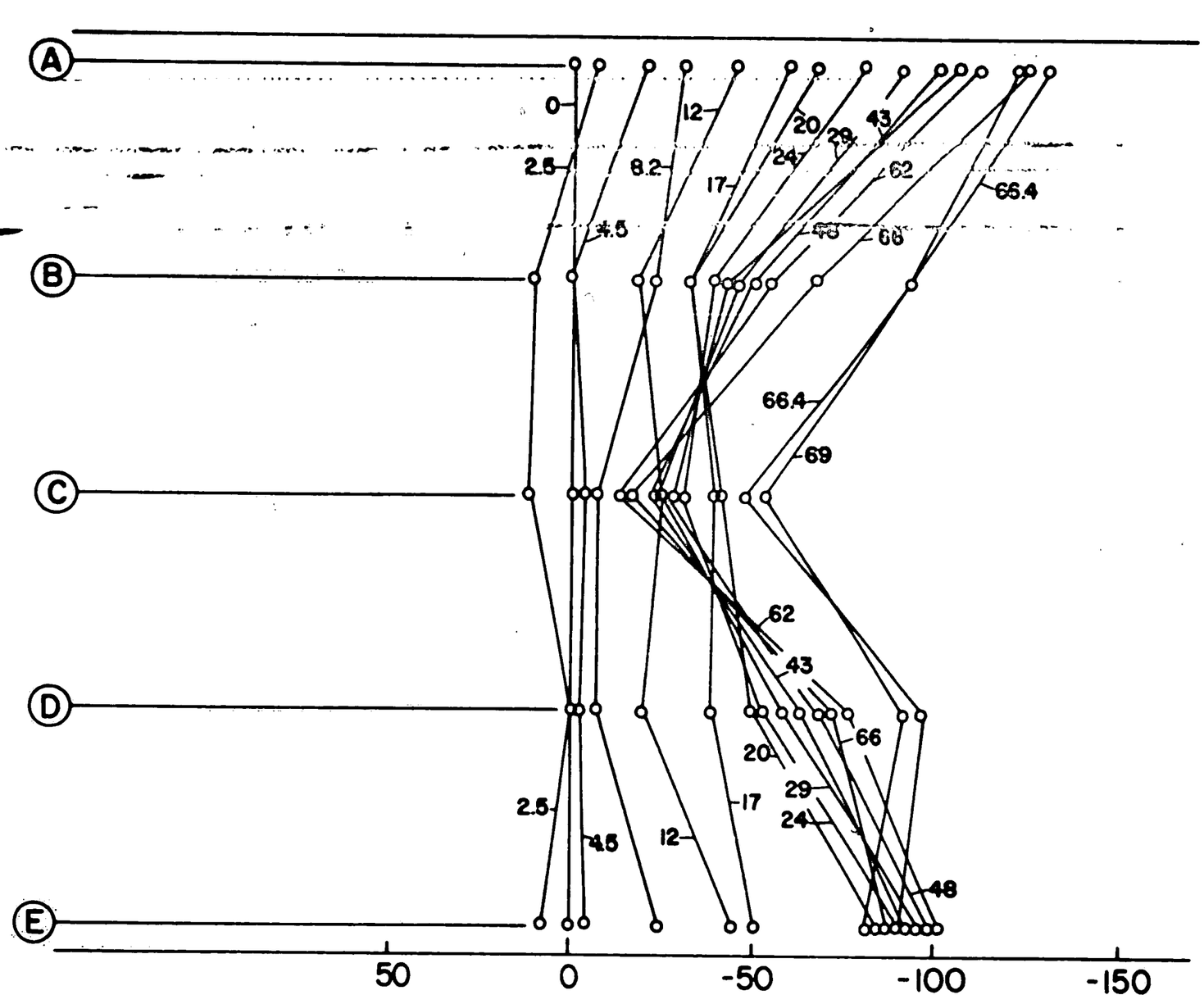

(e) LINE ④

Fig. 23 (cont'd)

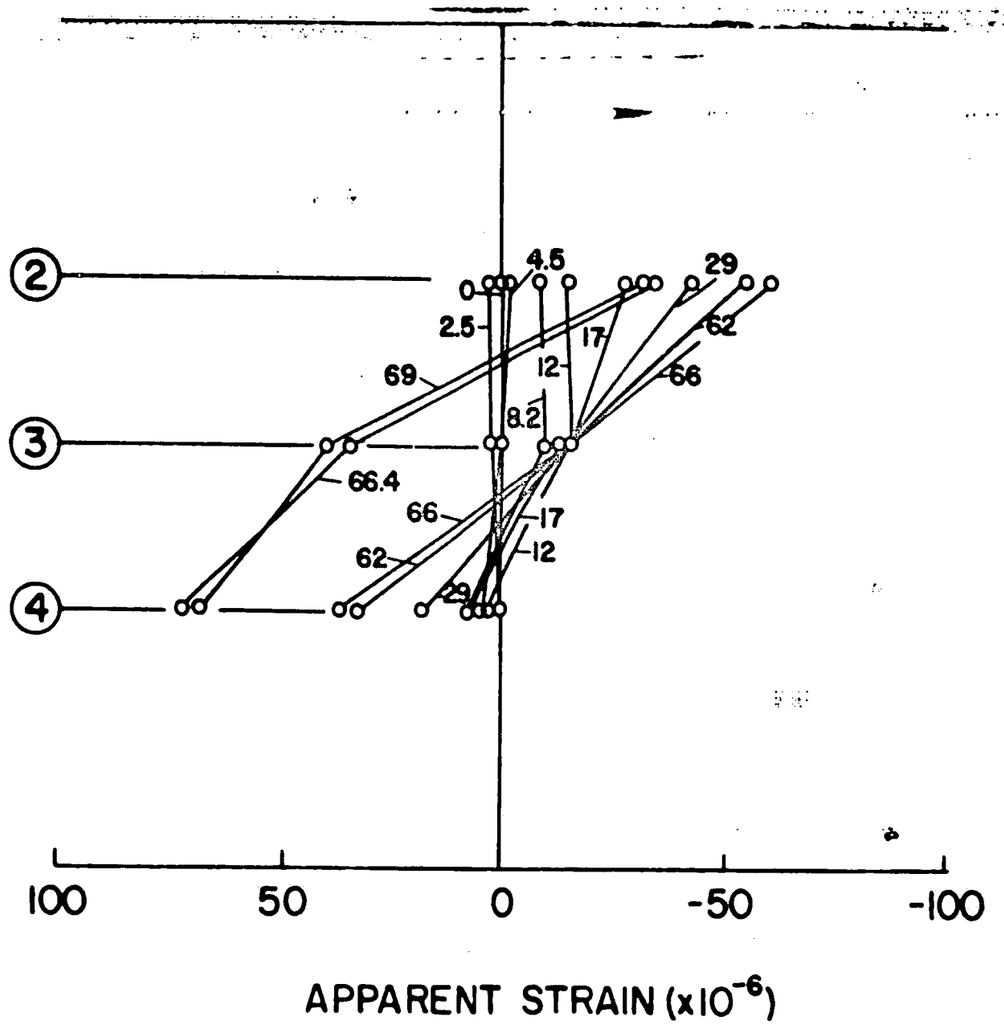

Fig. 24 Apparent Vertical Strain in Left End Face - Second Beam Test

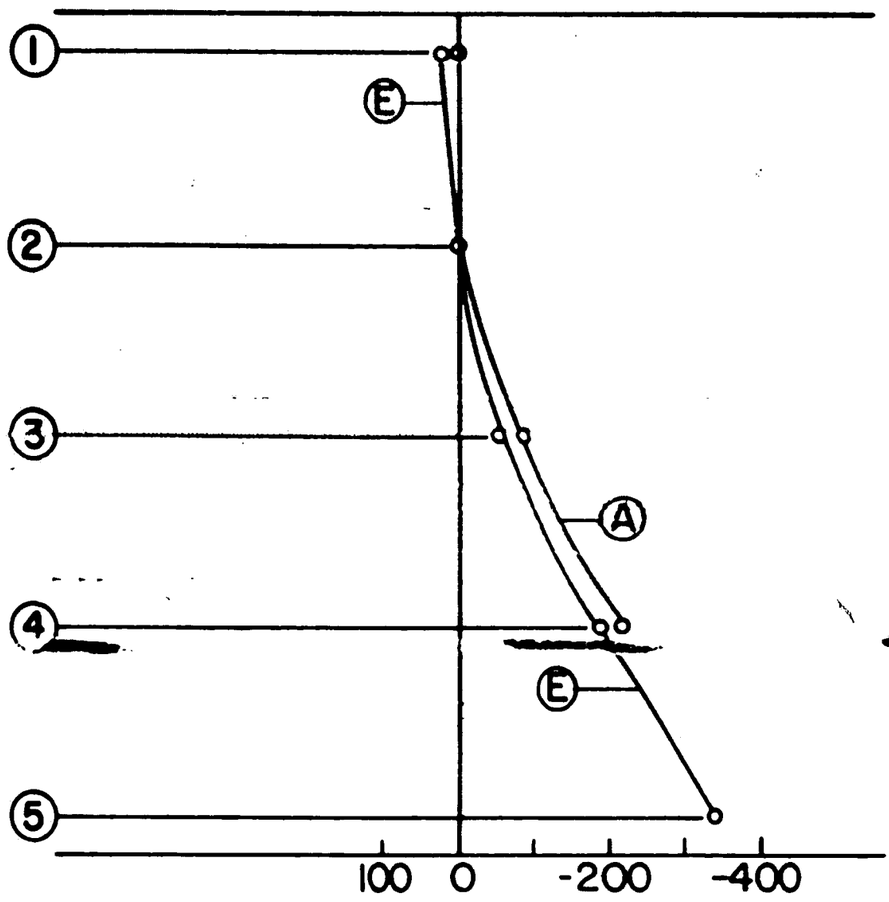

(a) SECTION I - ELEVATION

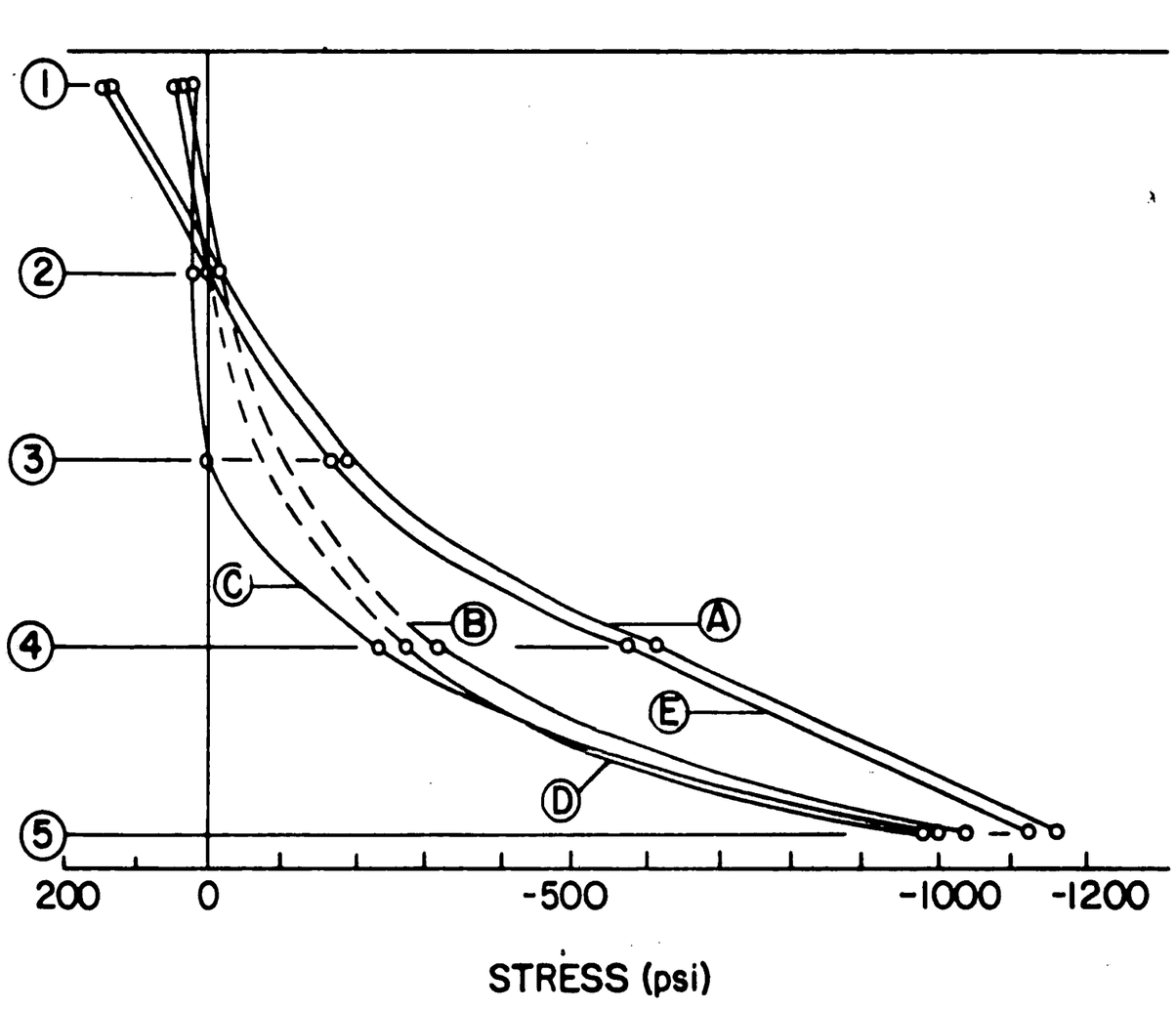

(b) SECTION II - ELEVATION

Fig. 25 Longitudinal Stresses Caused by Prestress Transfer in Second Test Beam

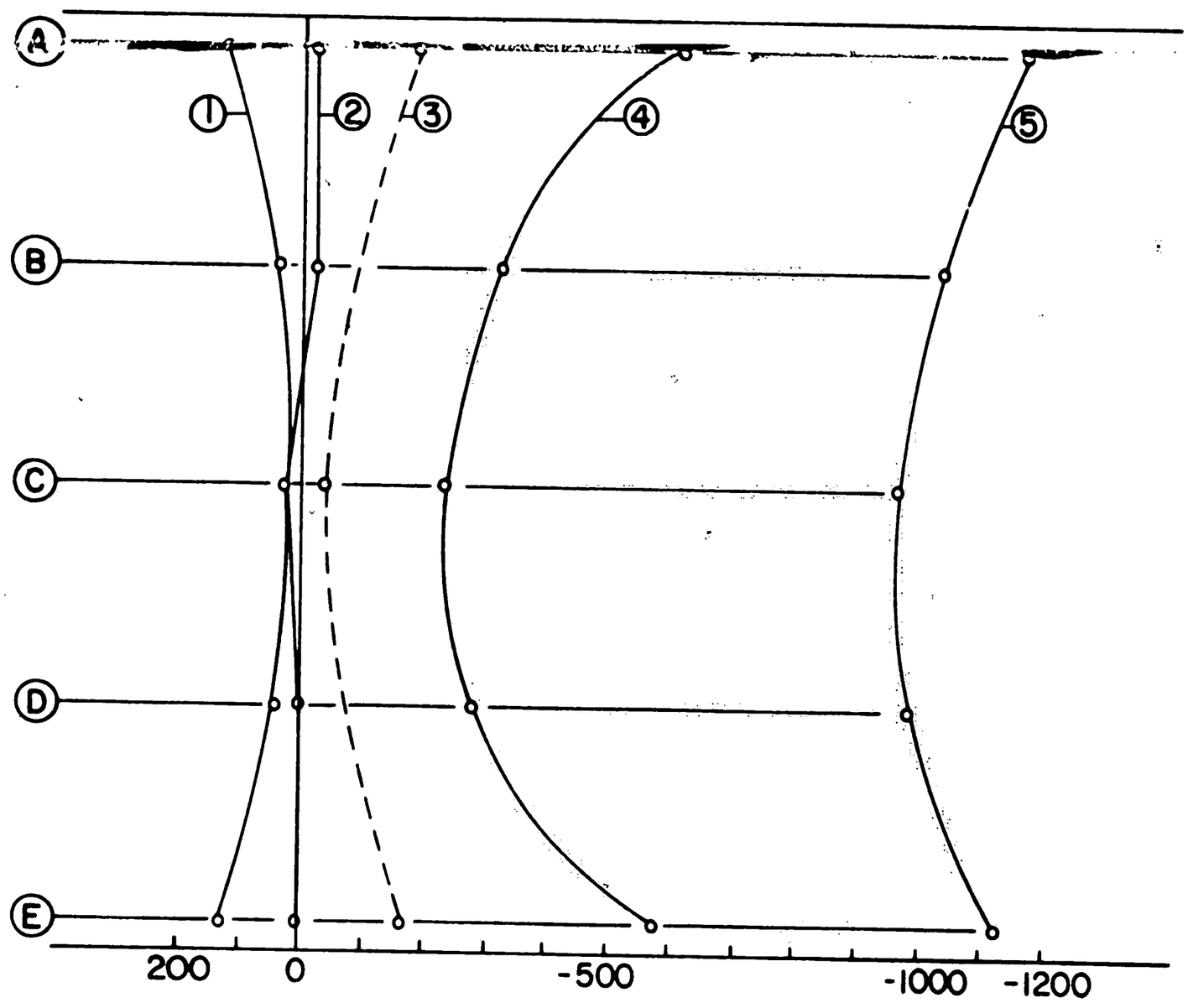

(c) SECTION II - TOP VIEW

Fig. 25 (cont'd)

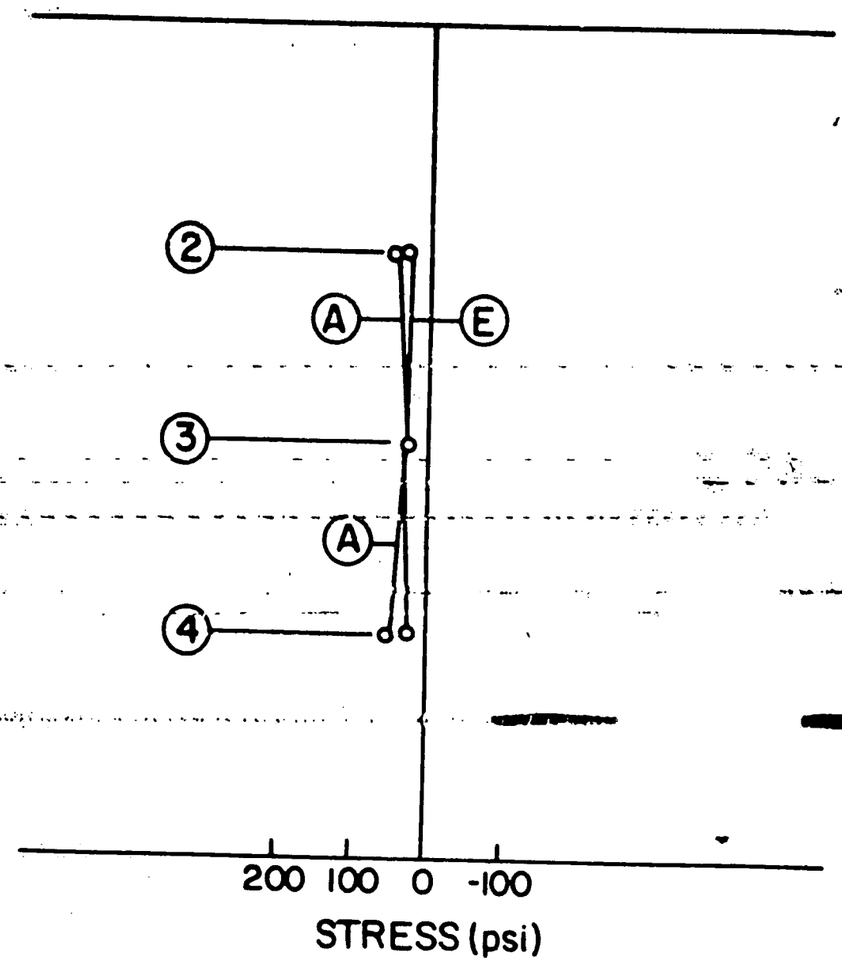

(a) SECTION I-ELEVATION

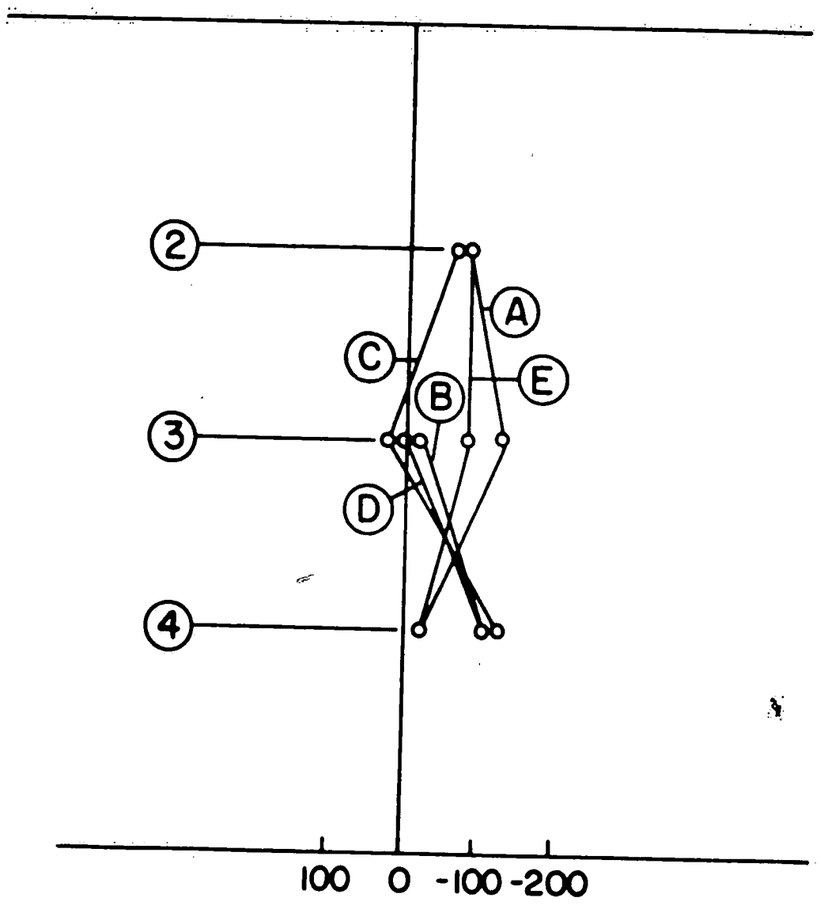

(b) SECTION II-ELEVATION

Fig. 26 Vertical Stresses caused by Prestress Transfer in Second Test Beam

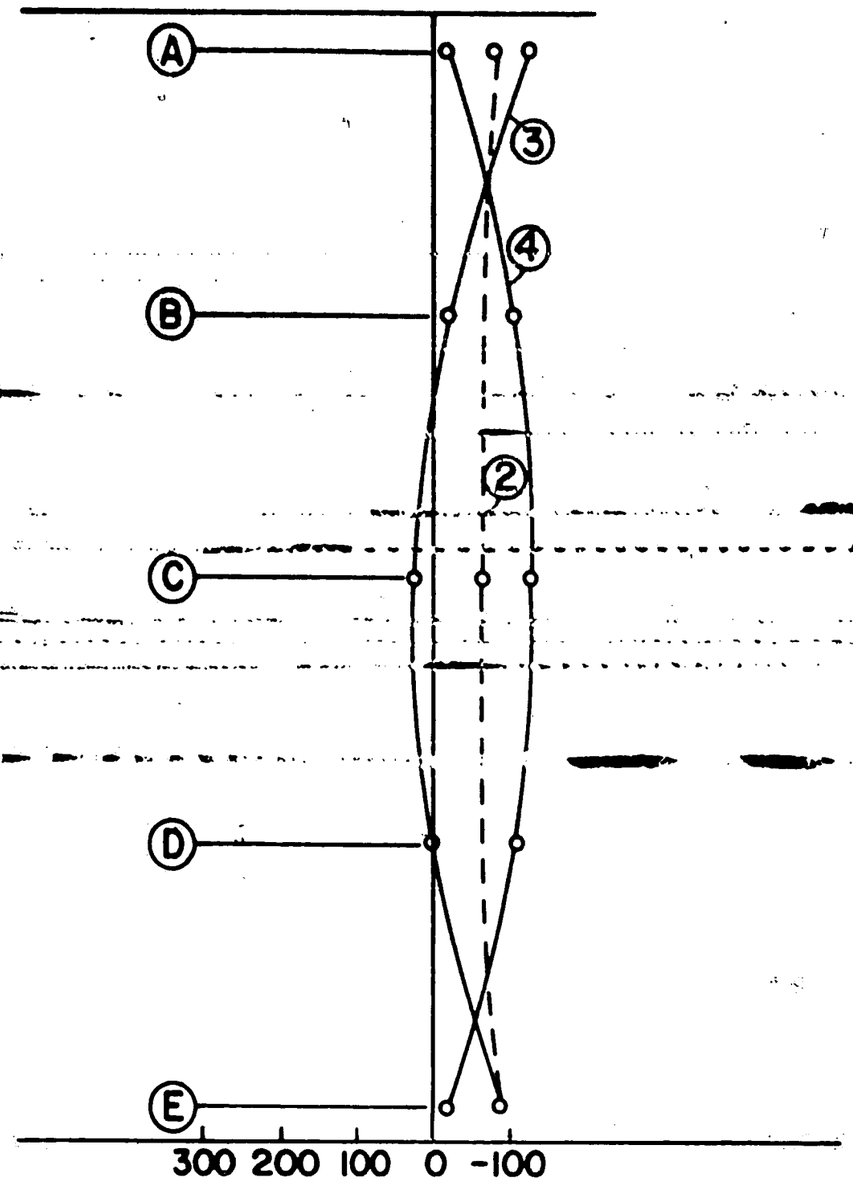

(c) SECTION II-TOP VIEW

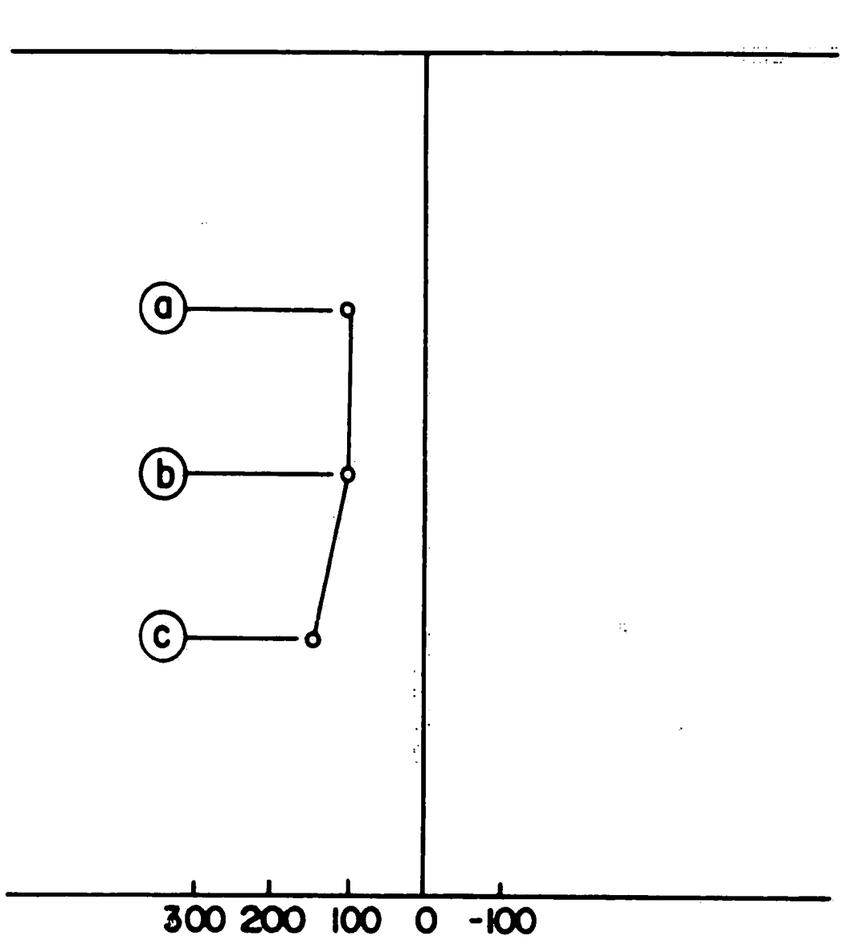

(d) LEFT END FACE

Fig. 26 (cont'd)

12. REFERENCES

1. Goodier, J. N.
THERMAL STRESS, American Society Mech. Engrg. Jour. Appl. Mech., Vol. 4, No. 1, March, 1937.

2. Guyon, Y.
PRESTRESSED CONCRETE, John Wiley & Sons, New York, 1953.

3. Lin, T. Y.
TESTS ON LUBABON COATED PRESTRESSING STRANDS AND WIRES, July 22, 1959, Sika Chemical Company, (Not Published).

4. Schupack & Zollman
DELAYED BONDING OF STRANDS IN THE END REGIONS OF PRETENSIONED BEAMS USING LUBABON COATING, Jan., 1960, (Prepared for Sika Chemical Company).

5. Timoshenko & Goodier
THEORY OF ELASTICITY, Second Edition, McGraw-Hill Book Company, New York, 1951, Chapts. 8, 14.

6. Perry and Lissner
THE STRAIN GAGE PRIMER, Second Edition, McGraw Hill Book Company, Inc., New York, 1962.

7. Hondros, G.
EPOXY RESIN PROTECTION OF ELECTRICAL RESISTANCE STRAIN GAUGES FOR GENERAL USE IN CONCRETE, Civil Engineering and Public Works Review, Vol. 57, No. 671, London, June 1962.

8. Weymouth, L. J.
A STRAIN GAGE FOR ELASTOMERIC EMBEDMENT, Journal of the Society for Experimental Stress Analysis, Experimental Mechanics, Vol. 3, No. 3, March, 1963.

9. Hanson, J. M. and Hulsbos, C. L.
ULTIMATE SHEAR TESTS OF PRESTRESSED CONCRETE I-BEAMS UNDER CONCENTRATED AND UNIFORM LOADINGS, Fritz Engineering Laboratory, Lehigh University, Report No. 223.27A, 1963.

10. Roark, Raymond J.
FORMULAS FOR STRESS AND STRAIN, Third Edition, McGraw Hill Book Company, Inc., New York.

11. Willis, T. F., and M. E. De Reus
THERMAL VOLUME CHANGE AND ELASTICITY OF AGGREGATES AND THEIR EFFECT ON CONCRETE, Proc. ASTM, Vol. 39, (1939), pp. 919-928.

12. Mitchell, L. J.
THERMAL EXPANSION TESTS OF AGGREGATES, NEAT CEMENTS, AND CONCRETES, Proc. ASTM, Vol. 53 (1953), pp. 963-977.

13. Baldwin-Lima-Hamilton Corporation
STRAIN GAGE HANDBOOK, Bulletin 4311A, 1963.

14. Pennsylvania Department of Highways Bridge Unit
PRESTRESSED CONCRETE BRIDGE STANDARDS, September 19, 1960.

15. Hanson, J. M. and Hulsbos, C. L.
OVERLOAD BEHAVIOR OF PRESTRESSED CONCRETE BEAMS WITH WEB REINFORCEMENT, Progress Report No. 25, Fritz Laboratory Report No. 223.25, p. 3.

16. Scarborough, J. B.
NUMERICAL MATHEMATICAL ANALYSIS, Fifth Edition, The John Hopkins Press, Baltimore, 1962, pp. 70-74.

17. Hanson, J. A.
OPTIMUM STEAM CURING PROCEDURE IN PRECASTING PLANTS, Proc. Journal of the American Concrete Institute, Jan. 1963, Vol. 60, p. 75.

18. Shideler, J. J. and Chamberlin, W. H.
EARLY STRENGTH OF CONCRETE AS AFFECTED BY STEAM CURING TEMPERATURES, ACI Journal, Proc. V. 46, No. 6, Dec. 1949, pp. 273-283.

19. Hulsbos, C. L. and Monson, E. M.
STRESS DISTRIBUTION IN THE ANCHORAGE ZONE OF A PRESTRESSED CONCRETE I-BEAM, Progress Report, Iowa Engineering Experiment Station, Iowa State College, Ames, Iowa, Sept. 10, 1957.

20. Bush, E. G. W., et. al.
DISCUSSION of the paper OPTIMUM STEAM CURING PROCEDURE IN PRECASTING PLANTS, Proc. Journal of the American Concrete Institute, Sept. 1963, Vol. 60, p. 1287.

21. Gonnerman, H. F. and Shuman, E. C.
COMPRESSION, FLEXURE, AND TENSION TESTS OF PLAIN CONCRETE, Proc. ASTM, Vol. 28, pt. II (1928), pp. 527-573.

22. American Association of State Highway Officials
STANDARD SPECIFICATIONS FOR HIGHWAY BRIDGES, 1961, Section 1.13.7: Allowable Stresses.

13. VITA

The author was born in Kansas City, Missouri, on May 12, 1934, the son of William Allen and Mary Elizabeth Miller. He completed his high school education in Jefferson City, Missouri in 1952, and attended pre-engineering classes at the Jefferson City Junior College during the following year. He received the remainder of his undergraduate civil engineering training at Washington University in St. Louis, Missouri where he was graduated in June, 1961.

In September, 1961 the author joined the staff of the Fritz Engineering Laboratory, Lehigh University as a research assistant in the concrete division, and in September, 1963 he was transferred to the structural metals division of the laboratory as a research assistant.